Biochemical characterization of the Structural Maintenance of Chromosomes (SMC) complex From *Bacillus subtilis*

Dissertation
for the doctor's degree in natural sciences
(Dr. rer. nat. corresponding to Ph.D.)
submitted to the Fachbereich Biologie
Philipps Universität Marburg

by
Arsen Volkov
From Moscow, Russia.

Marburg (Lahn)
2004

To my dear parents

Von Fachbereich Bioloogie der Philipps-Universität Marburg als Dissertation am 1 June 2004 angenommen.

Tag der mündlichen Prüfung: 15.06.2004

Erstgutachter: Dr. P. L. Graumann

Zweitgutachter: Prof. Dr. M. Bölker

Drittgutachter: Prof. Dr. U. Maier

Viertgutachter: Prof. Dr. A. Batschauer

Zusammenfassung

Structural Maintenance of Chromosomes (SMC) Proteine spielen eine zentrale Rolle in mehreren Aspekten von Chromosomen Dynamiken während des Zellzyklus in fast allen Zellen, von Bakterien bis zu Eukaryonten. Proteine der SMC Familie führen essentielle Funktionen in einer Vielzahl von Prozessen aus, wie bei der Chromosomen-Kondensation und Segregation, Schwesterchromosomen Kohäsion und DNA Doppelstrandbruch Reparatur. SMC Proteine besitzen eine ungewöhnliche Struktur, bestehend aus N- und und C-terminalen Domänen, die ATPase Motive beinhalten, aus einer Scharnier „hinge“ Domäne und zwei zentralen coiled coil Domänen. Die terminalen Domänen kommen zusammen und bilden die Kopfdomäne aus, während die coiled coil Domänen ein coiled coil bilden. SMC Proteine bilden intermolekulare Dimere aus, durch spezifische Interaktion der hinge Domänen. Alle SMC Proteine fungieren in Komplexen mit weiteren Nicht-SMC Untereinheiten, und kürzlich wurden zwei neuartige prokaryontische Proteine identifiziert, ScpA and ScpB, die mit bakteriellem SMC Protein *in vivo* interagieren.

In dieser Arbeit wurden biochemische Studien zur Eigenschaften und Funktion von SMC, ScpA und ScpB aus *B. subtilis in vitro* unternommen, um deren *in vivo* Funktion zu beleuchten. ScpB wurde in Lösung ausschließlich als Dimer vorgefunden, wohingegen ScpA in monomerer und in dimerer Form auftrat. Mit Hilfe von Gelfiltration, Gelshift Experimenten, Sucrose Gradienten Zentrifugation und Oberflächen Plasmon Resonanz (SPR) konnte ich nachweisen, dass SMC, ScpA and ScpB einen ternären Komplex ausbilden, höchst wahrscheinlich bestehend aus einem SMC Dimer, zwei ScpA und vier ScpB Molekülen. ScpA und ScpB interagierten spezifisch mit der SMC Kopfdomäne, jedoch nur, wenn beide Proteine vorhanden waren, wobei die Interaktion von ScpB nur indirekt über ScpA mit der Kopfdomäne erfolgte. ScpA und ScpB bildeten ebenfalls mindestens zwei Komplexe in Abwesenheit von SMC, die sich anscheinend aus einem ScpA Monomer und einem ScpB Dimer, bzw. aus einem ScpA und zwei ScpB Dimeren zusammensetzten. Gelfiltrationsexperimente legten nahe, dass der SMC Komplex durch Bindung des 2ScpA/4ScpB Komplexes an ein SMC Dimer erfolgt, und nicht durch Interaktion einzelner ScpA und ScpB Moleküle. Sucrose Gradienten zeigten, dass alle drei Proteine als Komplex und als separate Moleküle vorliegen, was auf einen dynamische Interaktion *in vivo* schließen lässt.

Des weiteren wurden die DNA Bindungseigenschaften des SMC Komplex und einzelner Domänen von SMC untersucht. SMC konnte Sequenz-unspezifisch an DNA binden, jedoch weder ScpA noch ScpB zeigten Affinität zu DNA, bzw. waren für die DNA Bindung des SMC Komplex notwendig. Die isolierte hinge oder Kopfdomäne von SMC waren ebenfalls unfähig, an DNA zu binden, was zeigt, dass das gesamte SMC Molekül zur effektiven Interaktion mit DNA notwendig ist. SPR Experimente zeigten, dass SMC als ringförmige Struktur an DNA bindet, vermutlich über Dimerisierung der Kopfdomänen, welches zum Ringschluß führt und zum Umschließen der DNA mit den langen coiled coil Armen. Kollaborative Atomic Force Microscopy Experimente konnten tatsächlich ringförmige SMC Strukturen nachweisen, sowie große, sonnenartige Strukturen in Lösung auflösen, welche eine Erklärung für die Beobachtung sein könnten, dass der SMC Komplex definierte, subzelluläre Strukturen auf dem bakteriellen Chromosom ausbildet und nicht über das gesamte Chromosom verteilt vorliegt.

SMC Proteine haben eine schwache ATPase Aktivität und besitzen typische ABC Typ ATPase Motive. Mutagenese Studien erbrachten den Nachweis, dass ATP Bindung, nicht aber Hydrolyse, zur DNA Bindung von SMC notwendig ist. Keine der Mutationen war jedoch zur Komplexbildung mit ScpA und ScpB notwendig, obwohl die Mutanten nur weniger effizient einen SMC Komplex ausbilden konnten. Aus diesen Daten lässt sich folgendes Modell ableiten: ATP Bindung führt zur Dimerisierung der SMC Kopfdomänen, wodurch DNA im Ring eingeschlossen wird. Dissoziation von DNA könnte über ATP Hydrolyse erfolgen. Gelfiltrationsexperimente legen nahe, daß ScpA in Abwesenheit von ScpB zur Ablösung von DNA führt, wohingegen alle drei Proteine (d.h. in Anwesenheit von ScpB) einen stabilen Komplex bilden, der durch Bindung von DNA Schleifen zur Kondensation der DNA führen könnte. Somit könnte der Kondensations-Grad des Chromosoms *in vivo* durch die Menge von ScpB in der Zelle kontrolliert werden.

Summary

Structural Maintenance of Chromosomes (SMC) proteins play a key role in the chromosome dynamics throughout the cell cycle in almost all species from bacteria to eukaryotes. Proteins from SMC family are involved in a number of processes, such as chromosomes condensation and segregation, sister-chromatid cohesion and DNA double strand break repair. All SMC proteins share a typical structure and consist of N- and C-terminal domains carrying the ATPase motif, the hinge domain and two central coiled-coil domains. Terminal domains come together to form one head domain**,** while coiled coil domains form a single coiled coil. SMC proteins form an intermolecular dimer via interaction of hinge domain**s**. All eukaryotic SMCs perform their function in complex with a number of other none SMC subunits and recently, two novel prokaryotic proteins, ScpA and ScpB, have been found to interact with bacterial SMC *in vivo*.

In this work, biochemical studies were performed to understand the properties of *B. subtilis* SMC, ScpA and ScpB *in vitro*, and to elucidate the mechanism of their action *in vivo*. The main state of ScpB in solution was found to be a dimer, while ScpA exists in both monomeric and dimeric forms. Using different approaches, such as size exclusion chromatography, gel shift assay and sucrose gradient ultracentrifugation, I found that SMC, ScpA and ScpB indeed form a ternary complex, which most likely consists of one SMC dimer, two ScpAs and two ScpB dimers. ScpA and ScpB were also able to form two types of complexes in absence of SMC: one formed by one ScpA and a dimer of ScpB, and a larger complex most likely consisting of two ScpAs and two ScpB dimers. ScpB was shown to interact with SMC indirectly only in presence of ScpA**,** and ScpA interacted stably with the SMC head domains only in the presence of ScpB. In addition, gel filtration assays suggested that the SMC complex is most likely formed by direct binding of the ScpA/ScpB complex to SMC, rather than through binding of individual ScpA and ScpB molecules to SMC. Sucrose gradient analysis also showed that ScpA, ScpB and SMC are present as a complex as well as in non-complexed form, indicating that the SMC complex is in a dynamic state *in vivo*.

Another aspect investigated here were the DNA binding properties of SMC, ScpA, ScpB as well as of different domains of SMC. I found that neither ScpA, nor ScpB are required for binding of SMC to DNA**,** and that they have no affinity to DNA in absence of SMC. Isolated hinge and head domains of SMC were also unable

to bind DNA, thus, the complete SMC molecule is needed for proper function. SMC bound to dsDNA in a sequence independent manner, and based on data obtained from surface plasmon resonance experiments, binding to DNA occurred via formation of a closed ring-like structure. The data suggest that SMC interacts with DNA via dimerization of its head domains leading to the formation of a ring-like structure with DNA trapped in between the coiled-coil (domains) arms of SMC. Collaborative AFM studies have also shown ring formation by SMC, and large complex structures formed by SMCs were detected in solution that could explain why SMCs in bacterial cells are concentrated in certain regions of the cells (foci) and are not distributed (throughout the inner cellular space) all over the chromosome.

Mutagenesis studies were another part of the project. SMC proteins have a weak ATPase activity and head domains contain conserved motifs that are typical for ABC-type ATPases. In this work I have shown, that ATP binding, but not ATP hydrolysis, is required for DNA binding of SMC. Additionally, none of these activities were required for complex formation with ScpA and ScpB, although formation of the SMC complex was less efficient in the mutant proteins. A model is suggested that ATP binding induces dimerization of head domains causing formation of a ring by SMC with DNA locked in the middle. Data obtained from gel filtration studies suggest that ScpA, in absence of ScpB, causes DNA release from SMC, while in the presence of ScpB, all three proteins form a stable complex. Therefore the condensation state of chromosomes *in vivo* could possibly be controlled by the levels of ScpB in the cell.

Contents **Page**

1. Introduction 8
1.1 SMC proteins family 8
1.2 Bacterial SMC and SMC-like proteins 13
1.3 Eukaryotic SMC proteins 16
1.3.1 Cohesin complex 16
1.3.2 Condensin complex 19
1.3.3 SMC5/SMC6 complex 21
1.4 Rad50 21
1.5 ABC-Transporters protein family 22
1.6 Aim of the work 24
2. Materials and methods 26
2.1 Materials 26
2.1.1 Equipments used in this study 26
2.1.2 Materials and reagents 27
2.1.3 Kits 28
2.1.4 Antibodies 29
2.1.5 Oligonucleotides 29
2.1.6 Bioinformatic tools and computer programs 30
2.1.7 Bacterial host strains 31
2.1.8 Plasmids used in this study 31
2.2 Molecular biology methods 34
Growth Medium 34
Antibiotic Solutions 35
Techniques related to DNA 36
2.2.1 Agarose gel electrophoresis of DNA 36
2.2.2 Digestion of DNA by restriction enzymes 36
2.2.3 Ligation of vector and insert DNA 37
2.2.4 E. coli transformation 37
2.2.5 Preparation of plasmid DNA 38
2.2.6 Polymerase chain reaction - PCR 39
2.2.7 DNA sequencing 40
2.2.8 Site-directed mutagenesis 40
2.4 Techniques related to protein 41
2.4.1 Small scale preparation of protein extracts 41
2.4.2 Separation of proteins by SDS-polyacrylamide gel electrophoresis 42
2.4.3 Separation of proteins by Native-polyacrylamide gel electrophoresis 44
2.4.4 Protein staining with Coomassie blue 45
2.4.5 Silver staining of proteins
2.4.6 Western blotting 46
2.4.6.1 Immunodetection 47
2.4.6.2 Chemiluminescence-detection of proteins on nitrocellulose membrane 48
2.4.7 Large scale purification of proteins 48
2.4.7.1 Large scale expression of proteins and preparation of protein extracts 48
2.4.7.2 Affinity purification of His-tagged proteins 49

2.4.7.3 Purification of Thermatoga maritima proteins 50
2.4.8 Surface plasmon experiments 50
2.4.9 Sucrose gradient centrifugation 50
2.4.10 Gel filtration assay 51
2.4.11 Sample preparation for ESI-TOF experiments 51
2.4.12 Sample preparation for atomic force microscopy 51
2.5 Bacillus genetics 52
2.5.1 Preparation of chromosomal DNA from Bacillus subtilis cells 52
2.5.2 Preparation of competent Bacillus subtilis cells 52
2.5.3 Transformation in Bacillus subtilis 54
2.6 Microscopic techniques 54
2.6.1 Fluorescence microscopy - Principles 54
2.6.2 Vital stains used in fluorescence microscopy 56
2.6.3 Media used for microscopy 57
2.6.4 Preparation of slides for microscopy 58
3. Results 59
3.1 ***Purification of SMC, ScpA and ScpB and of SMC domains*** 59
3.2 ***ScpA, ScpB and hinge domain of SMC form dimers*** *in vitro* 61
3.3 ***Full length SMC is needed to bind to dsDNA*** 65
3.4 ***SMC binds nonspecifically to DNA via a ring-like structure*** 68
3.5 ***ScpA and ScpB form two types of complexes*** *in vitro* 70
3.6 ***SMC is present in two distinct density fractions in cell extract, and co-elutes with ScpB in a high molecular weight fraction*** 73
3.7 ***SMC forms a stable complex with ScpA and ScpB*** 74
3.8 ***ScpA possibly causes release of DNA from SMC*** 77
3.9 ***ATP binding and hydrolysis are important but not required for SMC complex formation with ScpA and ScpB*** 79
3.10 ***ATP binding but not hydrolysis is needed for interaction of SMC with DNA*** 80
3.11 ***SMC possibly forms aggregates on AFM in solution*** 82
3.12 ***Purification and properties of Thermatoga maritima SMC*** 85
3.13 ***Localization of cold shock proteins to cytosolic spaces surrounding nucleoids in Bacillus subtilis depends on active transcription*** 85
4. Discussion 86

5. Appendix 96
5.1 Localization of cold shock proteins to cytosolic spaces surrounding nucleoids in Bacillus subtilis depends on active transcription 96
5.2 Strains used in this work 106
5.2.1 Plasmids and strains constructed in this work 106
5.2.2 Primers used in cloning 108
6. References 110

Abbreviations

ATP	Adenisine-5'- triphosphate
amy	gene coding for amylase
bp	base pair
cDNA	Complementary DNA
dH_2O	Distilled water
dsDNA	Double stranded DNA
EDTA	Ehtylene diamine tetraacetic acid
FPLC	Fast Performance Liquid Chromatography
FP	Fluoroscent protein
h	hour
IPTG	Isopropanol-b-D-thiogalactopyranoside
kb	Kilobase(s)
LB	Luria-Bertani medium
MCS	Multiple cloning sites
min	Minute(s)
nm	Nanometer
O.D.	Optical density
PCR	Polymerase chain reaction
RT- reaction	Reverse transcriptase reaction
rpm	Rotation per minute
SDS-PAGE	Sodium dodecylsulfate polyacrylamide gel electrophoresis
SPR	Surface Plasmon Resonance
T_m	melting temperature of dsDNA
TB	Tris. Boric acid buffer
TE	Tris EDTA buffer
Tris	2 amino 2-(hydroxymethyl)-1,3-proanediol
U	Unit of enzyme activity
UV	Ultraviolet light

1 Introduction

One of the central and crucial processes in the life of all living organisms is cell division. During the division both daughter cells are supposed to get an equal copy of genetic information as well as somewhat equal amounts of all cell components to provide cell survival. DNA segregation appears to be one of the most difficult tasks for the cells because of the huge size and high flexibility of the chromosomes. An average length of circular bacterial chromosome varies within a millimeter range, while typical bacterial cell has a length of few micrometers and volume of few cubic micrometers; therefore, chromosomes are compacted 10^3 to 10^4 times not only to fit into the cell, but to leave some space in the cell to make different cellular activities possible (Woldringh 2002). Chromosomes should not only be compacted but also organized in the cell to make it possible that different enzymes have access to all regions of the chromosomes and also to provide separation of daughter cells during cell division without damaging any DNA material. In eukaryotes, the organization and integrity of DNA is facilitated by the use of histones, which are not present in bacteria. Eukaryotic cells have an elaborate mitotic apparatus, while in bacteria, chromosomes are compacted and segregated in a much simpler manner, but nevertheless, as effective as in eukaryotic cells. Moreover, some bacteria have more than one chromosome or in some cases additional plasmids, which should also be segregated, and that requires a segregation apparatus, which is very precisely coordinated throughout the cell cycle. Although a number of DNA interacting proteins is present in bacteria, one of the key players in the processes of chromosome dynamics, segregation and condensation are Structural Maintenance of Chromosomes (SMC) proteins. The aim of this work was to investigate and characterize the properties and function of the bacterial SMC protein and its interacting partners *in vitro* using different biochemical techniques.

1.1 SMC proteins family

Structural Maintenance of Chromosomes (SMC) proteins form a protein family, members of which are ubiquitous in almost all species from prokaryotes to higher

eukaryotes and are involved in a number of processes in chromosome dynamics such as chromosome condensation, sister-chromatid cohesion, DNA repair and recombination, and gene dosage compensation (Jessberger 2002). In eukaryotes, there are at least 6 members of the SMC family which are the key components in at least three different multiprotein complexes. Unlike eukaryotes, bacteria have only one copy of a *smc* gene, with an exception in *E. coli*, which has an SMC-like protein MukB instead, very similar to SMC in its domain organization and functions. Moreover, at the moment only four genera are found that do not contain at all any type of SMC or SMC related protein: *Buchnera, Chlamydia, Chlamydophila* and *Helicobacter.*

Despite the variety of functions of the SMC proteins, they all share a similar structure. All SMCs have a high molecular weight which ranges from 110 to 170 kDa and consist of five domains: N-terminus and C-terminus domains that are connected to a central hinge domain via two long coiled-coil regions (Fig. 1).

Fig 1. SMC domain organization. N-terminal domain and C-terminal domains are connected to a central hinge domain via two coiled-coil domains.

SMC proteins were found to have a very weak ATPase activity and sequence analysis of SMC has shown that N-terminus and C-terminus domains contain highly conserved Walker A and Walker B motifs that are typical for ATP binding cassette (ABC)-transporters family of ATPases. Since Walker A and Walker B motifs are located in N- and C-terminus domains of SMC, respectively, these domains have to come together to form one functional head domain with ATPase activity, while coiled-coil domains interact with each other forming one stable structure. The main state of SMCs in solution is a dimer and crystal structure studies of the hinge domain of *Thermatoga maritima* SMC performed by Jan Löwe`s group (Haering, Lowe et al. 2002) has shown that dimerization of SMC occurs via the hinge and results in formation of a V-shape molecule (Fig. 2). The hinge domain contains the conserved sequence G(X)5GG(X)3GG for prokaryotes and G(X)6G(X)3GG for eukaryotes,

which seems to be highly important for the flexibility of SMC. Electron microscopy studies have shown that certain mutations in the hinge domain of *B. subtilis* SMC can change the flexibility of SMC while some mutations abolish dimer formation completely (Hirano, Anderson et al. 2001).

A **B**

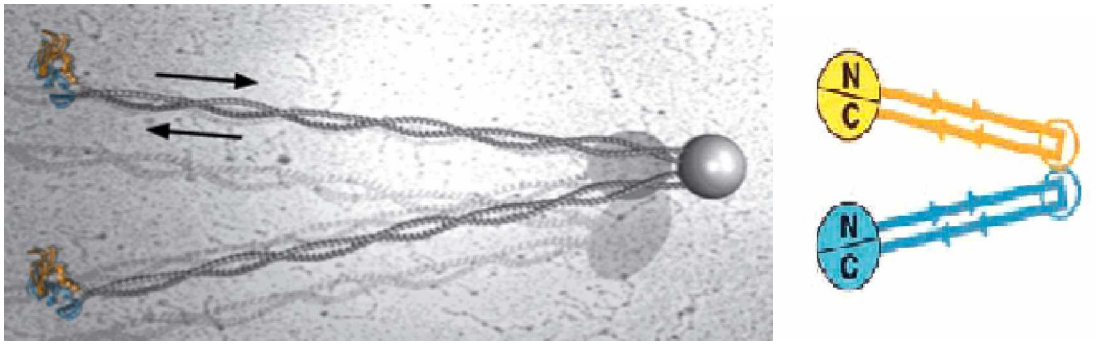

Fig. 2 Computer model (A) and schematic representation (B) of the SMC structure. SMCs form an inter-molecular dimer via dimerization of the hinge domain.

Being involved in such subcellular processes as DNA condensation, sister chromatid cohesion and DNA double strand brake repair, SMC proteins are supposed to be able to interact with distant regions on the DNA and this is provided by the long coiled-coil domains of SMCs that make it possible for proteins to interact with DNA strands, which are up to 50 nm apart from each other. The mechanism of binding to DNA for SMCs remained unclear after their discovery for quite a long time and one of the main models suggested that DNA binding occurs via the head domains of SMC. However, this model was not able to explain all aspects on how SMCs perform their function.

Besides true SMC proteins, there is a number of proteins related to the SMC family, such as bacterial RecN protein, involved in recombination and DNA double strand brake repair, archaeal and eukaryotic Rad50 involved in recombinational DNA double strand brake repair and its bacterial analogue, SbcC protein that is responsible for cleavage of hairpin structures on the ends of DNA, which is also involved in DNA double strand break repair (Fig. 3). Although their size may vary from that of SMCs and although these SMC like proteins do not possess a hinge domain, all these proteins have a SMC-like five domain organization and contain conserved Walker A and Walker B motifs, similar to ABC-transporters, in their N- and C-terminus.

Although all SMCs are evolutionary related to each other (Cobbe and Heck 2004), SMC1 was found to be more related to SMC4 and SMC2 is more related to SMC3 while SMC5 and SMC6 have evolved from a more ancient ancestor (Fig. 3). Due to the fact that bacterial SMC protein has most of the features typical of eukaryotic SMCs, understanding of mechanisms of its action would help to understand the function of all members of the SMC family.

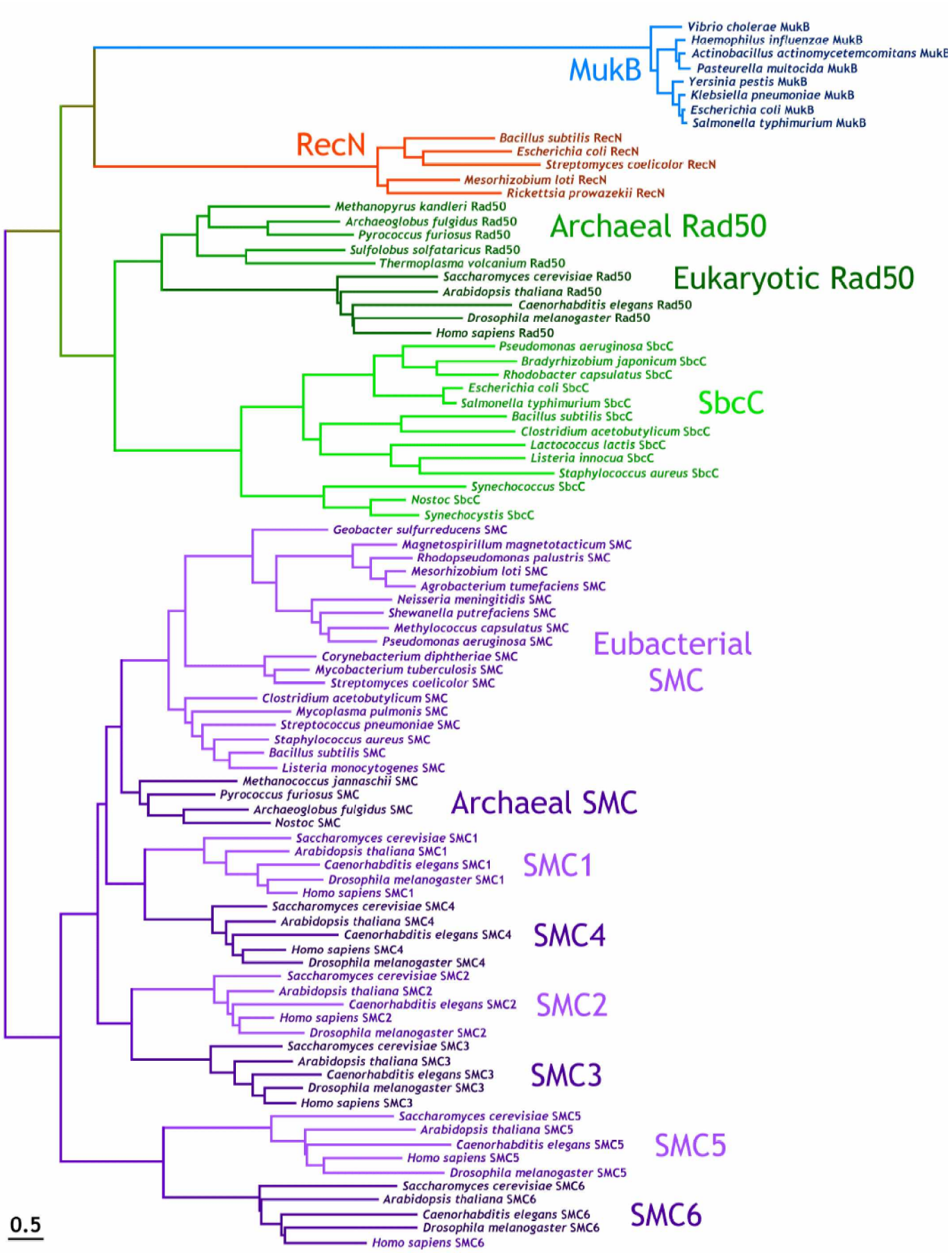

Fig. 3 Phylogenetic tree of SMCs and related proteins. The scale bar denotes the number of accepted substitutions in Whelan-Goldman distance units (Cobbe and Heck 2004)

1.2 Bacterial SMC and SMC-like proteins

Bacterial chromosomes are organized in a compact structure called nucleoid, which occupies the central part of a cell. DNA in the nucleoid is normally organized into separate supercoiled loops with overall negative supercoiling, which is provided by the regulated action of topoisomerases and SMCs. During cell division, newly replicated chromosomes should also be compacted and segregated into two separate nucleoids to make it possible for the cell to build septum in the middle and to separate daughter cells, so that each one will receive an equal number of undamaged chromosomes. Bacterial SMCs were found to play one of the central roles in the maintaining of condensation and segregation of chromosomes. The nucleoid in *smc* deletion mutants is not compact any more and DNA in such cells is distributed throughout the cell, filling all inner space (Fig. 4). Upon deletion of *smc* cells also become temperature sensitive, so that they are able to grow very slowly only at or below room temperature and additionally, mutant cells have a defect in segregation of chromosomes, so that about 15% percent of all cells are anucleate (i.e. do not contain any DNA).

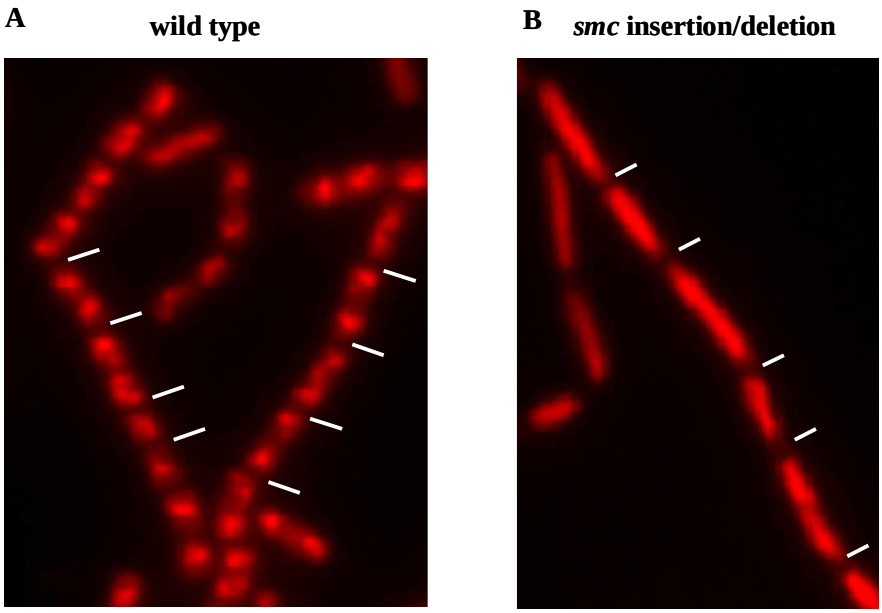

Fig. 4 PI DNA-stained wild type (A) and *smc* deletion mutant cells (B), courtesy P. Graumann

In the cells, SMCs are not distributed throughout the cells but on the contrary, they are concentrated in the certain foci, which are always located on the nucleoid, and most likely perform their function from these spots. *In vivo* studies of *B. subtilis* SMC, performed in our group have shown that in the beginning of replication, SMCs are concentrated into one focus that is located in a close proximity to the center of the cell, but as replication goes on, this focus separates into two foci which rapidly shift towards opposite cell poles (Fig. 5). Therefore, to fulfill their task, SMCs act from certain condensation centers, but the mechanism of their formation and the real role of these foci remains unclear.

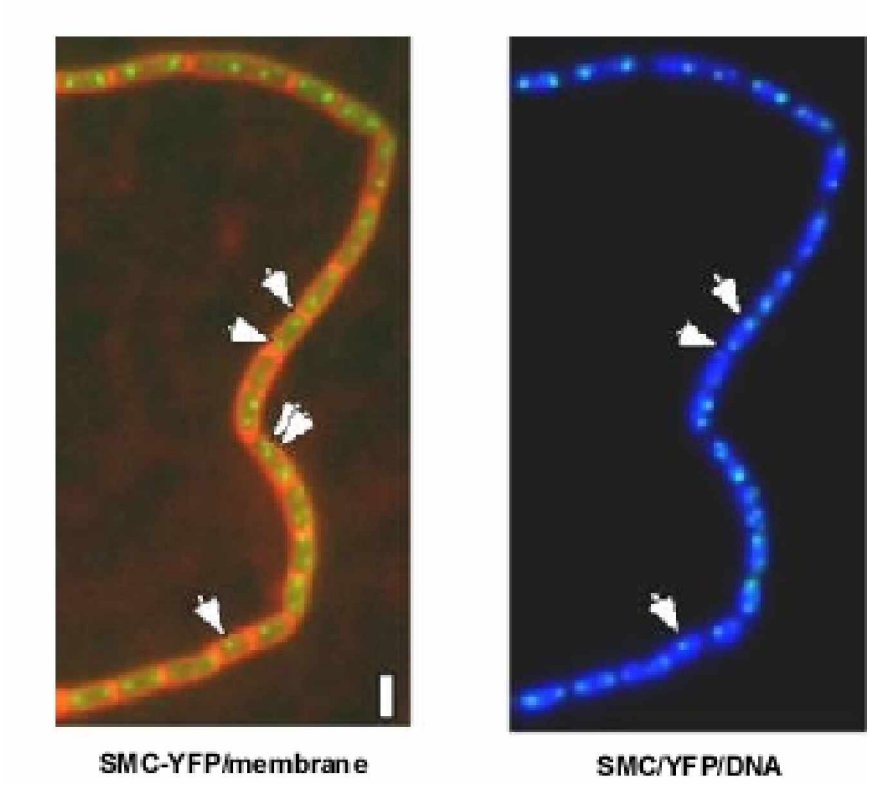

Fig. 5 Cell cycle dependent localization of SMC. Left panel represents an overlay of YFP-tagged SMC and membrane stain, right panel represents an overlay of YFP-tagged SMC and DNA stain. Arrows show the positions of certain SMC foci. (Volkov, Mascarenhas et al. 2003)

Bacterial SMCs have all structural features typical for all members of SMC family. However, in spite of the fact that all eukaryotic SMCs, as well as related proteins such as Rad50, perform their function in complex with different other non-SMC proteins, no interacting partners for bacterial SMC were known until recently.

Computer analysis of genome of *Halobacterium salinarum*, performed by Jörg Soppa, has shown that the *smc* gene is located in an operon with another downstream gene, which is conserved in almost all bacteria and achaea. Analysis of the *B. subtilis* genome has revealed that this gene (labelled as *ypuG* by the *B. subtilis* genome consortium) lies in an operon with two other genes, *ypuH* and *ypuI* (Fig. 6). It was found that *ypuG* is present in most bacterial species that possess SMC although some species do not have *ypuH*. Both *ypuG* and *ypuH* were previously reported to be essential, unlike *ypuI*. Investigation of *ypuG* and *ypuH in vivo*, performed in our group, showed that deletion of any of this genes results in a phenotype, similar to that of *smc* null mutant and evidence was obtained that SMC forms a complex with ypuG and ypuH *in vivo*. For this reason, ypuG and ypuH were renamed and are referred as Segregation and Condensation Proteins A and B respectively or ScpA and ScpB.

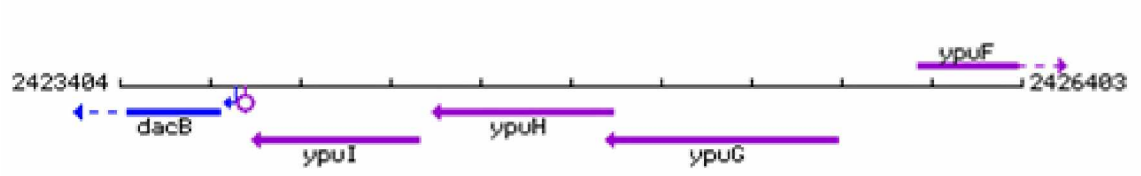

Fig. 6 Genomic organization of *B. subtilis ypuGHI* operon. Numbers represent coordinates on the chromosome.

E. coli, which does not have a SMC proteins have developed another protein related to SMC instead, which was named MukB. Although MukB does not have sequence similarities with SMCs, nevertheless it is very similar to SMC in structure and function. MukB proteins were found to form foci in the cell in a manner similar to SMC and *mukB* null mutants were found to have a similar phenotype to that of *smc* null mutants. MukB has a similar to SMC structure and is known to function in complex with two other proteins, MukE and MukF, and C-terminal domain of MukB was shown to take part in complex formation with MukE and MukF. However, similarly to ScpA and ScpB, the function of both MukE and MukF at the moment remains unclear.

1.3 Eukaryotic SMC proteins

Having a much more complex organization than prokaryotes, eukaryotes have developed a mitotic apparatus to provide the equal partitioning of newly replicated chromosomes, also called sister chromatids, into the daughter cells. During the process of mitosis, eukaryotic chromosomes have to undergo crucial changes, newly replicated chromosomes should be condensed, individualized and segregated into the daughter cells. Having a much more complicated chromosomes organization, eukaryotes evolved to have six different SMC proteins which form at least three different complexes with different non-SMC subunits that are involved in different stages of mitosis.

1.3.1 Cohesin complex

In the process of mitosis cohesion of replicated chromosomes, plays a crucial role. First of all, it allows attachment of sister kinetochores, which are located at the centromeric regions of the chromatids, to microtubules with opposite orientation (Nasmyth 2001). In this case, sister chromatid cohesion is needed to keep chromatids together until microtubules are connected in a proper orientation to ensure that the chromatids are pulled towards opposite cell poles. Cohesion also is very important since it resists the tension which was found to be crucial for stabile attachments between microtubules and kinetochores. The search for the proteins, important for cohesion of the sister chromatids resulted in identification of some dozen proteins. Four of these proteins, SMC1, SMC3, Scc1/(Mcd1 or Rad21) and Scc3 were found to form one stable complex in different organisms from yeast, worms and flies to vertebrates (Guacci, Koshland et al. 1997; Losada, Hirano et al. 1998; Toth, Ciosk et al. 1999), and all four components were found to be essential in the chromatid cohesion and for viability. While SMC1 and SMC3 belong to the SMC family of proteins, Scc1 was found to be a member of another wide spread protein family of so called “kleisins”, which consists of SMC-binding proteins and also includes Rec8s and bacterial ScpAs (Fig. 7A). The cohesin complex is loaded onto chromosomes

prior the beginning of replication and keeps sister chromatids together until metaphase in yeast and in higher eukaryotes. However, in vertebrates, most of cohesins are released from the chromosome arms in prophase while remaining in the centromeric regions of chromosomes and thus keeping sister chromatids connected. The prophase release of cohesin was found to be under control of the Aurora B and PLK kinases (Losada, Hirano et al. 2002; Sumara, Vorlaufer et al. 2002). In metaphase, cleavage of Scc1 cohesin subunit occurs, which allows for separation of the sister chromatids and movement towards opposite cell poles (Fig. 7B).

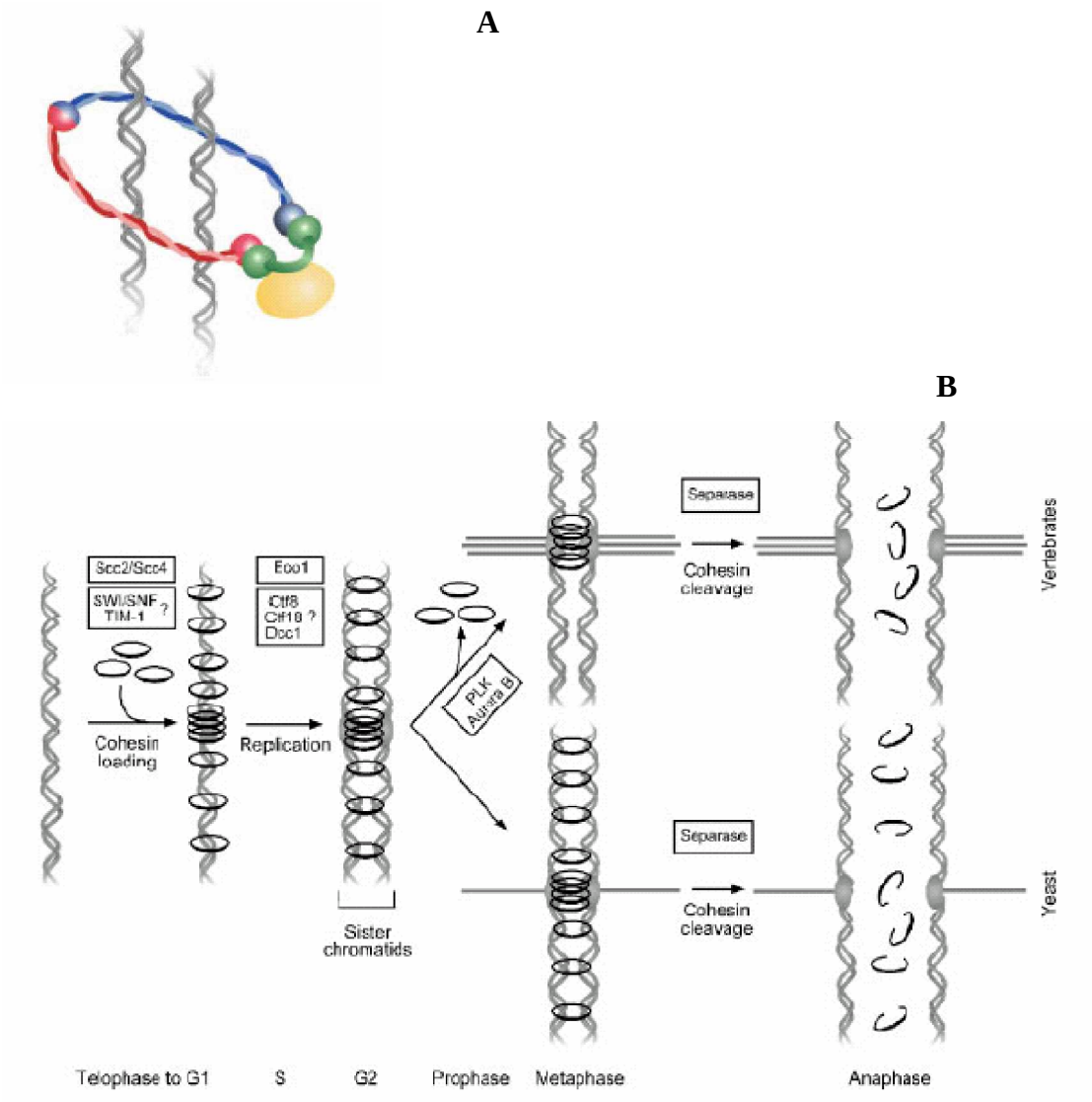

Fig. 7 (A) Model for cohesin binding to DNA. SMC1 and SMC3 (red and blue) embrace long arms around DNA while Scc1 (green) associated with Scc3 (yellow) bridges head domains, thereby locking the ring. (B) Cohesin cell cycle (Haering and Nasmyth 2003).

Biochemical analyses of the yeast cohesin complex together with electron microscopy studies have shown that while SMC1 and SMC3 form a dimer via hinge domain, Scc1 interacts with them in a close proximity to the head domains (Anderson, Losada et al. 2002) so that N-terminal part of Scc1 interacts with SMC3 and the C-terminal part with SMC1, bridging two heads and forming a closed ring (Haering, Lowe et al. 2002). Scc3 binds to the center of Scc1 making the complex complete. *In vivo,* sister chromatids are trapped inside the ring formed by long coiled-coil arms of SMC1 and SMC3 with their heads bridged by Scc1 (Gruber, Haering et al. 2003). Having about 35 nm in diameter, cohesin can easily hold two chromatids. At the moment not much is known about the mechanisms of cohesin loading on the chromosomes, although recently it was shown that it needs to hydrolyze ATP to load on the DNA and it needs a chromatin remodeling factor (Arumugam, Gruber et al. 2003; Weitzer, Lehane et al. 2003). At the transition from metaphase to anaphase, release of the sister chromatids is provided by the cleavage of the Scc1 at two specific sites by an enzyme named “separase”, which thereby opens the cohesin rings and frees chromatids (Uhlmann, Lottspeich et al. 1999; Uhlmann, Wernic et al. 2000). Separase, in turn is controlled by the protein named “securin” which binds to separase and keeps it inactive until metaphase to anaphase transition, when securing is proteolysed by the Anaphase Promoting Complex (APC) (Funabiki, Yamano et al. 1996; Cohen-Fix and Koshland 1997).

Cohesin was also fond to be essential in the process of meioses. Most of organisms have developed a meioses specific cohesin complex with Rec8 protein instead of Scc1. During the Meioses I, cohesin is located all along chromosomes (Fig. 8). At the end of Meioses I, cohesins are released from the chromosomes arms to make segregation of homologues possible while remaining in the centromeric regions to keep sister chromatids until the meioses II (Klein, Mahr et al. 1999; Buonomo, Clyne et al. 2000; Pasierbek, Jantsch et al. 2001; Watanabe, Yokobayashi et al. 2001).

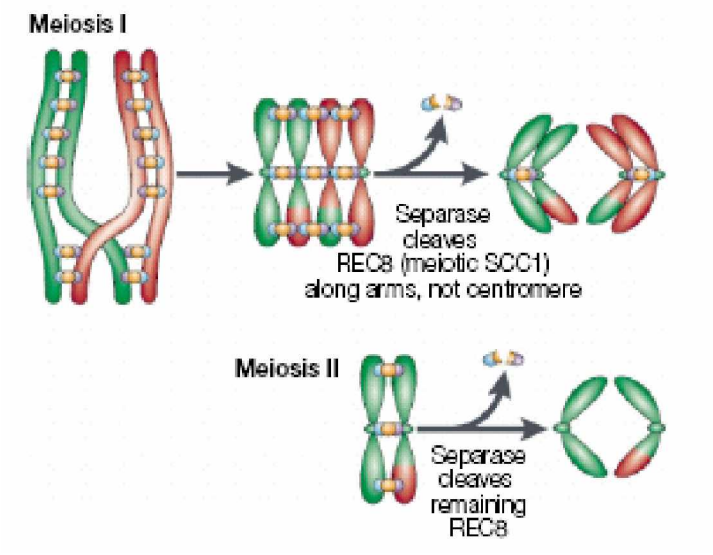

Fig. 8 Schematic representation of cohesion in the Meioses I and II, (Hagstrom and Meyer 2003).

1.3.2 Condensin complex

While cohesin is responsible for cohesion of sister chromatids, the condensin complex plays a totally different role in mitosis and is responsible for chromosome compaction and organization. Disruption of condensin in cells leads to severe defects in chromosome condensation (Hirano and Mitchison 1994; Hirano, Kobayashi et al. 1997) and segregation and is deleterios for resolving of the sister chromatids in prophase (Steffensen, Coelho et al. 2001). Found in different eukaryotic species from yeasts (Freeman, Aragon-Alcaide et al. 2000) to humans (Sutani, Yuasa et al. 1999; Kimura, Cuvier et al. 2001), condensin consists of five subunits (Fig.9): the core SMC subunits SMC2 and SMC4, two subunits which share a motif known as HEAT repeat (Neuwald and Hirano 2000), namely CAP-D2 and CAP-G and a subunit CAP-H, which belongs to the family of kleisins, together with ScpA, Scc1 and Rec8 (Schleiffer, Kaitna et al. 2003).

The mechanism of action for the condensin complex remains unclear until now. It was found that condensin is able to introduce positive supercoils into DNA in an ATP dependent manner (Kimura and Hirano 1997; Hagstrom, Holmes et al. 2002) and knots in the presence of topoisomerase II (Kimura and Hirano 2000) which can be one of the ways to condense DNA. Recent atomic force microscopy studies of *S.*

pombe condensin showed that all non-SMC subunits are bound to the head domain of SMCs (Yoshimura, Hizume et al. 2002) and a similar to cohesin model of binding to DNA via ring formation was proposed for condensin. Recently, a second condensin complex named condensin II was discovered in vertebrates, which consists of the same core SMC2 and SMC4 subunits but has different non-SMC subunits named CAP-D3, CAP-G2 and CAP-H2 (Fig. 9) (Ono, Losada et al. 2003).

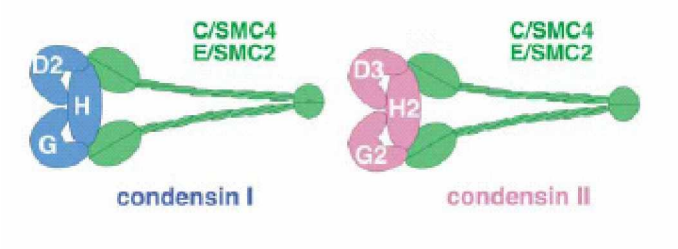

Fig. 9 Structures of condensin I and II (Ono, Losada et al. 2003)

Condensin I and II are loaded separately on the chromosomes and have a different effect on the shape of the chromosomes. Both complexes form a spiral like structures in the chromosomes and while condensin I is mainly responsible for organization of chromatin fibers, condensin II affects the final shape of the chromosomes. Both complexes are supporting function independently of each other and depletion of the complexes results in swollen chromosomes in case of condensin I depletion, or in curly chromosomes for condensin II (Ono, Losada et al. 2003).

Mitosis seems not to be the only process where condensin is involved and genetic studies of dosage compensation in *C. elegans* revealed the presence of dosage-compensation factors similar to condensin subunits (Meyer 2000). Factors mix-1 and dpy-27 were found to be homologues of SMC2 and SMC4, respectively (Chuang, Albertson et al. 1994) and DPY-26 and DPY-28 are similar to CAP-H and CAP-D2 (Lieb, Capowski et al. 1996). The dosage-compensation complex functions on the X-chromosome, where it is targeted by two proteins SDC-2 and 3, which help in finding and assembling on the X-chromosome. Possibly, the dosage compensation complex controls repression of the X chromosome via compaction of the chromosomes and therefore by gene silencing, although the mechanisms of its action remain unclear (Martinez-Balbas, Dey et al. 1995).

1.3.3 SMC5/SMC6 complex

One of the multiple functions performed by SMC protein family is DNA repair. The eukaryotic SMC5/SMC6 complex was recently reported to be involved in recombination and DNA repair, and is present in *S. cerevisiae* (Fujioka, Kimata et al. 2002), *S. pombe* (Fousteri and Lehmann 2000) as well as in mammalian cells (Lehmann, Walicka et al. 1995). SMC5/SMC6 also forms a complex with other non-SMC subunits including protein Nse1 and was identified as a complex involved in a postreplicative pathway of DNA repair. It is mainly responsible for repair of radiation DNA (Lehmann, Walicka et al. 1995), although it is also reported to be involved into the cell cycle arrest caused by DNA breaks (Verkade, Bugg et al. 1999) and somehow also in chromatin organization (Lehmann, Walicka et al. 1995; Fousteri and Lehmann 2000). However, at the moment it is not clear how the SMC5/SMC6 complex performs its function.

1.4 Rad50

Rad50 is a protein conserved throughout eukaryotes and archae bacteria, and was found to play a very important role in DNA double strand brake (DSB) repair (Sharples and Leach 1995; Hopfner, Karcher et al. 2000), cell cycle checkpoint activation in response to a DSB, DNA end processing and maintenance of telomere length (Luo, Yao et al. 1999; Zhu, Kuster et al. 2000). Sequence analyses of Rad50 has shown that it is related to the SMC family of proteins, consisting of the domains typical for this family, although Rad50 lacks a hinge domain. However, different from SMC proteins, Rad50 contains a conserved CXXC motif that is involved in the formation of a so called “zinc hook”. This domain provides dimerization of Rad50 in presence of zinc ion that is coordinated by four Cys residues, two from each Rad50 molecule (Hopfner, Craig et al. 2002). *In vivo* and *in vitro* studies showed that Rad50 functions in a complex with two other proteins, with a dimer of Mre11 and with Nbs1 (Xrs2 in *S. cerevisiae)*. The Mre11 dimer was shown to interact with Rad50 close to its head domain forming one big globular head domain, which is able to bind to the

end of broken dsDNA. It is not clear how the complex manages to bring DNA ends together, but it is probably facilitated by interaction of the hinge domains of the complexes bound to opposite ends of broken DNA. After DNA ends are brought together and kept by the Rad50/Mre11/Nbs1 complex, they become available for other enzymes to provide subsequent reactions such as meiotic recombination, DNA double strand brake repair or telomere maintenance (Fig. 10). In case when repair is performed by homologues recombination with another DNA molecule, it can be also held trapped in between the coiled-coil regions of Rad50 in a manner similar to the cohesin complex (the right part of the Fig. 10).

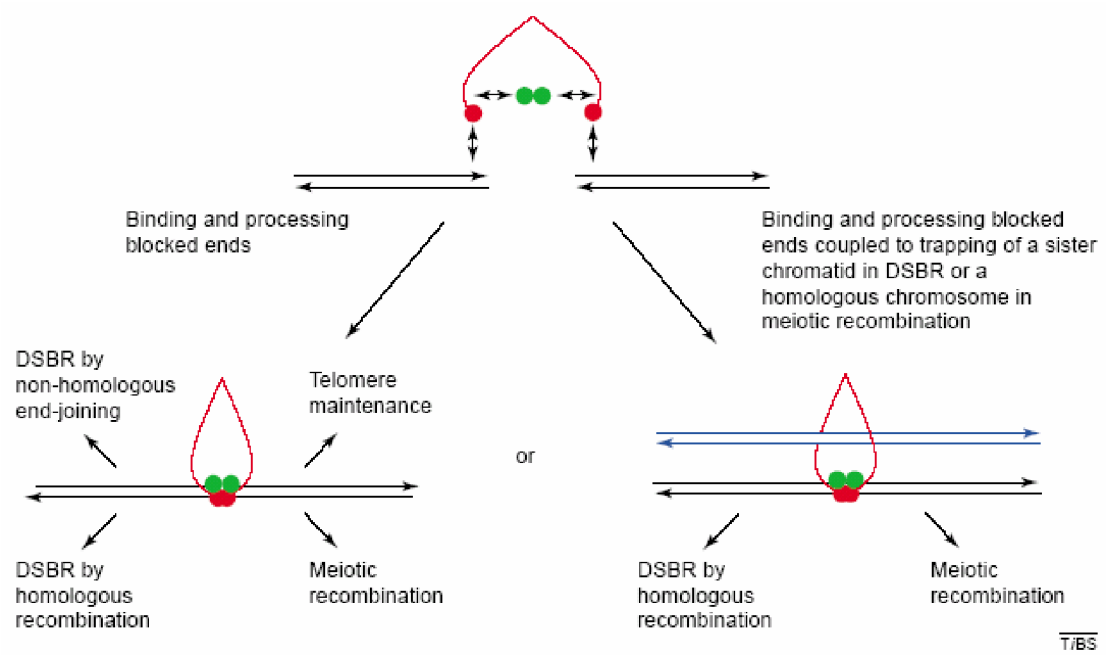

Fig. 10 Model for the action of the Rad50(red)/Mre11(green)/Nbs1 complex (Connelly and Leach 2002).

1.5 ABC-Transporters protein family

ATP-binding cassette (ABC) transporters are ubiquitous multi domain proteins, which form one of the largest protein families with members conserved across archaea, bacteria and eukaryotes (Jones and George 2004). There are at least 80 identified ABC transporters just in *E. coli*, which corresponds to approximately 5% of the genome. Similarly, in humans, ABC transporters also form one of the biggest

protein families and current data suggest that most likely they are present in all species (Higgins 1992). Although most of the enzymes from ABC-transporters family are membrane proteins and are responsible for selective transport through membrane , there are a number of cytosolic proteins containing ABC-type ATPase domains such as MutS, responsible for DNA mismatch repair (Junop, Obmolova et al. 2001), UvrA, responsible for nucleotide excision and SMC-related proteins. In spite of the fact of the difference in functions, ABC ATPase domains of all these proteins have a very high structure similarity and similar mechanism of action with the only difference that ATPase activity of SMC-proteins very low as compared to other ABC ATPases.

Most of ABC transporters share a similar structure and normally consist of two transmembrane domains and two ABC ATPase domains(Higgins 1992). Two transmembrane domains are very hydrophobic and are responsible for a formation of a channel in the membrane as well as they probably contain binding sites for substrate while nucleotide binding domains serve as ATP-dependent gate-keepers (Fig.11). Frequently, ABC transporters also contain an additional substrate binding protein on the outside of the cell membrane.

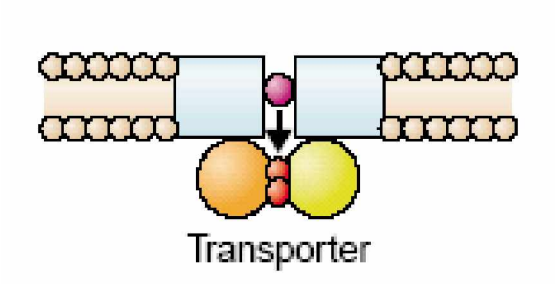

Fig.11. Architectural principle of ABC transporter. Two substrate specific transmembrane domains (blue squares) form a membrane channel and are connected via dimerization of ABC ATPase domains (yellow/orange) with two ATP molecules sandwiched in between (Hopfner and Tainer 2003).

ABC ATPase domains contain two highly conserved motifs that are responsible for nucleotide binding and hydrolysis: Walker A and Walker B motifs and a so called “signature” motif also known as C-motif, which appears to be important for a dimer formation and ATP hydrolysis. The crystal structures of ABC domains have shown that the Walker A motif (G-X-X-G-X-G-K-S/T) main function is nucleotide binding while Walker B (Φ-Φ-Φ-Φ-D, where Φ is a hydrophobic residue) is mainly responsible for stabilization and maintaining of the geometry of the nucleotide binding site (Schmitt and Tampe 2002). The C-motif consists of the sequence

LSGGQ and is distantly separated from the ATP binding pocket formed by Walker A and Walker B motifs (Hung, Wang et al. 1998). This problem of the distance is resolved by dimerization of ABC domains so that signature motif from one domain comes together with the ATP-binding pocket from the second domain and vice versa. It was shown that the signature motif is highly important for the function of ATPase, and lack of it abolishes ATPase activity in ABC transporters. Comparison of crystal structures of ABC ATPases in presence or absence of ATP has shown that the signature motif binds to the γ-phosphate of ATP and this binding results in structural rearrangement of the enzyme via reorientation of α-helices. These ATP-driven conformational changes seem to be the main mechanism of function for all proteins from family of ABC-transporters (Fig. 12).

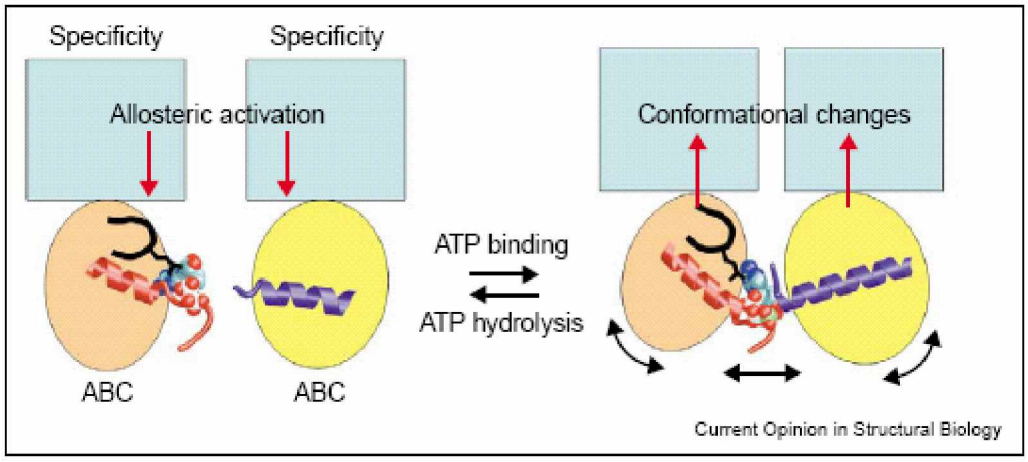

Fig. 12 Mechanism for ABC switching. Binding of ATP to ABC domains induces their dimerization and rearrangement of α-helices. This rearrangement presumably causes conformational changes in substrate-specific domains (shown in blue) to complete enzymatic cycle (Hopfner and Tainer 2003).

1.6 Aim of the work

At the onset of this work, the function and mechanisms underlying properties of SMC proteins were poorly understood. This work aimed to investigate and characterize the *in vitro* properties of *B. subtilis* SMC protein using different biochemical approaches. A further goal of the work was to study function of the

novel recently discovered proteins ScpA and ScpB, which were proposed to form a complex with SMC.

Material and methods

2.1 Materials

2.1.1 Equipment used in this study

Table 1

Equipment	Manufacturer
Automated DNA sequence analyser	ABI PRISM 301 Genetic analyzer, Perkin Elmer
Western blotting chamber	Semi dry blotting chamber Trans-Blot SD, Sigma-Aldrich
Centrifuges	Heraeus Microfuge pico, Eppendorf 5415 D
Digital pH meter	CG8400 Schott
Documentation of agarose gel	Videocamera Cybertech CS1
DNA thermocycler	Eppendorf Mastercycler personal
Digital camera for microscope	MircoMax CCD
Fluorescence microscope	AX70, Olympus
Electroporation system	Biorad Gene pulser II
French Press	
Gel electrophoresis apparatus	Philipps-Universität Marburg workshop
ÄKTA™FPLC™	Amersham Pharmacia
ÄKTA™prime	Amersham Pharmacia
Photometer	Pharmacia Ultraspec 3000 UV/Visibile spectrophotometer
UV transilluminator	
Water bath shaker	C76, New Brunswick scientific
Speed-Vac	Uniequip Univapo 150H

2.1.2 Materials and reagents:

Most of the chemicals were of analytical grade and were purchased from Fluka (Deisenhofen), Gibco BRL (Karlsruhe), Merck (Darmstadt), Roth (Karlsruhe), Serva (Heidelberg), and Sigma (München).

Table 2

Materials	manufacturer
Sterile filters - 0.45 µm and 0.2 µm	Roth(Karlsruhe)
Electroporation cuvettes	Eurogenetic (Belgium)
Spectrophotometer cuvettes	Roth(Karlsruhe)
Quartz cuvettes	Hellma
<u>For western blotting</u>:	
Whatman 3MM filter paper	Schleicher and Schüll (Dassel)
Nitrocellulose membrane type BA85	Schleicher and Schüll (Dassel)
Conjugatd secondary antibody	Amersham life sciences
X-ray film Biomax MR	Kodak (Rochester, USA)
ABI Prism dRhodamine terminator cycle sequencing ready reaction kit	ABI (Foster City, USA)
Strep-Tactin Sepharose column	IBA (Göttingen)
<u>Enzymes for molecular biology</u>:	
Restriction endonucleases, DNA modifying enzymes, DNA and protein markers	New England Biolabs (Schwalbach)
Expand Long template PCR system	Boehringer (Mannheim)
Turbo *pfu*	
<u>Columns for FPLC</u>:	
Superdex 200 10/300 GL	Amersham Pharmacia Biotech
Superdex 200 26/60	Amersham Pharmacia Biotech
HiTrap™ Desalting columns	
<u>Vital stains for microscopy</u>:	
DAPI, FM646, Syto59	Molecular Probes TM

Computer software:	Chromas 1.45, DNAstar 5.0, Clone manager, Metamorph 4.6 (Universal Imaging), UNICORN™ Control System

Only deionised and/or distilled water was used for the preparation of buffer solutions and growth media, and was sterilized prior to use in all the enzymatic reactions.

2.1.3 Kits

Table 3

Kit designation (manufacturer)	**a) Usage description**
QIAquick PCR purification kit (Qiagen)	Purification of DNA fragments from PCR reactions
QIAquick gel extraction kit (Qiagen)	Purification of DNA fragments from agarose gels
Nucleospin Extract (Macheary Nagel AG)	Plasmid extraction
DyeExSpin kit (Qiagen)	Purification of sequencing reaction
Silver Staining Kit (Amersham Pharmacia Biotech)	Visualization of proteins on the gel
Protein Standarts Kit for gel filtration (Bio-Rad)	Calibration of gel filtration columns
Protino 2000	Purification of His-tagged proteins
Sequenase Version 2.0 DNA Sequencing Kit (USB)	Manual sequencing reactions

2.1.4 Antibodies

Table 4

Primary antibodies	**Proteins purified, Antibody Source**
Rabbit anti SMC	A. Strunnikov
Rabbit anti ScpB	A. Volkov, Eurogenetics
Secondary antibodies	
goat-anti-Rabbit-IgG, peroxidase-conjugated	Sigma
goat-anti-mouse-IgG, peroxidase-conjugated	Sigma

2.1.5 Oligonucleotides

Synthetic oligonucleotides for PCR were supplied by MWG-Biotech AG and Qiagen- Operon. The annealing temperature was calculated using an empirical formula provided by MWG-Biotech AG:

$$Tm = 69.3 + 0.41 \cdot \left(\frac{100 \cdot \sum G + C}{L} \right) - \frac{650}{L}$$

with Tm = annealing temperature of the primer, L = length of the primer, and $\Sigma G+C$ = sum of G and C residues within the primer sequence. For a more convenient use, an easy look table was constructed (see table 16 in the appendix).

2.1.6 Bioinformatics tools and computer programs

All sequence comparisons, restriction analysis and *in silico* cloning procedures were performed using Clone Manager version 5.0 from Scientific and educational software, DNA sequencing data analysis was carried out using chromas 1.45 software.

Analysis of all chromatography results was done using UNICORN™ Control System software.

Surface Plasmon Resonanse experiments were analysed using BiaCore software.

Most of other bioinformatics analyses were undertaken using public internet resources:

Table 5

b) Task:	**reference:**
BLASTP protein similarity searches	http://www.ncbi.nlm.nih.gov/blast/
retrieval of *B. subtilis* genome data	http://genolist.pasteur.fr/SubtiList/ http://locus.jouy.inra.fr/cgibin/genmic/madbase/progs/madbae.operl
retrieval of *E. coli* genome data	http://genolist.pasteur.fr/Colibri/
multiple protein sequence alignments using ClustalW	http://www.ebi.ac.uk/clustalw/
collection of bioinformatic tools	http://us.expasy.org/tools/ http://www.ncbi.nlm.nih.gov/

2.1.7 Bacterial host strains

Table 6

Escherichia coli	**Genotype**	**reference**
XL1-Blue	*recA1 endA1 gyrA96 thi-1 hsdR17 supE44 relA1* lac[F' proAB lacI^{q}ZΔM15 Tn10 (Tet^{r})]	Stratagene
Top10F'	F- *mcr*A (*mrr-hsd*RMS-*mcr*BC) 80*lac*Z M15 *lac*X74 *rec*A1 *ara*D139 *gal*U *gal*K (*ara-leu*)7697 *rps*L (StrR) *end*A1 *nup*G	Invitrogen
M15	*Lac, ara, gal, mtl, recA_, uvr_,* [pREP4, *lacI, kanr*]	Qiagen
Bacillus subtilis		
PY79	prototrophic, *Bacillus subtilis* subsp. *subtilis*	P.Youngman (BGSC) (Webb, Teleman et al. 1997)

2.1.8 Plasmids used in this study

pBluescript®SKII(+) is a derivative of pUC19 [Yanish-Perron, 1985 #210] from Stratagene. It possesses a filamentous phage origin of replication. The plasmid harbours the β-lactamase gene conferring ampicillin resistance to the bacteria and thus helps in the selection of transformants. The multiple cloning cassette is inserted in frame at the 5' of β-galactosidase which is under the control of IPTG inducible lac promoter. β-galactosidase hydrolyses Xgal (an analogous substrate of β-galactosidase) present in the bacterial growth medium resulting in blue coloured colonies. Insertion of a DNA fragment in the cloning cassette disrupts the β-

galactosidase gene and consequently the expression of the protein. In addition the plasmid vector has promoter sequences of RNA polymerases of T3 and T7 phages flanking the multiple cloning cassette. In this study this plasmid was used to subclone various resistance genes selectable in *Bacillus subtilis*.

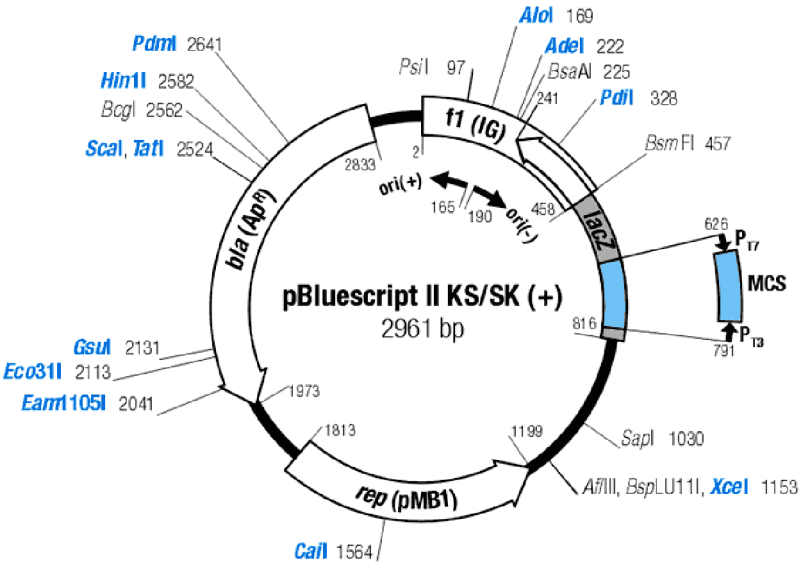

Fig. 13 pBluescript®SKII(+) map

pQE60 (Qiagen)

QIA*express* pQE vectors combine a powerful phage T5 promoter (recognized by *E. coli* RNA polymerase) with a double *lac* operator repression module to provide tightly regulated, high-level expression of recombinant proteins in *E. coli*. Protein synthesis is effectively blocked in the presence of high levels of *lac* repressor and the stability of cytotoxic constructs is enhanced. The pQE vectors (see Fig.) enable placement of the 6xHis tag at either the N- or C-terminus of the recombinant protein. pQE60 plasmid that as used in most of the constructs in this work provides a C-terminal 6xHis tag.

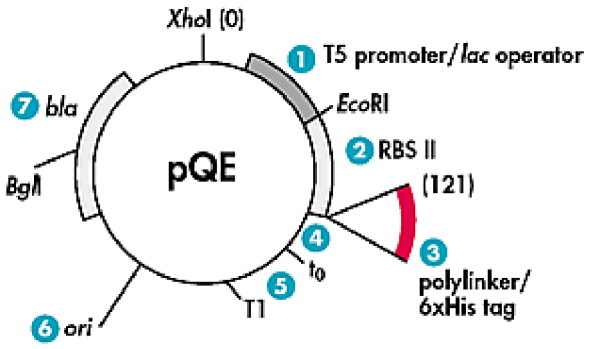

Fig. 14 pQE vectors. (1) Optimized promoter/operator element, (2) Synthetic ribosomal binding site RBSII, (3) 6xHis-tag coding sequence, (4) Translational stop codons, (5) Two strong transcriptional terminators, (6) ColE1 origin of replication, (7) beta-lactamase gene (*bla*)

pET101 (Invitrogen)

The Champion™ pET Expression System is based on expression vectors originally developed by Studier and colleagues, and takes advantage of the high activity and specificity of the bacteriophage T7 RNA polymerase to allow regulated expression of heterologous genes in *E. coli* from the T7 promoter (Rosenberg *et al.*, 1987; Studier and Moffatt, 1986; Studier *et al.*, 1990). The Champion™ pET Expression System uses elements from bacteriophage T7 to control expression of heterologous genes in *E. coli*. In the pET TOPO® vectors, expression of the gene of interest is controlled by a strong bacteriophage T7 promoter that has been modified to contain a *lac* operator sequence (see below). Inbacteriophage T7, the T7 promoter drives expression of gene 10 (φ10). T7 RNA polymerase specifically recognizes this promoter. To express the gene of interest, it is necessary to deliver T7 RNA polymerase to the cells by inducing expression of the polymerase or infecting the cell with phage expressing the polymerase. In the Champion™ pET Directional TOPO® Expression System, T7 RNA polymerase is supplied by the BL21 Star™(DE3) host *E. coli* strain in a regulated manner (see below). When sufficient T7 RNA polymerase is produced, it binds to the T7 promoter and transcribes the gene of interest.

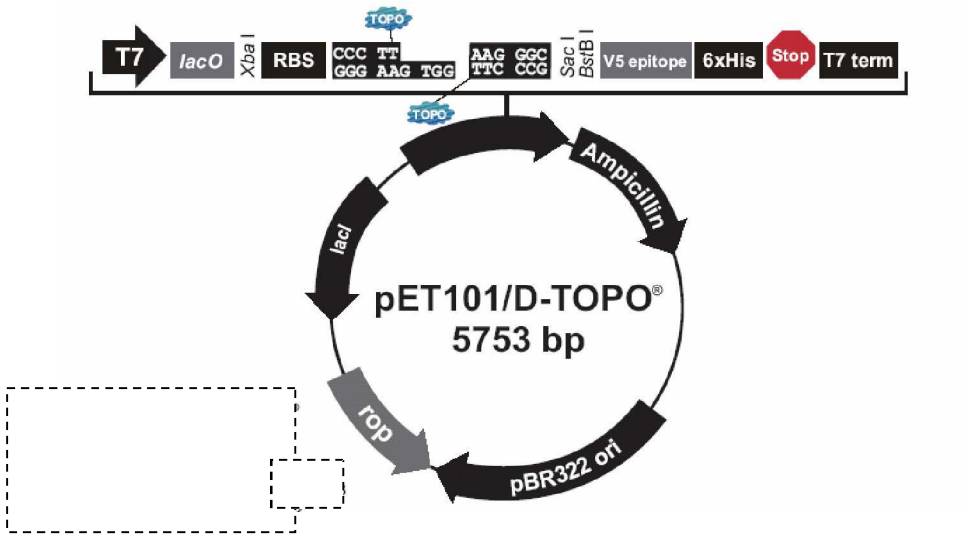

Fig 15. Map of the pET101 plasmid (Invitrogen)

List of plasmids and strains constructed and used in this work are listed in tables 13 and 14 in appendix (5.2 and 5.2.1)

2.2 Molecular biology methods

Growth Medium

LB / LB agar medium, (Sambrook et al., 1989):

Bactotryptone	10g
Yeast extract	10g
NaCl	5g
dH_2O to 1L	

Ingredients were dissolved in water, the resulting solution adjusted to pH 7.4 using 1M NaOH and sterilized by autoclaving at 121°C, 1.5bar for 30min. LB agar, 1.5% agar was added to LB medium before autoclaving. After autoclaving, the medium was cooled down to approx. 50°C and the antibiotics (Table 9) were added, swirled to mix and poured into Petri dishes.

Antibiotic Solutions

Table 9

c) Antibiotics	**stock solution**	**working solution**
Ampicillin	50 mg/ml in H_2O	50µg/ml (*E. coli*)
Kanamycin	10 mg/ml in H_2O	50µg/ml (*E. coli*)
Kanamycin	10mg/ml in H_2O	10µg/ml (*B. subtilis*)
Chloramphenicol	25 mg/ml in EtOH	7.5µg/ml (*B. subtilis*)
Spectinomycin	25mg/ml in 50%EtOH	25µg/ml (*B. subtilis*)
Tetracycline	20mg/ml in 50%EtOH	20µg/ml (*B. subtilis*)
		..... continued
Erythromycin [1]	4 mg/ml in EtOH	1 µg/ml (*B. subtilis*)
Lincomycin [1]	25 mg/ml in 50% EtOH	25 µg/ml (*B. subtilis*)

[1]MLS - collective term addressing the macrolide lincosamine streptogramidine B antibiotic family which is applied as a combination of lincomycin and erythromycin

All stock solutions listed above were sterile filtered and the antibiotic stocks were stored at -20°C.

2.2.1 Agarose gel electrophoresis of DNA

DNA molecules can be separated according to their sizes by electrophoretic migration. Depending on the sizes of the DNA fragments to be resolved, for preparation of agarose gels 0.8-2 % (w/v) agarose was suspended in TB buffer, 0.5 µg/ml of ethidium bromide were added and the mixture was heated until the agarose had completed dissolved. After cooling to approx. 50°C, the gel was poured, cooled to room temperature and supplemented with TB buffer. DNA samples suspended in DNA loading buffer and electrophoresis was carried out at 50-75 mA. After the run, DNA was visualized by ultraviolet (UV) irradiation.

DNA loading buffer:	50% (v/v) glycerol
	0.1 M EDTA
	0.1% (w/v) SDS
	0.05% (w/v) bromo-phenol blue
	0.05% (w/v) xylene cyanol FF
TB buffer:	90 mM Tris-HCl pH 8.0
	90 mM boric acid

2.2.2 Digestion of DNA by restriction enzymes

The digestion of plasmids/DNA by restriction enzymes was carried out according to the manufacturer's instructions (NEB). Typically, a restriction digest reaction contained 1-2µg of DNA, 1/10 volume of an appropriate 10x restriction buffer, 1-2 units of the restriction enzyme. Preparative digestion was carried out in 50µl volume and qualitative digestion in 10µl final volume. The reactions were carried out by incubation for 2h at 37°C and analysed by agarose gel electrophoresis.

For preparative digestions, the DNA fragment of interest was excised from the gel and purified through QIAquick gel extraction kit following the manufactures protocol.

2.2.3 Ligation of vector and insert DNA

Vector and insert DNA were digested with appropriate restriction enzymes to generate compatible ends for cloning. A typical ligation reaction was carried out in a total volume of 10 µl containing vector and insert DNA (molar ratio vector:insert was approx. 1:5), 1/10 volume of 10x T4 ligase buffer and 3 U of T4 Ligase. The ligation reaction was carried out at room temperature or at 16°C overnight.

2.2.4 E. coli transformation

Electrocompetent bacteria were prepared by repeatedly washing bacteria harvested in the exponential growth phase (OD_{600}=0.6-0.75) with sterile ice cold water to remove salt and were then conserved at -80°C in 10% glycerol. 1 µl of a typical ligation reaction (or the whole ligation mix after dialysing against water for 15 minutes on 0.025 µm membrane) was mixed with 40 µl of electrocompetent bacterial cells and transfered into a 0.2 cm electoporation cuvette and placed into the Biorad Gene Pulser electroporator. Settings were 25 µFD capacity, 12.5 kV/cm field strength, 200 Ω resistance. The electric pulse creates transitory pores in the bacterial cell wall which allows the entry of the DNA. The transformed bacteria were diluted in 1 ml of pre-warmed LB medium and incubated at 37°C for 45 minutes. This incubation permits the bacteria to reconstitute their cell walls and start to express the antibiotic resistance gene present on the plasmid. For selection of transformants, bacteria were plated on LB-Agar plates containing the appropriate antibiotic and incubated overnight at 37°C.

2.2.5 Preparation of plasmid DNA

In order to check transformants for the presence of the expected plasmid, small scale DNA plasmid preparation (mini-prep) was carried out. Individual transformant colonies were grown under vigorous shaking by overnight incubation at 37°C in 3 ml LB medium supplemented with appropriate antibiotics. Cells were harvested by centrifugation and the cell pellet was resuspended in 300 µl of solution I and then lysed by alkali treatment in 300 µl of solution II, which also denatures the chromosomal DNA and proteins. The lysate was neutralized with 300 µl of solution III and plasmid DNA was then precipitated by adding 600 µl of isopropanol. The precipitated pellet was washed with 70% ethanol, dried and resuspended in 40 µl of dH_2O.

solution I :	25 mM Tris/HCl pH 8.0
	10 mM EDTA pH 8.0
solution II :	0.2 N NaOH
	1% w/v SDS
solution III :	60 ml of 5 M potassium acetate
	11.5 ml glacial acetic acid
	28.5 ml $d.H_2O$

For large scale isolation of plasmids (midi-prep) the cultures were grown in 50 ml and treated similarly as above with volumes of solution I, II, and III adjusted to 5 ml each.

2.2.6 Polymerase chain reaction - PCR

PCR allows for the exponential amplification of DNA by utilizing repeated cycles of denaturation, annealing and elongation. The reaction essentially requires a thermostable DNA polymerase, primers, dNTPs, and a DNA template. A typical 50 µl PCR reaction mix contained:

5 µl of 10x DNA polymerase buffer

20 pmol of each primer

200 µM of dNTPs

10-100 ng (approx. 1 µl) of template DNA (1:100 from chromosomal DNA and 1:1000 from plasmid from standard preparations)

1-2 U (1 µl) of DNA polymerase preparation (Turbo pfu or pol mix-Expand Long template PCR system polymerase)

The reaction was carried out in a PCR thermocycler, using the following program cycles:

A typical PCR reaction programm is listed below:

	Temperature	Time (min)	Cycles
Initial denaturation:	95°C	2 :00	
Denaturation:	95°C	0 :30	10
Primer annealing:	T_m - 2°C	0 :30	
Extension :	72°C (for pfu)	1:00 / kb	
	68°C (for pol mix)	1:20 / kb	
Exponential amplification:	95°C	0 :30	25
	T_m+ 5°C	0 :30	
	72°C / 68°C	1:00 / kb	
Final extension :	72°C / 68°C	4:00	
	4°C		

The resulting PCR products were analyzed on an agarose gel. For cloning purposes the PCR product was purified over the column using the QIAquick PCR purification kit before subjecting to endonuclease digestion.

2.2.7 DNA sequencing

In order to verify clones for the presence of any point mutations, appropriate DNA preparations were sequenced utilizing a fluorescent dye technique. Clean plamids were prepared using the Nucleospin plasmid prep kit or QIA plasmid prep kit. The purity and concentrations were analyzed spectroscopically using DNS method mode. For a sequencing PCR reaction, plasmid concentrations of 100 ng/kb were used in a reaction mix of 10 µl which contained 1 µl of 10 pmol primer and 3 µl of termination mix (dNTP's, ddNTP's, buffer, Ampilitaq DNA polymerase FS). A standardized PCR reaction programm was used with an initial denaturation at 95°C for 60 sec, 30 cycles of denaturation at 95°C for 10 sec, primer annealing at T_m-2°C for 5 sec, extension at 60°C for 4 minutes, and terminated with 60°C for 5 min to facilitate the completion of extension reaction. After PCR completion, the products were purified either using a column from the Dye Ex kit (Qiagen) or were precipitated with 1µl 3M sodium acetate and 25µl absolute ethanol, the pellet was washed with 70% ethanol dried and resuspended in 40 µl HPLC-grade H_2O the sample was denatured at 95°C for 2 min. before subjecting to analysis by the ABI 310 sequence analyser.

Mannual sequencing reactions for primer extension studies were carried out using the 'Sequenase Version 2.0 DNA Sequencing Kit' from USB.

2.2.9 Site-directed mutagenesis

In vitro site-directed mutagenesis is a valuable technique for studying protein structure-function relationships. This procedure utilizes a vector carrying the gene to be modified and two complementary primers carrying the desired point mutation.

These two complementary primers were designed such that the mutation region is located at the center:

(15-18 bp)-(mutation region)-(15-18 bp)

The primers each complementary to opposite strands of the vector, are extended in the PCR reaction with a *turbo pfu* polymerase. The PCR reaction was carried out in a reaction volume of 50 µl containing 1 µl of the plasmid (from standard plasmid prep).

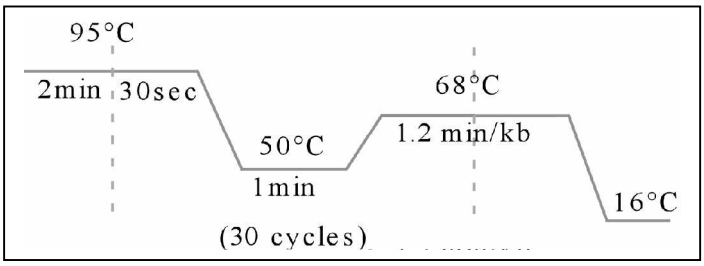

The PCR reaction allows for the incorporation of the primers which results in a mutated plasmid with staggered nicks. In order to get rid of the parental vector the reaction was digested with *Dpn*I for 2-3 hours. *Dpn*I endonuclease is specific for methylated and hemimethylated DNA which is the case only for the parental vectors. The product was then purified through the column and used for transformation in *E. coli*. The presence of mutations was confirmed by sequencing the plasmids after their isolation from the transformants.

2.4 Techniques related to protein

2.4.1 Small scale preparation of protein extracts

For the preparation of protein extracts from cell lysates, cell density was monitored spectroscopically at 600 nm (OD_{600nm}), culture volumes corresponding to OD_{600nm} values of 0.5 or 5 were harvested, and cells were isolated by centrifuging at 4°C. This procedure ensured that comparable amounts of cells were withdrawn for protein extract preparation even when cells of different growth stages had to be

compared. The isolated cell pellets were lysed either by sonicating or by lysozyme treatment as follows.

For sonication, cells were resuspended in 400 µl of ice cold water supplemented with 1 mM of EDTA and PMSF as protease inhibitors. Cells were repeatedly (6 times) sonicated for 30 sec on ice using a sonicator. Between each repetition cycle, a 1 min pause was applied. The sonifier was set to deliver 80 % power, with a 25 % cycle. For cell lysis by lysozyme treatment, the cell pellet was resuspended in a lysis buffer (50 mM EDTA, 0.1 M NaCl, pH 7.5) containing 50 µg/ml of lysozyme and incubated for 10-15 min at 37°C until the dense solution started clearing.

Independent of the lysis method applied, the cell lysates were centrifuged to remove the cell debris. An aliquot of each lysate was stored at -20°C for future purpose and 100 µl of the lysates were boiled with the denaturing protein loading buffer and equal volumes of these samples were loaded on a SDS gel for inspection of whether the protein contents were of comparable concentration.

2.4.2 Separation of proteins by SDS-polyacrylamide gel electrophoresis

The protein sample to be resolved was denatured by heating at 95°C for 2 min in the presence of SDS and β -mercaptoethanol (see protein loading buffer composition below). While β-mercaptoethanol reduces disulfide bonds, SDS denatures and anneals to the amino acid chains of the proteins giving each protein a negative net charge that is proportional to the polypeptide chain length. As a consequence, the proteins are separated essentially based on their molecular mass (Laemmli, 1970). The sieving effect of the gel matrix is achieved by adjusting an appropriate ratio of acrylamide to N,N' methylene bisacrylamide (37.5/1). The polymerization of acrylamide is catalyzed by 0.1% APS (w/v) and 0.05% TEMED. The migration of the proteins was carried out in running buffer under a constant current of 25 mA for 2 h.

Table 10: Composition of gel for SDS-PAGE

compounds	**separating gel (10ml)**		**stacking gel (5ml)**
	10%	7.5%	4%
acrylamide/bisacrylamide	3.33 ml	2.5 ml	0.66 ml
separating buffer (1.5 M Tris/HCl, pH 8.8)	2.5 ml	2.5 ml	-
Stacking buffer (0.5 M Tris/HCl, pH 6.8)	-	-	1.2 ml
distilled water	4.0 ml	4.8 ml	3.01 ml
1% SDS	100 µl	100 µl	50 µl
10% ammonium persulfate	50 µl	50 µl	25 µl
TEMED	5 µl	5 µl	5 µl

*The volume corresponds to 2 gels, each of size: 8 cm x 10 cm x 0.1 cm

Loading buffer:
100 mM Tris/HCl, pH 6.8
10 % (v/v) glycerol
2 % (w/v) SDS
3 % (v/v) β-mercaptoethanol
0.1 % (w/v) bromophenol blue

Running buffer (Laemmli):
25 mM Tris/HCl, pH 8.3
250 mM Glycine
0.1% (w/v) SDS

2.4.3 Separation of proteins by Native-polyacrylamide gel electrophoresis

Protein samples before loading on the gel were mixed with loading buffer. Because of the absence of SDS and of the -mercaptoethanol in the gel and in the running buffer proteins remained their folding and protein activity wasn't lost. As a result proteins were separated according to their combination of their mass, size and charge.. The polymerization of acrylamide is catalyzed by 0.1% APS (w/v) and 0.05% TEMED. The migration of the proteins was carried out in running buffer (TBE) under a constant current of 10 mA for 2 h (per one gel).

Table 11: Composition of gel for Native-PAGE (7%)

Compounds	**Amounts**
acrylamide/bisacrylamide	2.8ml
10xTBE	1.2ml
Glycerine 50%	1.44ml
dH_2O	6.47ml
10% ammonium persulfate	80µl
TEMED	10µl

*The volume corresponds to 2 gels, each of size: 8 cm x 10 cm x 0.1 cm

Loading buffer:	Glycerin	10%(v/v)
	Bromphenolblue	0.1%(w/v)
10xTBE:	Tris	163.5 g/l
	Boric acid	29.86 g/l
	EDTA	11.3 g/l
10xBinding buffer	Tris/HCl, pH 8.6	200mM
	NaCl	500mM
	$MgCl_2$	50mM

2.4.4 Protein staining with Coomassie blue

After electrophoresis, the proteins in the gel were fixed and stained in staining solution with gentle agitation for 1-2 hours. In order to remove non-specific dye from the protein gels, the gel was destained in the destaining solution.

staining solution: 0.125% (w/v) Coomassie blue
10% (v/v) acetic acid
25% (v/v) ethanol

destaining solution: 10% (v/v) acetic acid
20% (v/v) ethanol

2.4.5 Silver staining of proteins

In case of low concentration of proteins silver staining method was used instead of Coomassie blue staining. Silver staining technique allows detection very low amounts of proteins down to nanogram range and is much more sensitive than Coomassie staining.

After electrophoresis in the gel, gel was fixed in the fixing solution for 30 min, transferred to sensitizing solution for 30 min and washed 3 times in water for 5 minutes. Next step was Silver reaction in silver solution for 20 min followed by washing in water for 1minute 2 times. Final steps were developing for 2-5 minutes, stopping developing reaction with stop solution for 10 minutes and washing off stop solution by washing gel in water 3 times for 5 minutes each.

Solution	Compounds	Amounts
Fixing solution	Ethanol	100ml
	Glacial acetic acid	25ml
	Make up to 250 ml with distilled water	
Sensitizing solution	Ethanol	75ml
	Glutardialdehyde (25% w/v)	1.25ml
	Sodium thiosulfate (5% w/v)	10ml
	Sodium acetate	17g
	Make up to 250 ml with distilled water	
Silver solution	Silver nitrate solution (2.5% w/v)	25ml
	Formaldehyte (37% w/v)	0.1ml
	Make up to 250 ml with distilled water	
Developing solution	Sodium carbonate	6.25g
	Formaldehyte (37% w/v)	0.05ml
	Make up to 250 ml with distilled water	
Stop solution	EDTA-Na_2x2H_2O	3.65g
	Make up to 250 ml with distilled water	
Washing solution	Distilled water	

2.4.6 Western blotting

For the detection of specific proteins on protein gels, a technique termed western blot was applied in which the protein bands were first transfered to a polyvinylidene floride (PVDF) 0.45 µm microporous membrane (Immobilon-P, Millipore). An air bubble-free sandwich was formed from Whatman 3MM filter papers embedding the membrane and the gel. All components were presoaked in transfer buffer and the electro transfer was carried out in a semi dry transfer system (Sigma-Aldrich) for 90 minutes under a constant current calculated by the area of the gel (in cm) multiplied by 0.8 mA. After transfer, the proteins were visualised by staining the membrane with amido black solution for 1-2 minutes and destaining with dH_2O.

transfer buffer: 48 mM Tris base
39mM glycine
1.3mM SDS
20% methanol, pH 9.2

amido black solution:	0.1% amido black 25% isopropanol 10% acetic acid

2.4.6.1 Immunodetection

After transferring the proteins to a PVDF membrane, the non-specific sites were blocked by incubating the membrane in blocking buffer for 30 min at room temperature. The membrane was then incubated in blocking buffer with a defined dilution of the primary antibodies (see below) overnight at 4°C or for 1 hour at 37°C. The membrane was washed to eliminate the unbound antibodies, once for 10 minutes and twice for 5 minutes with PBS-T at room temperature. The membrane was then incubated in blocking buffer with the secondary antibody coupled to horse-radish peroxidase (1:10000 dilution of anti-rabbit or 1:5000 anti-mouse) for 1 hour at 37°C. The membrane was washed again as described earlier to eliminate the unbound secondary antibodies. The proteins recognized by the primary antibodies were detected using ECL (enhanced chemiluminescence).

PBS-T:	80 mM Na_2HPO_4 20 mM NaH_2PO_4 100 mM NaCl, pH 7.5 0.2% (v/v) Tween-20
primary antibody dilution:	
Rabbit anti SMC	1:1000
Rabbit anti ScpB	1:1000
Rabbit anti GFP	1:1000
Mouse anti His	1:1000
secondary antibody dilution:	
goat-anti-Rabbit-IgG, peroxidase-conjugated	1:10000
goat-anti-mouse-IgG, peroxidase-conjugated	1:5000

2.4.6.2 Chemiluminescence-detection of proteins on nitrocellulose membrane

Immunolabeling was visualized by adding the luminol and H_2O_2 to the peroxidase-conjugated antibodies. The reaction was carried out in the dark by mixing two solutions:

solution1: 100 µl of 250 mM Luminol
44 µl of 90 mM caumaric acid
1 ml of 1M Tris-HCl pH 8.5
add H_2O to give 10 ml

solution 2: 6 µl of 30% H_2O_2
1 ml of 1M Tris- HCl pH 8.5
add H_2O to give 10 ml

The membrane was soaked for 1 minute in solution mix and luminescence was recorded by exposing the blots to an X-ray film for 5-30 min.

2.4.7 Large scale purification of proteins

2.4.7.1 Large scale expression of proteins and preparation of protein extracts

For expression of proteins cells were inoculated into 300ml of LB media with antibiotics and grown at 37°C, 250rpm. Growth of cells was monitored until OD_{600nm} was 0.5. Expression of protein was induced by addition of IPTG to final concentration of 1mM. After induction cells were grown for 2 hours at 37°C or for 5 hours at 30°C, depending on protein. Cells were harvested, spinned at 5000rpm for 15 minutes and resuspended in 10 ml of HepesA buffer. Three cycles of lyses on French

press were used to break open *E. coli* cells and 5 or more cycles to break *B. subtilis* cells open at pressure of 1100 psi. Cells lysate was spun at 17000rpm for half an hour and supernatant was collected and kept on ice before loading onto a column for purification.

2.4.7.2 Affinity purification of His-tagged proteins

Prior to purification column was packed with Ni-NTA matrix according to manufacturers recommendations. 1ml of matrix was normally used for purification of protein from 300 ml culture. After equilibration of column with 5 column volumes of buffer HepesA cell extract was loaded onto column at flow rate of 0.8 ml/min. All unbound proteins were washed from the column with 8 column volumes of HepesA buffer. For elution of His-tagged protein off the column 0 to 250mM gradient of imidazol was applied and eluate was fractionated and fractions were analysed on the SDS-PAGE. For polishing and dialyses against HepesA buffer protein containing fractions were applied to the gel filtration column or onto desalting column depending on the required purity of protein. After gel filtration protein was stored at +4°C until further experiments.

HepesA buffer	Hepes 50mM
	NaCl 300mM
	pH 8.0 was adjusted with NaOH
HepesB buffer	Hepes 50mM
	NaCl 300mM
	Imidazol 250mM
	pH 8.0 was adjusted with NaOH

*2.4.7.3 **Purification of** Thermatoga maritima **proteins***

All *Thermatoga maritima* were expressed in the *E.coli* cells. After the lyses of the cells, crude protein extract was fractionated transferred into 2 ml Eppendorf tubes. To precipitate *E. coli* proteins, protein extract was transferred to a water bath and incubated there for 30 minutes at 80° C. After incubation samples were cooled on ice for 5 minutes and all denatured *E. coli* proteins were precipitated by centrifugation for 20 minutes at 13000 rpm. Supernatant was collected and kept at +4° C until further experiments. Due to high thermostability of *Thermatoga maritima* proteins, they remain stable and soluble after the heat denaturation of *E. coli* proteins and supernatant contains protein of interest that is normally clean enough for further experiments, although in some cases an additional step using gel filtration or ion exchange column is needed.

2.4.8 Surface plasmon experiments

Interactions were analyzed by surface plasmon resonance with a Biacore X instrument. Proteins were dialyzed in HEPES buffer. CM5 chips were derivatized with proteins by amine coupling according to the manufacturer's recommendations, and SA chips were used for biotin coupling. The signal in the reference cell was subtracted online during all measurements. The soluble binding partner (analyte) was injected at a range of concentrations at a flow rate of 10µl/min. For the removal of unbound analyte, 50 mM NaOH was used; for the complete removal of DNA from SA chips, 250 mM NaOH was used. All measurements were done at room temperature.

2.4.9 Sucrose gradient centrifugation

For gradient centrifugation, 5 to 20% sucrose gradients were spun at 165,000 x *g* for 15 h at 4° C. 1 ml fractions were withdrawn and subjected to SDS-PAGE analysis. Standard proteins used were thyroglobulin (670 kDa), γ-globulin (158 kDa),

bovine serum albumin (66 kDa), ovalbumin (44 kDa), chymotrypsinogen (25 kDa), myoglobin (17 kDa), cytochrome C (14 kDa), and aprotinin (6.5 kDa).

2.4.10 Gel filtration assay

Gel filtration was performed on Superdex 200 10/300GL or on Superdex 200 26/60 column from Amersham-Pharmacia Biotech. Proteins were mixed so that final volume was 500 µl or 2 ml depending on the column and were incubated for 30 min before applying to the column. Proteins were loaded and run on the column at 0.8 ml per minute and fractionated into 1 ml fractions. Peak fractions were analyzed on the SDS-PAGE.

2.4.11 Sample preparation for ESI-TOF experiments

After purification proteins were concentrated on the spin-columns until minimum concentration of 3 µg/µl and dialyzed against 10mM ammonium acetate buffer at pH 8.0.

2.4.12 Sample preparation for atomic force microscopy

Prior to application of the sample to a mica SMC protein was diluted in distilled water for a dry AFM or in HepesA buffer for an AFM in a liquid media, to a final concentration of 0.2 ng/µl.

2.5 Bacillus genetics

2.5.1 Preparation of chromosomal DNA from Bacillus subtilis cells

The cells of a 2 ml overnight culture was harvested and resuspended in 0.5 ml of lysis buffer (50 mM EDTA, 0.1 M NaCl, pH 7.5) and incubated with 1mg/ml lysozyme for cell lysis. The lysate was then extracted once with phenol and then with phenol:chloroform (1:1). Chromosomal DNA was precipitated by adding 40 µl of 3 M sodium acetate and ethanol. The precipitated DNA was spooled with a pasteur pipette, and washed by dipping in 70% EtOH, it was then air dried before dissolving it in TE buffer, pH 8.

2.5.2 Preparation of competent Bacillus subtilis cells

B. subtilis develops a competent state at the onset of stationary growth phase during which exogenous DNA is trapped and processed to yield single-stranded DNA in cytoplasm. Through recombinational and replicational processes such DNA is either established as a plasmid or integrated into the genome where homologous sequences are present (Dubnau 1991). Preparation of competent *B. subtilis* cells is based on a modified two step procedure from Dubnau and Davidoffabelson (1971) and requires cells growing in SpC medium until the cells enter the stationary growth phase where they become naturally competent.

Overnight cultures were used to inoculate in 20 ml of freshly prepared SpC medium. Growth was maintained until the cells reached the stationary phase. When the OD_{600} remained unchanged for 20-30 min, the culture was diluted 1:10 into pre-warmed SpII medium and allowed to grow for 90 min. The cells were then pelleted by centrifugation at RT and resuspended in a mixture of 20 ml of supernatent containing 10% glycerol and aliquoted for storage at -80°C.

T-Base :	per litre	
	2 g	$(NH_4)_2SO_4$
	18.3 g	$K_2HPO_4 \cdot 3H_2O$
	6 g	KH_2PO_4
	1 g	trisodium citrate$\cdot 2H_2O$

Sterilized by autoclaving at 121°C at 1.5 bar for 30 min.

SpC Medium:

T-Base	20 ml
50 % (w/v) glucose	0.2 ml
1.2 % (w/v) $MgSO_4 \cdot 7H_2O$	0.3 ml
1 % (w/v) casamino acids	0.5 ml
10 % (w/v) bacto yeast extract	0.4 ml

SpII medium:

T-Base	200 ml
50 % (w/v) glucose	2 ml
1.2 % (w/v) $MgSO_4 \cdot 7H_2O$	14 ml
1 % (w/v) casamino acids	2 ml
10 % (w/v) bacto yeast extract	2 ml
0.1 M $CaCl_2$	1 ml

SpC and SpII media were prepared fresh from the sterile stock solutions and sterile filtered.

2.5.3 Transformation in Bacillus subtilis

100-200 µl of competent *Bacillus subtilis* cells were used for each transformation. Two different dilutions of the plasmid DNA (5 µl and 15 µl from normal plasmid mini-prep) or the chromosomal DNA (0.05 µl and 0.5 µl) were mixed with the competent cells in a culture tube and incubated at 37°C for 20-30 min in a roller drum. The cells were then plated on selective plates and incubated overnight. In case of temperature sensitive mutants the transformation was carried out at room temperature or 25°C for 30-40 min incubation.

2.6 Microscopic techniques

2.6.1 Fluorescence microscopy – Principles

Flourescence microscopy is an useful tool to examine the location or concentration of molecules *in vivo* and can be performed with high sensitivity and specificity. The ability to view activities of proteins within a single living cell began with the discovery of a green fluorescent protein (GFP) from the jellyfish *Aequoria victoria*. The elaborate use of this protein has allowed for sophisticated insight into the microscopic cell world (Gordon *et al*., 1997; Lemon and Grossman, 2000; Margolin, 2000; Phillips, 2001; Li *et al*., 2002; Southward and Surette, 2002).Due to which GFP has been subjected to exhaustive mutagenesis to improve the brightness and alter the spectral properties of fluorescence to allow simulatneous labelling of different proteins in the cell. Various GFP varients and its spectral details are presented in table below:

GFP varients	exitation /emission (nm)	a.a substitutions in GFP
GFPmut1	488/507	2
BFP	380/440	4
YFP	513/527	4
CFP	433/ 475(major) 453/ 501(minor)	6

Fluorescent microscopes are based on the principle of fluorescence which uses high-energy, short-wavelength light to excite electrons within certain molecules inside a specimen, causing these electrons to shift to an energetically elevated state. When they fall back to their original energy levels, they emit lower-energy, longer-wavelength light in the visible spectrum. The fluorescent microscope possesses a light source that emits a broad spectrum of light. A filter is used to allow only certain wavelengths of light to pass into the microscope. The light of these wavelengths is focused on the specimen to be studied through a lens. When the proper wavelength of light hits the specimen, the fluorescent protein (e.g. GFP) that might be attached to a cells natural protein begins to glow, making the protein glow as well. The hereby emitted light goes back through the lens, which also contains an emission filter that enables the appropriate image to be seen through the microscope's eyepiece or by a camera that create a digital image on a computer screen. A dichroic beam splitter attached to the microscope allows to select the proper wavelength to pass through. The emitted light is always produced at a longer wavelength than that originally absorbed (the stokes shift). This shift is crutial for the detection of fluorescence as it differentiates the excitation and the emission wavelengths (Emptage 2001).

The interactions of proteins can be visualized *in vivo* using fluorescence resonance energy transfer (FRET) technique. FRET is a distance-dependent effect between two interacting molecules (e.g. FP-tagged proteins) in which the excitation energy of one molecule (the donor) can be transferred to its partner (acceptor). For FRET to occur, molecules must be at close proximity of within 100 Å and the absorbtion spectrum of the recipient molecule must overlap the emission spectrum of

the donor. The use of a pair of proteins of which one is tagged to CFP and the other tagged to YFP is ideal for FRET and allows for colocalization studies (Emptage 2001).

In this work, fluoroscence microscopy was performed on Olympus AX70 microscope. Images were acquired with a digital micromax CCD camera, signal intensities and cell length were measured using the Metamorph 4.6 programme (Universal Imaging). By default, the shape of the cell/nucleoid was examined in bright field light using nomarski differential interface contrast which resolves different refractive indices.

2.6.2 Vital stains used in fluorescence microscopy

DAPI (4',6-diamidino-2-phenylindole) is a blue fluorescent nucleic acid stain that preferentially stains double-stranded DNA (dsDNA). This stain was used to visualize the nucleoid. DAPI attaches to AT clusters in the DNA minor groove. Binding of DAPI to dsDNA produces an approximate 20-fold fluorescence enhancement, apparently caused by the displacement of water molecules from both DAPI and DNA. The excitation maximum for DAPI bound to dsDNA is 358 nm, and the emission maximum is 461 nm. DAPI was used at a final concentration of 0.2 ng/ml.

Syto59 is a cell-permeant red fluorescent nucleic acid stain that exhibits bright, red fluorescence upon binding to nucleic acids. It has the absorbtion at 622nm and emission at 645nm

FM4-64(N-(3-triethylammoniunpropyl)-4-(p-diethylaminophenylhexatrieny) pyridinium dibromide) is a lipophilic styryl dye, with red fluorescence (excitation/emission spectra approx. 515/640 nm). The stain intercalates into the outer surface of the membrane but is unable to cross the lipid bilayer, therefore only the membrane surface which is directly exposed to the FM 4-64 is stained. FM4-64 was used at the final concentration of 1 nM.

2.6.3 Media used for microscopy

The cells were visualized live under the microscope after being grown in a specialized $S7_{50}$ complete medium that had low level of background fluorescence.

$S7_{50}$ complete media: The media was prepared fresh, from stock solutions (table12) and sterile filtered

Table 12

Stock solutions	Final concentration
10x $S7_{50}$ salts	1x $S7_{50}$ salts
100x metals	1x metals
50% glucose*	1 % glucose*
10 % glutamate	0.1 % glutamate
casamino acids	40 µg/ml
	dH_2O to 1 l

* glucose was substituted with fructose for cultures consisting of strains that had genes with xylose inducible promoters because presence of glucose represses xylose uptake.

10x $S7_{50}$ salts:	MOPS (free acid)	0.5 M (104.7 g)
	$(NH_4)_2SO_4$	100 mM (13.2 g)
	KH_2PO_4	50 mM (6.8 g) adjusted pH 7 with KOH dH_2O to 1 l
100x metals:	$MgCl_2$	0.2 M
	$CaCl_2$	70 mM
	$ZnCl_2$	0.1 mM
	$MnCl_2$	5 mM

2.6.4 Preparation of slides for microscopy

In order to view live cells under the microscope, the cells were spread on a glass slide coated with a thin layer of $S7_{50}$ agarose medium: About 800 µl of the $S7_{50}$ medium with 1% molten agarose was spread on a glass slide and covered with another glass slide so that a thin layer is formed between them, after the medium solidified one of the slide was carefully removed by sliding. 2-3 µl of growing cell culture were applied on the agarose coated slide and spread with a cover slip.

Results

3.1 Purification of SMC, ScpA and ScpB and of SMC domains.

B. subtilis SMC is a very large molecule with a molecular weight of 135.51 kDa. Its size and probably some other factors were the reason that SMC has not been a very easy protein for purification and not many groups in the world succeeded in its purification. The first part of this work was to find conditions for purification of active proteins in amounts sufficient for all types of further biochemical experiments. Ni-NTA chromatography was chosen as a method for purification of proteins since this method proved itself highly efficient and allows to get protein of high purity after a one step purification. It was known from the experience of different groups that attempts to get N-terminal His_6-tagged SMC were not successful, so plasmid pQE60 which provides a C-terminal His_6-tag was chosen for cloning of genes of all proteins of interest for further purification. Results of purification can be seen in Fig 16, after all steps of purification SMC, ScpA, B and hinge domain were > 95% pure with no detectable by Coomassie staining impurities, which allows us to assume that all activities detected in experiments, described in this work, belonged to the corresponding proteins. To make sure that His_6-tagged SMC will be as functional *in vitro* as wild type SMC, a strain of *B. subtillis*, carrying smc-his6 at the amylase (*amy*) locus on the chromosome, was created in our group. This tagged SMC could complement the function of wild type SMC at room temperatures but not at 37°C. Due to this fact all further experiments with His_6-tagged SMC were performed at room temperature.

ScpA and ScpB, which have molecular weights of 30 and 23 kDa respectively, were found easy to purify using Ni-NTA chromatography and after purification under native conditions amounts of soluble proteins, sufficient for all further experiments, were obtained. However, for SMC and ScpB any attempts to get concentrations higher than what was obtained after purification, resulted in precipitation of proteins, thus limiting all further experiments which required titration of proteins. To obtain the isolated hinge domain, the central part of SMC between the two coiled-coil regions was amplified (residues from 1440 to 2040) and cloned into pQE60 plasmid.

The resulted hinge domain had a molecular weight of ~25 kDa and was purified under native conditions.

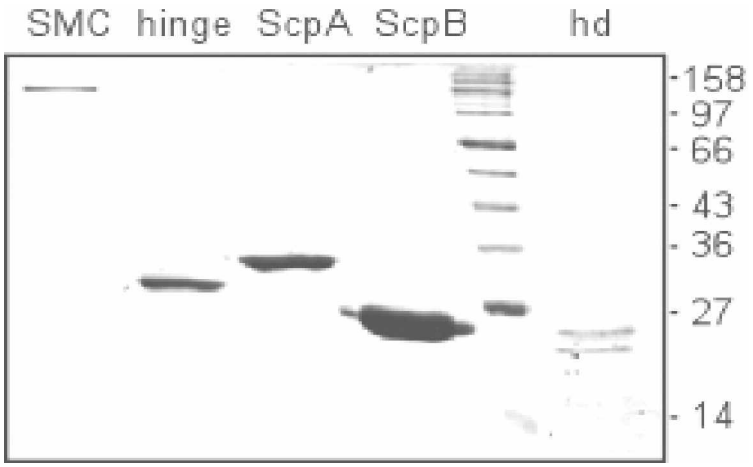

Fig.16 Coomassie blue-stained 15%-polyacrylamide gel of purified proteins. Hd corresponds to head domain of SMC. Selected sizes of marker proteins are indicated on the right in kilo Daltons.

It was found in this work that the activity of SMC and complex formation of SMC with ScpA and ScpB are strongly inhibited by imidazol even at very low concentrations. Gel filtration (using HiTrap desalting or in some cases Superdex200 10/300GL columns from Amersham/Pharmacia) was used to remove all residual imidazol. The final yield from 1L of culture was 2.5 mg of protein for SMC, ~10 mg of ScpA or of hinge domain**,** 22 mg of ScpB, and ~1.5 mg of head domain of SMC. Purified proteins remained active for about 2 month upon storage at plus 4°C (except for ScpA which remained stable for approximately one month).

To express the isolated head domain of SMC, a construct was created with both fragments of *smc* encoding for N-terminal and C-terminal domains of SMC on one plasmid (pQE60). Both domains were under control of their own yet identical promoters. Native-PAGE assay was used to confirm proper formation of a single head domain. As can be seen on the Fig. 17, N and C terminal domains of SMC migrated as a single band under native conditions, confirming proper folding of N- and C-termini to a single head.

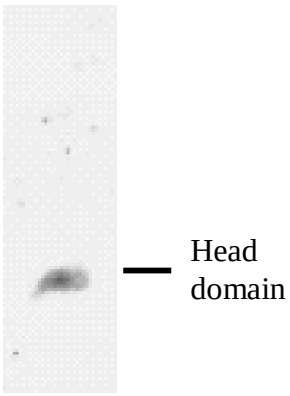

Fig. 17 Coomassie blue-stained 7.5% native polyacrylamid gel with 1.8 µM head domain of SMC.

*3.2 **ScpA, ScpB and hinge domain of SMC form dimers** in vitro*

Computer analyses of ScpA and ScpB based on coiled-coil prediction algorithm (Combet C. 2000) showed high probability of coiled-coil regions in both proteins. ScpA has two regions that can possibly form coiled-coil domains, one in the center with a very high probability and second closer to the C-terminus of the protein, which has much less probability over a short length (Fig. 18A). ScpB sequence showed high probability of coiled-coils only in one short region close to C-terminus of protein (Fig. 18B)

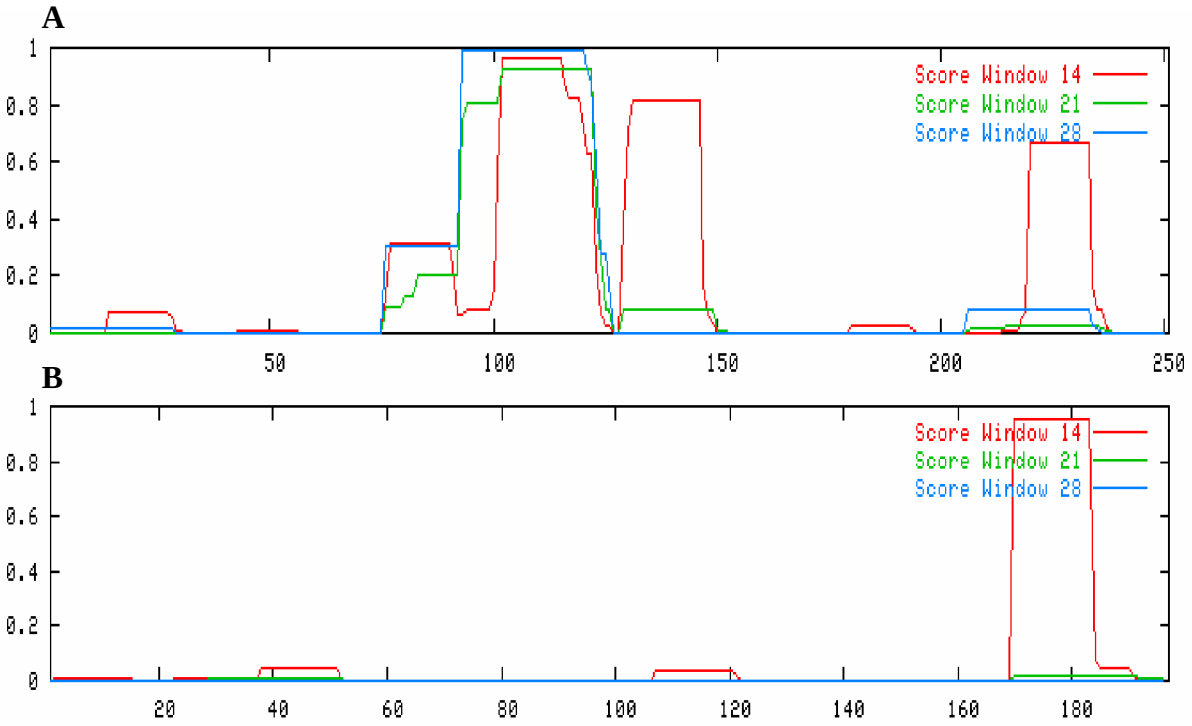

Fig. 18 Coiled-coil prediction for (A), ScpA and (B), ScpB. Y-axis shows the probability of coiled-coils in the defined region.

Very often, the presence of coiled-coil regions in proteins indicates high probability of multimer formation. To investigate if ScpA and ScpB form dimers or even higher order multimers**,** gel filtration assay was performed on both proteins and on hinge domain of SMC. For further estimation of proteins sizes, the gel filtration column was calibrated with standard proteins (bovine serum albumin, ovalbumin, chymotrypsinogen, cytochrome c and aprotinin of sizes 66, 45, 25, 14 and 6.5 kDa, respectively). As expected from the X-ray crystallography data suggesting that SMC forms a dimer via hinge domains interaction (Haering, Lowe et al. 2002), hinge domain (25 kDa) eluted as a single peak at 160 ml which corresponded to size of 50 kDa, exactly matching the size of a dimer (Fig 19). ScpB eluted as a single peak at 149.5 ml, corresponding to a size of 65 kDa and to a Stokes radius of 3.4 nm**.** The ScpA elution profile consisted of one major peak at 176 ml and of a second small peak at 152 ml, which corresponded to sizes of 35 and 60 kDa and Stokes radii of 2.8 and 3.3 nm**,** respectively.

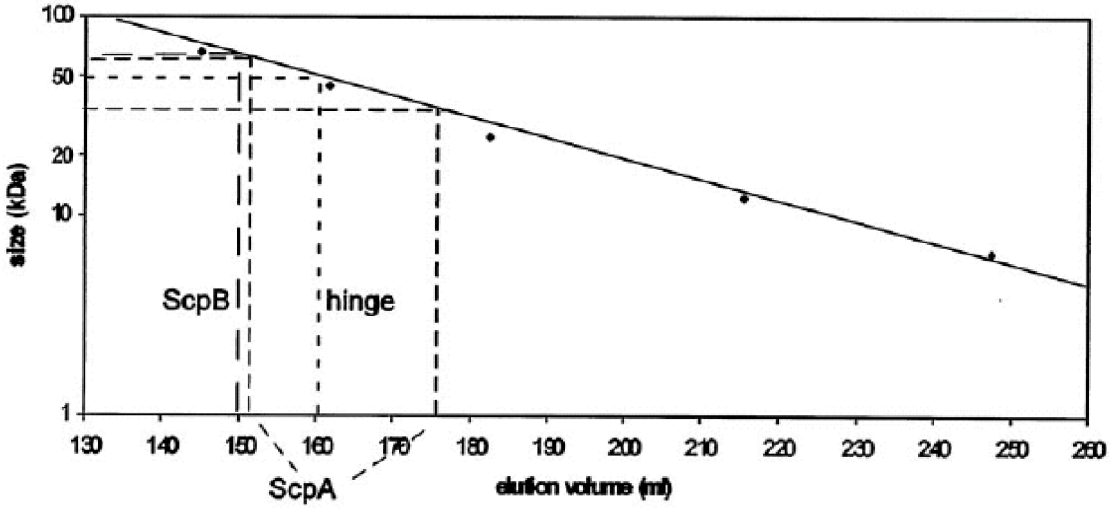

Fig. 19 Gel filtration assay for ScpA, ScpB and hinge domain of SMC on **a** Superdex200 26/60 column (Amersham Pharmacia Biotech). Elution peaks for calibration proteins are marked with diamonds. Arrows indicate elution peaks for ScpA, ScpB and hinge.

Since data received from size exclusion chromatography reflect the size and shape of molecules rather than weight, additional experiments were required for proper analyses of ScpA and ScpB. Gradient ultracentrifugation provides data on

proteins size and densit**y,** which when combined with data from gel filtration experiments allows one to estimate proteins weight. Weight can be calculated using empirical formula for proteins in solution: **$\underline{M = 3.909 S x R_s}$**, where S is in Svedberg units and R_s is Stokes radius in nm (Erickson 1991).

To calculate the masses of ScpA and ScpB in solution, sucrose gradient ultracentrifugation was performed using sucrose gradients from 5 to 20%. Approximate sedimentation coefficients for ScpA and ScpB were obtained from comparison with elution peaks of standard proteins with known sedimentation coefficients (Fig. 20). The peak fraction of ScpA corresponded to a sedimentation coefficient of approximately ~2.0S (similar to cytochrome c with sedimentation at 1.8S). Combined with Stokes radii that were obtained from gel filtration where ScpA eluted in two peaks that correspond to native weights of 35 and 60 kDa, it can be concluded that ScpA mainly exists in a monomeric state but can probably also form a dimer. The peak fraction from sucrose gradient centrifugation for ScpB corresponded to **a** sedimentation coefficient of 2.8S. After substitution of this value together with Stokes radius into the equation described above, a molecular weight of 37.2 kDa can be deduced. Since the molecular weight of ScpB is ~23 kDa, the native weight of 37.2 kDa can be explained by a dimeric form of ScpB, although that would expected to be around 44 kDa.

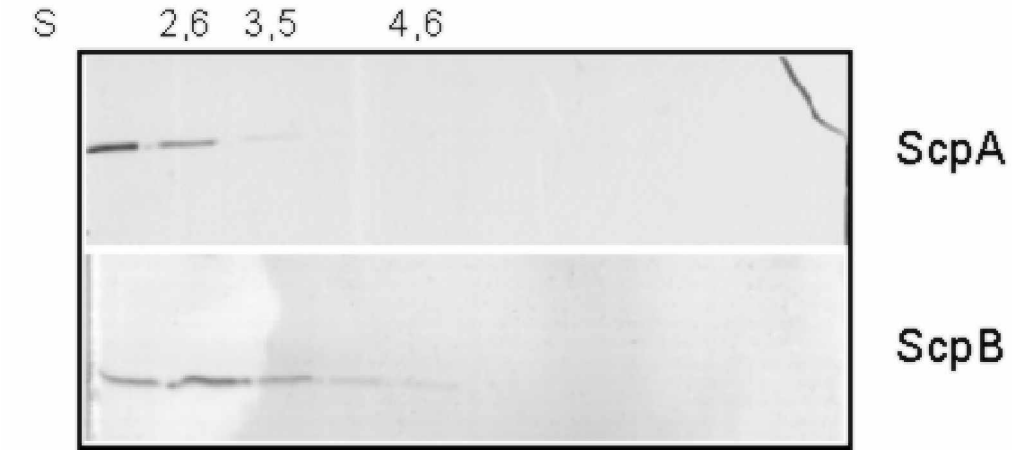

Fig. 20 Coomassie blue-stained 15% SDS polyacrylamide gel from 5-20% sucrose gradient centrifugation assay for ScpA and ScpB. Each line corresponds to a 1 ml fraction, 5 to 20% of sucrose from left to right. Sedimentation coefficients of selected standard proteins are indicated on the top of the gels.

For a final confirmation of a dimer formation, mass spectroscopy was performed for highly concentrated ScpB (Fig. 21). Measurements were made for a set of different dilutions of ScpB (concentrations from 3 to 10 µg/µl) showing two mass peaks, 22972 Da for the monomer of ScpB, and 45944 Da for a dimer. No masses that could belong to other multimers but dimer of ScpB were detected.

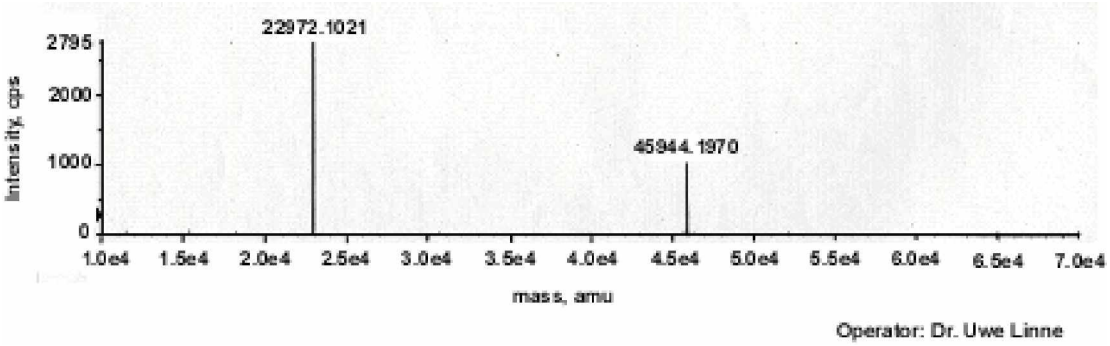

Fig. 21 ESI-TOF analysis of ScpB(3 µg/µl in 10 mM ammonium acetate buffer, pH 8.0).

Therefore, it was proved that the native form of ScpB is a dimer, while ScpA mainly exists as a monomer although can also be in a dimeric form. The ScpB dimer appeared to be very stable, even under denaturing conditions of SDS-PAGE buffer with 2 % (w/v) SDS, a band corresponding to the dimer could be seen on the gel. After boiling a sample of ScpB at 95°C for 2 min, denaturing was complete and the dimer band was eliminated (Fig. 22).

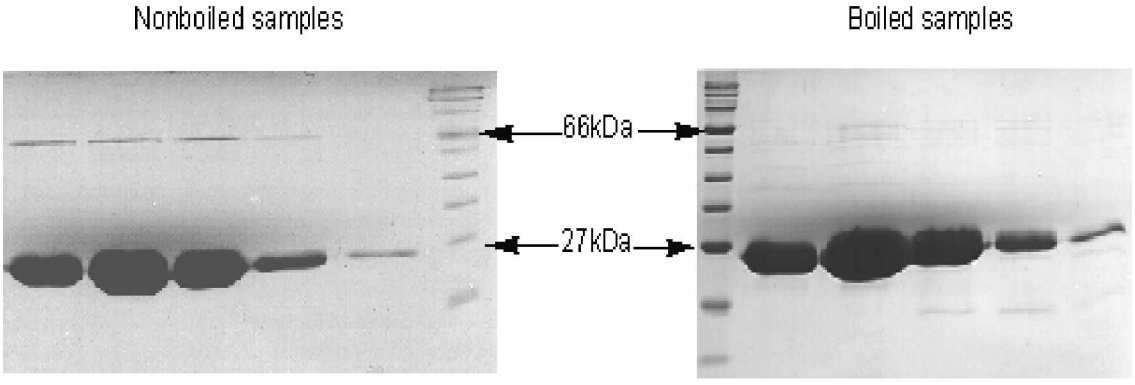

Fig. 22 Coomassie blue-stained 15% SDS-PAGE with ScpB samples right after purification (left picture) and with ScpB samples boiled prior applying to the gel at 95°C for 2 min samples (right picture).

All attempts to get mass spectroscopy data for ScpA were unsuccessful because it was impossible to concentrate the protein to a sufficient concentration for mass spectroscopy. All attempts to concentrate ScpA resulted in protein precipitation.

3.3 Full length SMC is needed to bind to dsDNA

Since SMC is a DNA condensation factor in cells, the next step of this work was to investigate a possible DNA binding activity of all SMC complex proteins, and the importance of different SMC domains for DNA binding. DNA gel shift assays were used to answer these questions. Assays were performed with dsDNA amplified with PCR from different regions of chromosome with different length**,** as well as with plasmid DNA. Results were similar to all types of DNA and were not dependent on the DNA sequence. ScpA, ScpB as well as hinge and head domains shared similar behavior and showed no DNA binding (Fig. 23). Increase of concentration of ScpA, ScpB or of SMC domains had no effect on DNA binding. On the contrary, SMC showed interaction with DNA, although the shift was not very clear and looked like smearing of DNA. Since SMC has a weak ATPase activity, DNA binding of SMC was tested in the presence of different concentrations of ATP**,** but no significant effect was detected. The presence of ScpA or of ScpB in different combinations also did not influence DNA binding of SMC.

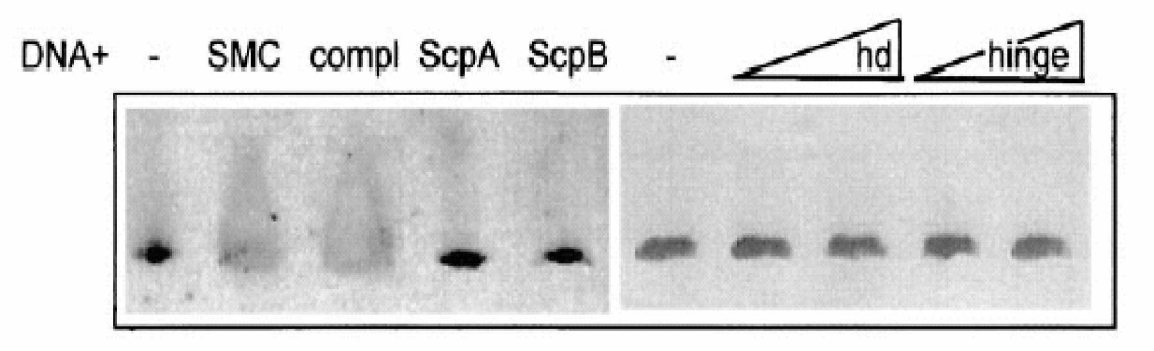

Fig. 23 Ethidium-bromide stained 7% native polyacrylamide mobility shift assay. Linear DNA (1.5 pmol; 500 ng; 500 bp) was run in the absence (minus) or presence of SMC (20 pmol); SMC, ScpA, and ScpB (20 pmol each; compl); ScpA

(20 pmol); ScpB (20 pmol); head domain (hd; 20 and 40 pmol, from left to right); or hinge (20 and 40 pmol).

To confirm gel shift results, the DNA binding activity of all protein was tested using Surface Plasmon Resonance (SPR). 100 and 500 bp fragments of DNA from an rRNA operon close to the replication origin and from 90° region on the chromosome were amplified by PCR using two biotinylated primers, so that both ends of the DNA were immobilized on the chip. SMC showed strong non specific binding to DNA**,** and was retained on the chip after washing (Fig. 24A). Consecutive addition of SMC resulted in a similar pattern of binding. Such pattern of binding can be explained by nonspecific interaction of SMC with DNA**,** because more binding is observed as more protein is flowing over the surface of the chip. If binding was specif**ic,** this would result in rapid occupying of all specific sequences of DNA by the protein and therefore in saturation of binding sites, followed by flat curve and therefore a state of equilibrium**,** in which dissociated protein is replenished by protein flowing over the surface. On the contrary, as can be seen on the graph, binding after second addition of SMC was similar to the first one and no saturation was observed. After washing of SMC from the chip, the experiment could be repeated and no changes in the kinetics of SMC binding were observed. When the experiment was repeated with DNA from different regions on the chromosome, no significant difference in the binding of SMC to DNA was detected, giving another prove for DNA sequence-independent binding of SMC. Similar experiments were performed with ScpA, ScpB and hinge and head domain of SMC and showed similar to gel shift experiment results (Fig. 24B), as ~~it~~ was expected. The absence of DNA binding activity of hinge and head domains can have two explanations. Either**,** coiled-coil domains have DNA binding activity per se**,** or this activity can be only established by all three domains connected together into a complete SMC molecule.

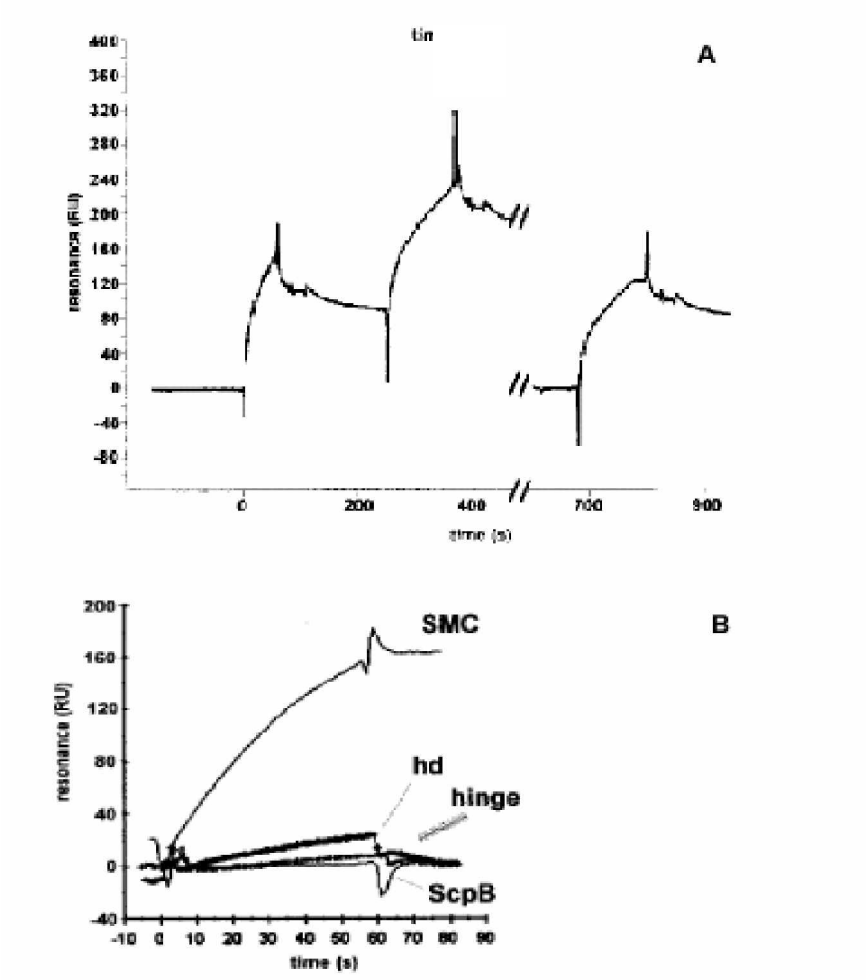

Fig. 24 Surface plasmon resonance experiments. (A) A Streptavidin chip was coated with 350 RU of a 500-bp linear DNA fragment carrying biotin labels at both ends (closed). SMC (2 µM) was injected, followed by a second injection (2 µM, double amount at 250 s). The chip was washed with 50 mM NaOH, and SMC (2 µM, double amount at 680 s) was injected. (B) Binding of different proteins to closed DNA: SMC (2 µM), head domain (hd; 2 µM), hinge (2 µM), or ScpB (20 µM).

Also, reversed experiments for DNA binding were performed with SMC. SMC was immobilized on the surface of the chip through covalent binding to a layer of carboxymethylated dextran and DNA was injected into the flowpath. Although some interaction with SMC was detected, it was considerably lower than in the case of free SMC (data not shown). This can be explained by the fact that SMC might need flexibility of its arms for proper DNA binding which is abolished when different parts of one SMC molecule are bound to the surface of the chip. Another explanation can be that SMC needs to interact with other SMC molecules to bind to DNA.

3.4 SMC binds nonspecifically to DNA via a ring-like structure

Since SMC did not show any specificity to DNA sequence, the question arises if the structure of DNA might be important rather than any sequence. The same DNA sequences that were used to investigate the DNA binding activity of SMC (see chapter 3.1) were used to answer this question. The only difference was that in this case, amplification of DNA with PCR was performed only with one biotinylated primer out of two. For this reason, unlike DNA with two biotinylated ends that could bind to the surface of Streptavidine-coated chip with both ends, forming "closed" bridge-like structure, DNA with just one biotinylated end could bind to the surface of the chip only with this end, forming an "open" structure (Fig. 25, right panel). When SMC binding to this type of DNA was measured, it showed similar kinetics for SMC binding to "closed" form of DNA; but after the washing step**,** the picture was different. Unlike experiment with "closed" DNA (Fig. 25, left panel), SMC was not retained on the DNA but was washed off the chip.

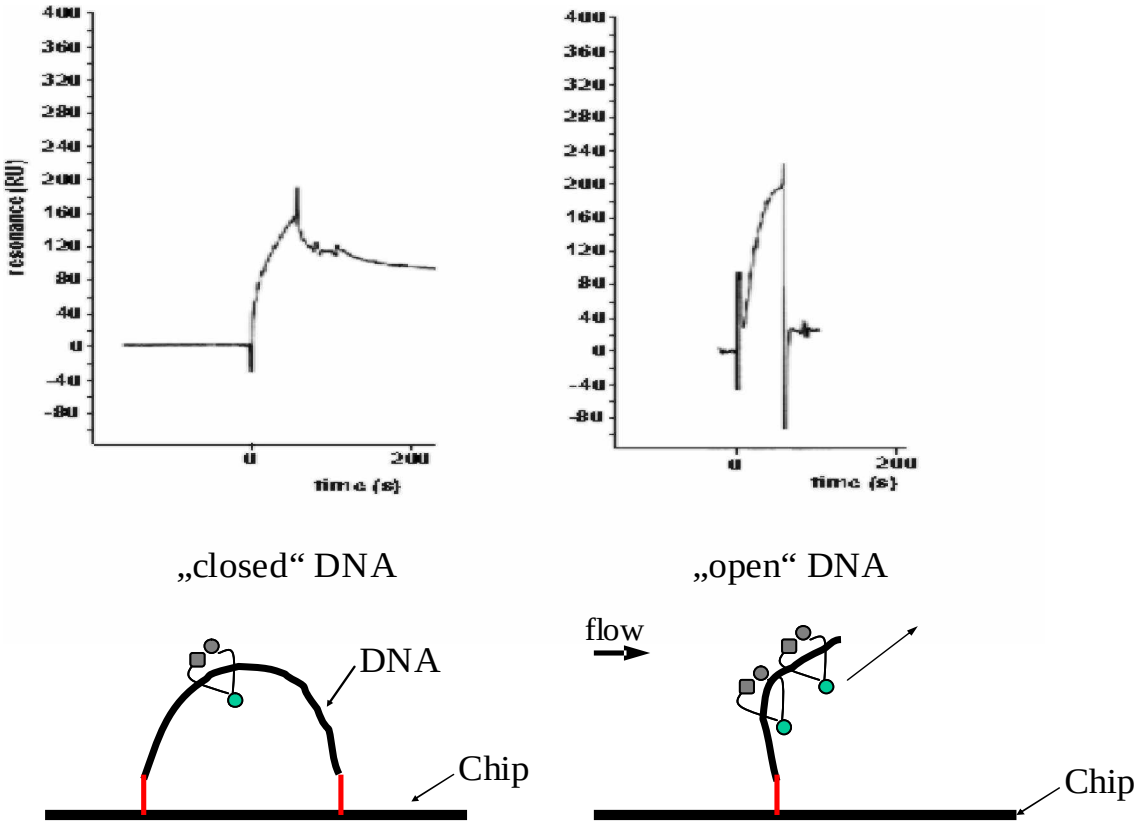

Fig. 25 Surface plasmon experiments for SMC (2 µM) binding to biotinylated DNA immobilized on the streptavidin coated chip. Left panel represents binding to

"closed" DNA with two biotinylated ends and right panel shows binding to "open" DNA with one biotinylated end. SMC molecules bound to DNA (biotinylated ends are represented in red) are shown schematically below the Biacore results.

This result suggests that SMC binds to DNA by bringing its heads together, forming a ring-like structure and holding DNA in between its arms. In case of "open" DNA SMC can be easily washed off with the flow of the buffer, which is impossible with "closed" DNA.

As a control, similar experiments were repeated with two other proteins, *B. subtilis* AbrB and *E. coli* Fis. Both proteins are global transcription factors (Klein W 2002; Muskhelishvili G 2003) and have DNA binding activity. As can be seen in Fig. 26, although binding of AbrB to "open**"** DNA was slightly stronger, there was no principle difference in interaction of the protein with "closed" or "open" DNA in the end of injection and during the washing step. Fis showed a behavior similar to AbrB although it had similar affinity to both types of DNA (data not shown). Unlike SMC**,** both proteins were released from DNA with a constant off rate regardless of the type of DNA.

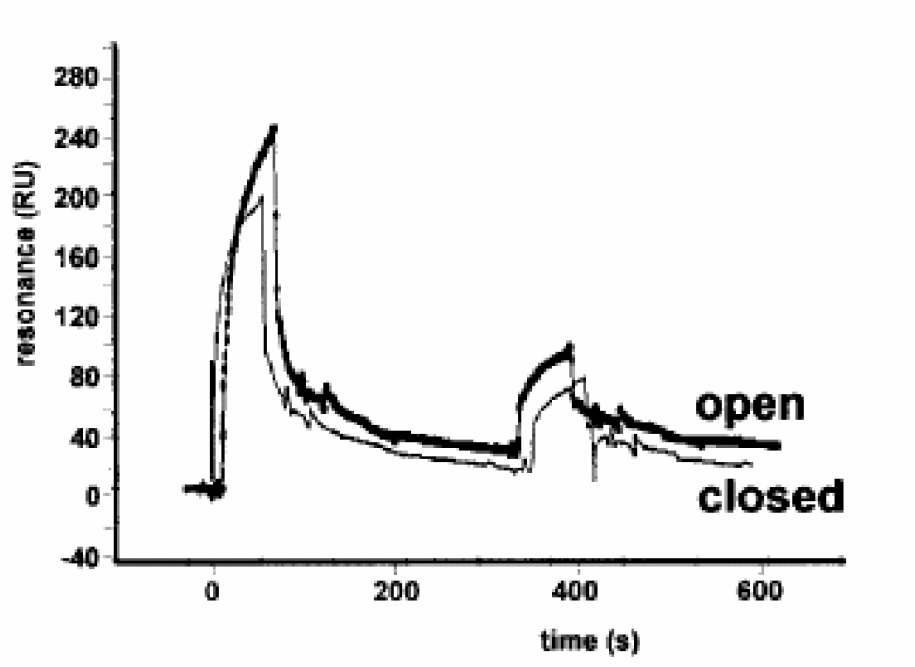

Fig. 26 Surface plasmon resonance experiment for AbrB. Binding to "open" DNA is shown with thick line. First injection, 12 µM AbrB; second injection, 6 µM AbrB.

*3.5 **ScpA and ScpB form two types of complexes** in vitro*

As was shown above, in previous chapters, although SMC needs ScpA and ScpB *in vivo* for proper function, no dependence on ScpA or ScpB in DNA binding of SMC was detected *in vitro.* For a proper understanding of the function of ScpA and ScpB in formation of the SMC complex**,** it was important to reconstitute the SMC complex *in vitro.* Investigation of ScpA and ScpB interactions was the first step. The first method of choice was native polyacrylamid gel assay. Unfortunately no interaction was detected using this method so other methods were tried. Sucrose gradient ultracentrifugation and analytical gel filtration were chosen for the second attempt since they are much gentler than electrophoresis and do not require electrical forces which can disturb proteins in complex. Also during electrophoresis a significant change in pH is possible**,** which also can affect complex formation.

Sucrose gradient centrifugation showed that elution peaks for ScpA and ScpB corresponded to sedimentation values of 2.0S and 2.8S (Fig. 27, two upper panels**),** but the elution pattern for ScpA changed when both proteins were mixed and applied to sucrose gradient together. The elution peak of ScpA in the mixture shifted from 2.0 to 2.6**,** indicating either multimer formation or association with ScpB. Although this assay showed some interaction between ScpA and ScpB, gel filtration experiments were needed to get more quantitative results.

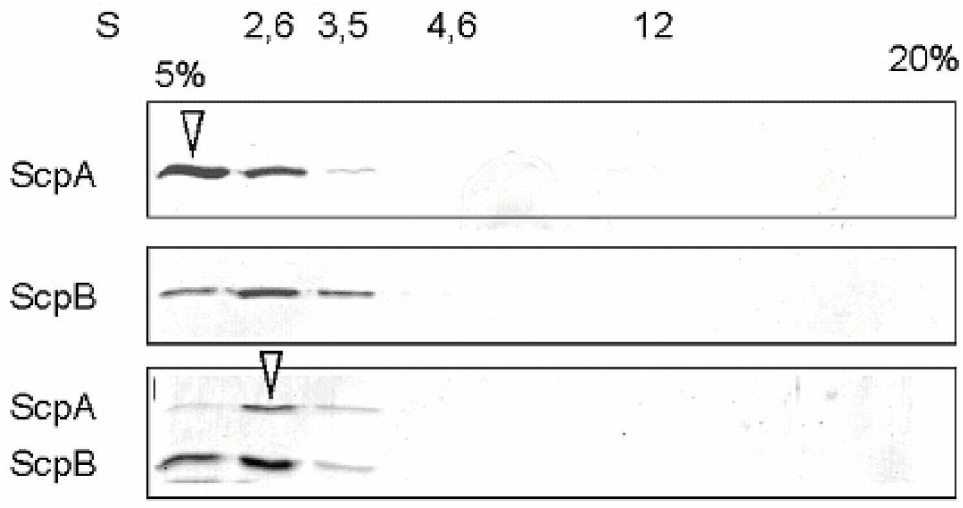

Fig. 27 Sucrose gradient centrifugation using 5 to 20 % sucrose concentration. 0.4 nmol ScpA (upper panel), 0.4 nmol ScpB (middle panel), or 0.2 nmol ScpA and

0.2 nmol ScpB (lower panel). Elution of standard proteins is indicated, arrowheads indicate the shift in elution maximum for ScpA

For these experiments, an analytical gel filtration column that allows work with small amounts of proteins was used. As can be seen on figures 28B and 28C, both ScpA and ScpB eluted as single distinct peaks (corresponding to monomer of ScpA and dimer of ScpB), when they were loaded separately. But the elution profile changed significantly when ScpA and ScpB were premixed and incubated for half an hour at room temperature before loading to the column (Fig. 28D). Original ScpA and ScpB peaks were reduced in size in favor of two new peaks at 13.9 and 12.0 ml, which corresponded to sizes of ~110 and ~ 210 kDa, when compared to calibration curve based on standard proteins (Fig. 28A). Since ScpA and ScpB elute as proteins with molecular weights of about 35 and 65 kDa respectively, the two new peaks that appeared after loading of the mixture most likely correspond to complexes that consist of one ScpA and one ScpB dimer **(**110 kDa peak) and of two ScpA and two dimers of ScpB (210 kDa peak).

The ratio between two new peaks appeared to depend on the ratio of ScpA and ScpB in the initial mixture. In excess of ScpB, ScpA and ScpB peaks reduced mainly in favor of the peak at 13.9 ml with formation of a much lower amount of the bigger complex (Fig. 28D, lower graph). The picture was different when the initial ratio of ScpA and ScpB was equal, or an excess of ScpA was loaded. In this case ScpA and ScpB were present mainly in form of the bigger complex (Fig. 28D, upper graph). ScpA is likely to form a dimer (see chapter 3.2), for this reason one can suggest that a higher molecular weight ScpAB complex is possibly formed by interaction of two small ScpAB complexes.

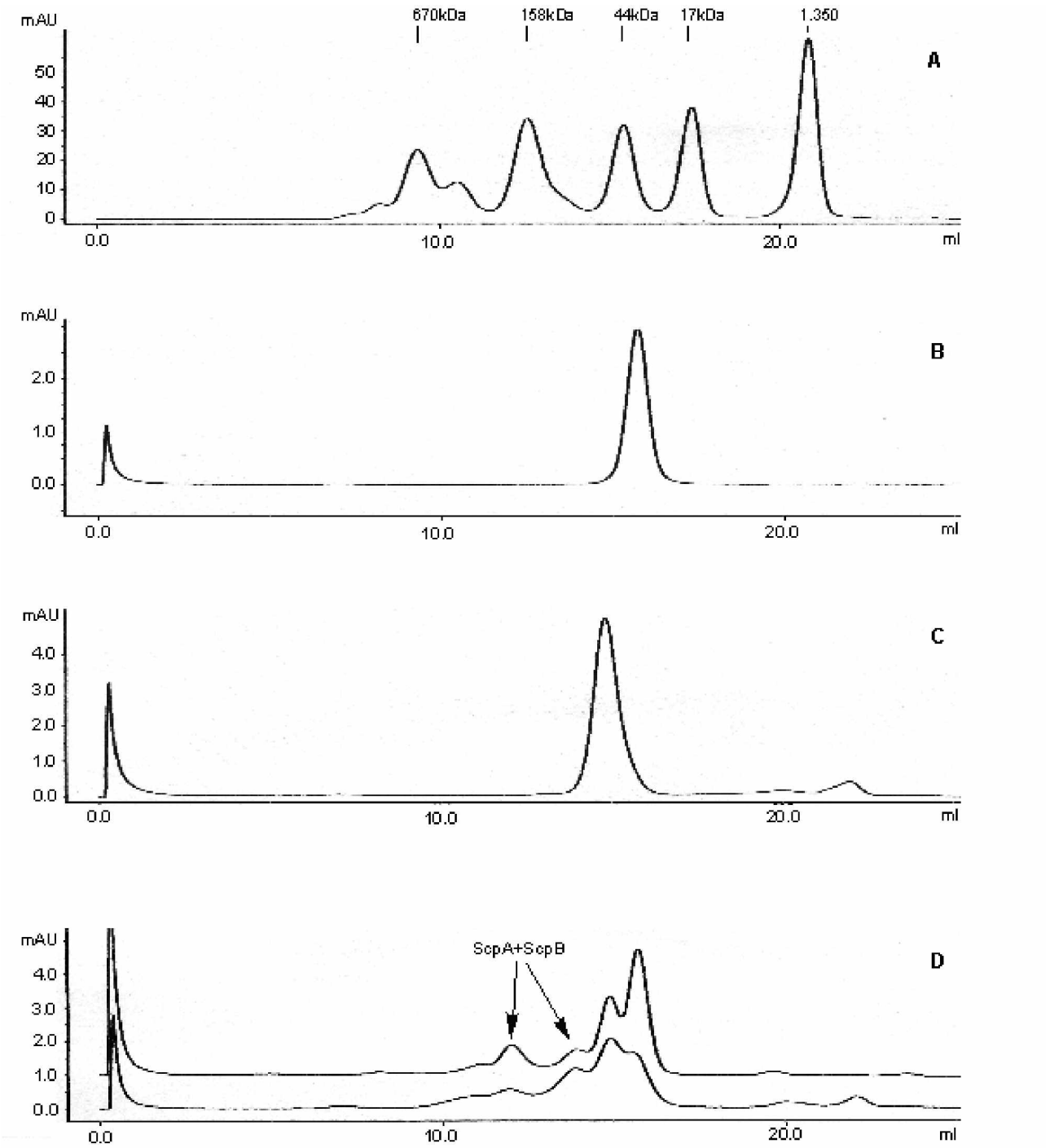

Fig. 28 Analytical gel filtration assay with ScpA and ScpB. (A) Calibration of the column with gel filtration standard proteins (BioRad). (B) 0.4 nmole of ScpA. (C) 1 nmole of ScpB. (D) ScpA mixed with ScpB in two different proportions, 0.4:1 nmole (lower graph) and 1.2:1 nmole (upper graph).

3.6 SMC is present in two distinct density fractions in cell extract, and co-elutes with ScpB in a high molecular weight fraction

Sucrose gradient centrifugation was used to detect interactions between SMC and ScpB. A crude extract of proteins from wild type *B. subtilis* was loaded onto the sucrose gradient and after centrifugation was subjected to Western blot analyses with antibodies against SMC or against ScpB. It was not possible to use ScpA antibodies since all attempts to produce them failed, possibly due to ability of ScpA to form multimers. Results received from Western blot analyses were compared with sedimentation profiles of ScpB and SMC. As it was shown above, after centrifugation, when loaded alone, ScpB elutes at fraction that corresponds to sedimentation value of 2.8S. Unlike pure protein, in the crude extract ScpB eluted in two fractions, one that corresponded to a pure form and the second corresponded to a much higher molecular weight with sedimentation of about 13S (Fig. 29, middle panel). The picture was similar with SMC whose sedimentation coefficient is reported to be about 6.6S (Hirano and Hirano 1998). In crude extract SMC also eluted in two fractions, one with a sedimentation coefficient corresponding to pure SMC and a second with sedimentation coefficient similar to the second peak of ScpB (Fig. 29, lower panel). Therefore, since high molecular weight fractions of SMC and ScpB correspond to similar sedimentation coefficients they most likely represent the SMC complex. The presence of SMC and ScpB both in unbound form and in complex shows that *in vivo*, the complex probably exists in a dynamic equilibrium with "free" SMC and ScpB although this is not necessarily true for intact cells due to the fact that complex could be broken down in the cell extract after cell disruption.

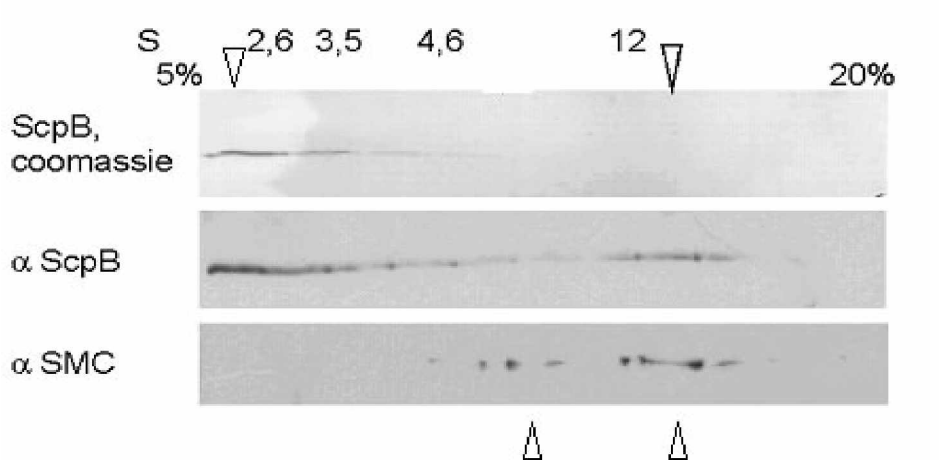

Fig. 29 5 to 20% sucrose gradient ultracentrifugation. 1 nmol of purified ScpB (upper panel), cell extract probed with ScpB antiserum (middle panel) or with SMC

antiserum (lower panel). Arrowheads pointing upwards indicate the elution peaks for SMC. Arrowheads pointing downwards indicate the elution peaks for ScpB. Note that the first fraction shown in Fig. 4 is not shown on this figure.

3.7 SMC forms a stable complex with ScpA and ScpB in vitro

To confirm formation of the SMC complex and interaction of SMC with ScpA and ScpB *in vitro,* native PAGE and surface plasmon resonance assays were used. On native PAGE**,** SMC migrated as two separate bands (Fig. 30) which most likely represented different conformations of the SMC arms. When SMC was premixed with ScpA and ScpB**,** this pattern changed and additionally, a band most likely corresponding to the complex appeared. Similar results were obtained when SMC was premixed only with ScpA or ScpB, although in case of ScpB the new band was rather diffuse contrarily to the complete complex and appeared only at high concentrations of ScpB.

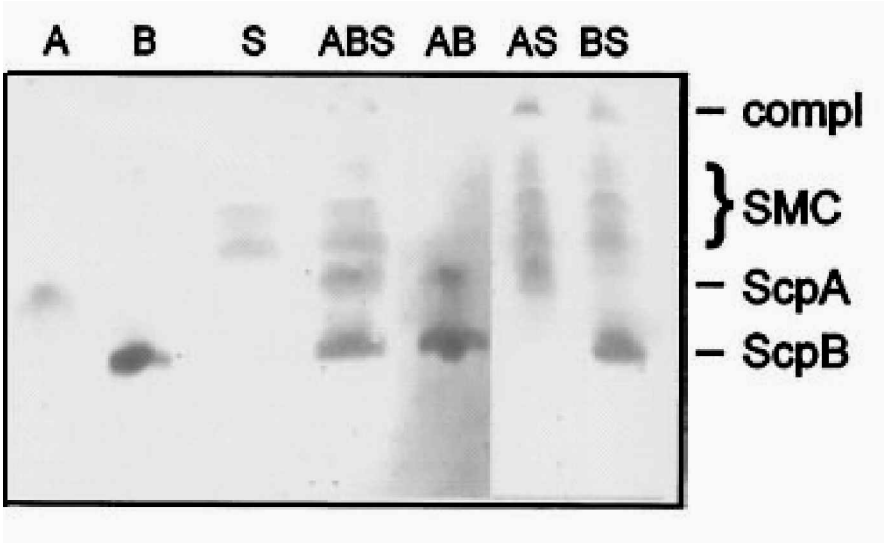

Fig. 30 Coomassie blue-stained 7.5% native polyacrylamide gel. Lanes: A, ScpA (2 µM); B, ScpB (10 µM); S, SMC (2 µM); hd, head domain (1.8 µM; this lane was taken from another gel at its appropriate position relative to ScpB and ScpA); other lanes, combinations of A, B, and/or S. Lines at right indicate migration positions for ScpA, ScpB, and the complex (compl); the brace indicates the migration position for SMC.

The head domain of SMC was also investigated in these experiments, to find out whether ScpA and ScpB bind to it or to the coiled-coil or to the hinge domains. Contrarily to SMC, the head domain did not show any interaction with ScpA and ScpB when native PAGE assay was used. In SPR experiments, when purified ScpA was covalently immobilized on a Biacore chip**,** a weak interaction with head domain but not with the hinge domain of SMC could be detected (Fig. 31), showing the approximate area of ScpA/ScpB binding. This interaction could be stabilized when the head domain was added together with ScpB. The presence of DNA, on the other hand did not show any significant influence on the kinetics of interaction.

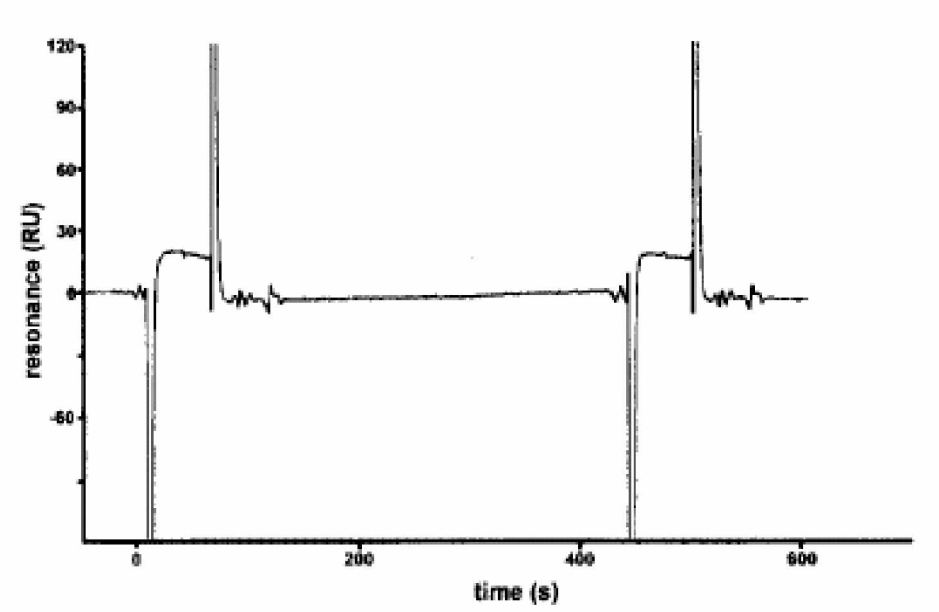

Fig. 31 Surface plasmon resonance experiments. (A) ScpA (180 resonance units [RU]) was covalently immobilized on a Biacore chip. An equimolar mixture of the head domain and ScpB (2 µM each) was injected, followed by injection (at 450 s) of the head domain and ScpB (2 µM each) and a 500-bp linear DNA fragment.

Unlike head domain, ScpB was not able to bind to immobilized on the chip ScpA in SPR experiments. One could argue that ScpA needs to be mobile to be able to form a complex with ScpB which supports data for 2ScpA4ScpB complex. To support the ScpA/ScpB interactions found in native PAGE and surface plasmon resonance experiments, size exclusion chromatography was used, also to get more quantitative data. SMC alone eluted at a volume that corresponded to a Stokes radius of about 9 nm (Fig. 32A). Such a big Stokes radius (similar to protein of 670 kDa) can be explained by the elongated shape of the SMC molecule, which makes SMC

behave on gel filtration matrix like a much bigger molecule than it is. This Stokes radius combined with the sedimentation value of SMC of 6.6S from sucrose gradient centrifugation results in the mass of approximately 230 kDa (comparable with the weight of SMC dimer, 270 kDa). When SMC was loaded together with ScpA and ScpB, a shift of the SMC peak accompanied by increase in height of the peak was observed**,** showing an interaction of proteins and formation of the stable complex (Fig. 32B). Samples from fractions corresponding to all detected peaks were subjected to SDS-PAGE analyses to determine the compounds of the peaks. The silver stained gel clearly showed presence of both ScpA and ScpB in the shifted SMC peak (first two samples on the gel, Fig. 32B). Both peaks that corresponded to the ScpA/ScpB complex also appeared in this run although their intensity was strongly reduced in favor of the SMC complex. SDS-PAGE analyses also showed that the ratio of ScpA to ScpB in the SMC complex is similar to that in the ScpA/ScpB complex and is approximately 1:2 (or more correctly one ScpA to one ScpB dimer).

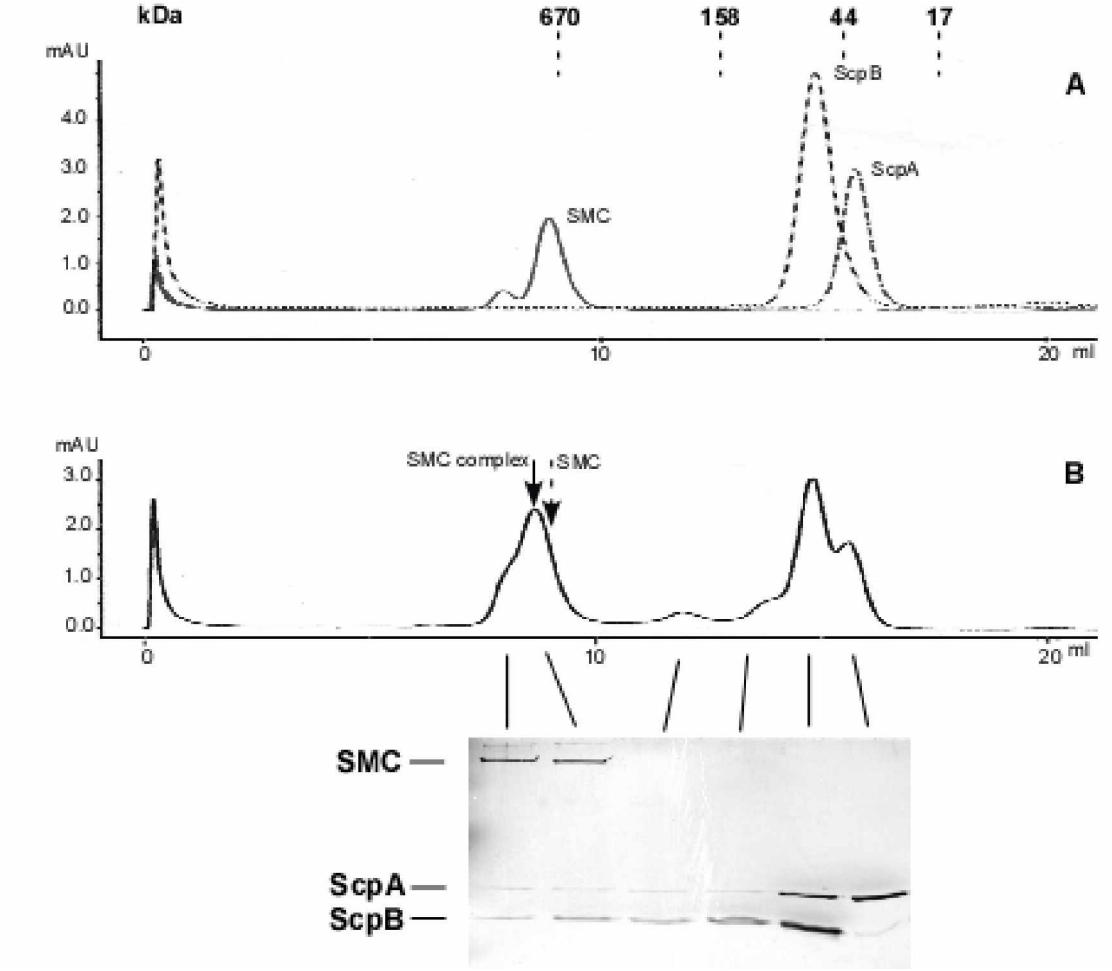

Fig. 32 Analytical gel filtration assays with SMC and ScpA and ScpB. (A) Reference runs for purified SMC (0.3 nmole), ScpA (0.4 nmole) and ScpB (1 nmole),

all three profiles were merged. Dashed lines show position of peaks for proteins from gel filtration standards. B) SMC incubated with ScpA and ScpB, same amounts as in (A). Dashed arrow shows the position of SMC in the absence of Scps, and arrow shows the peak of the SMC complex. Bottom panel shows silver stained SDS-PAGE with fractions loaded corresponding to peaks from gel filtration (indicated by arrows) of SMC mixed with ScpA and ScpB.

Due to the elongated shape of SMC, binding of ScpA and ScpB does not change its Stokes radius very much**,** which resulted in a small shift of the peak. Therefore, combination of Stokes radius of the complex (9 nm) and of the sedimentation coefficient (13S, see chapter 3.6) reveals a native weight of the complete SMC complex of ~460 kDa. Since the weight of SMC is 270 kDa, about 190 kDa remains for ScpA/ScpB**,** and most likely corresponds to a 2 ScpA/ 4 ScpB complex (two ScpA monomers and two ScpB dimers). These experiments were repeated with different ratios of SMC, ScpA and ScpB loaded**,** but no major change in complex formation was observed. Although these findings leave open a question, whether SMC interacts with a complete established ScpA/ScpB complex, or with ScpA and ScpB bind directly to SMC one by one to form a complete complex, my data argues in favor of a 2 ScpA/ 4 ScpB complex binding because its amount decreases considerably upon formation of the SMC/ScpA/ScpB complex.

3.8 ScpA possibly causes release of DNA from SMC

Although some interaction of SMC with ScpA and very minor interaction with ScpB was detected with Native-PAGE assay (Fig. 30)**,** the data are not very convincing without further proves. For this reason these interactions were investigated using gel filtration assays. Consistent with results of native PAGE assays, no shift of the SMC peak occurred when SMC was loaded together with ScpB (Fig. 33A), and no traces of ScpB were visible on a silver stained SDS-PAGE when peak fractions from elution were loaded. The results were completely different when SMC was loaded in a mixture with ScpA. Although no ScpA was detected on SDS-PAGE analysis of peak fractions containing SMC, and no reduction of the original ScpA peak was observed, the elution profile for SMC has significantly changed (Fig.

33B). Unlike shift to a bigger size and increase in a UV light absorption like it was observed in case of SMC/ScpA/ScpB complex formation in this case SMC peak reduced its size and slightly shifted to a smaller size. To explain this fact a conjecture was made that since SMC is a DNA binding protein, even after all purification steps it might remain bound to some amount of none released DNA. If this conjecture is correct, the decrease of size in SMC peak and shift to a smaller size can be explained if bound to SMC DNA is released upon addition of ScpA.

Additional experiment was made to verify presence of DNA in SMC fraction. Purified SMC was mixed with DNase A and incubated for periods of times from half an hour to an hour. After incubation, DNA peak was completely degraded and SMC peak behaved exactly as in case with ScpA, it reduced its size and shifted to a smaller position (Fig. 33C). Therefore this experiment supported possibility of DNA release from SMC by ScpA.

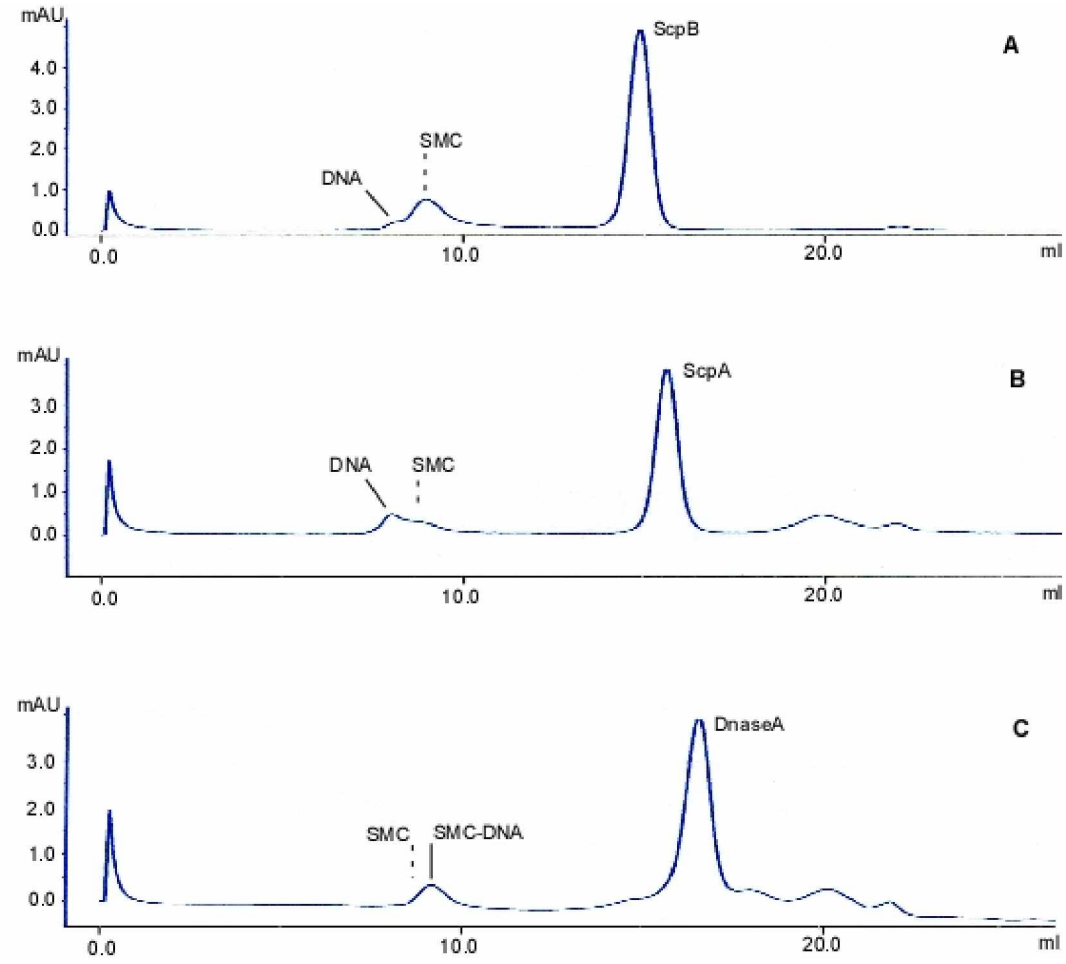

Fig. 33 Analytical gel filtration assays with SMC, ScpA, ScpB and DNase A. Arrows show positions of DNA and protein peaks. Dashed arrow shows the position of SMC in the absence of Scps. (A) Purified SMC (0.3 nmole) with ScpB (2 nmole)

premixed half an hour before the run. (B) SMC incubated with ScpA (0.4 nmole). (C) SMC with DNase A (1 nmole), incubated for half an hour at 37°C before the run.

3.9 ATP binding and hydrolysis are important but not required for SMC complex formation with ScpA and ScpB

The head domains (hd) of SMC proteins share three conserved motifs with the ATP-binding cassette (ABC) family of ATPases: Walker A and Walker B motifs and the so called "C motif", also known as "signature" motif. To study the importance of the ATPase activity for complex formation in SMC, two point mutations were introduced into SMC. A K37I substitution in the Walker A motif abolishes ATP binding activity (Hirano, Anderson et al. 2001), and a S1090R substitution in the "C motif" allows for ATP binding but prevents ATP hydrolysis (Hirano, Anderson et al. 2001). The importance of ATPase activity was investigated using gel filtration assay. Both mutants showed the ability to form complex with ScpA and ScpB (Fig. 34). But although the peaks of the SMC mutants shifted to a similar position (compared to wild type SMC) and increased their sizes, the increase was lower in case of the SMC Walker A mutant and even smaller for the C motif mutant protein, compared to the wild type protein. Analyses of elution on silver stained SDS-PAGE also showed that although ScpA and ScpB were present in peak fractions that correspond to mutant SMC protein complexes, their amounts were considerably lower than in case of wild type SMC (Fig. 34, compare with gel on Fig. 32B). From these results we can draw the conclusion that ATPase activity of SMC is not required for complex formation but affects the efficiency of interaction with ScpA and ScpB.

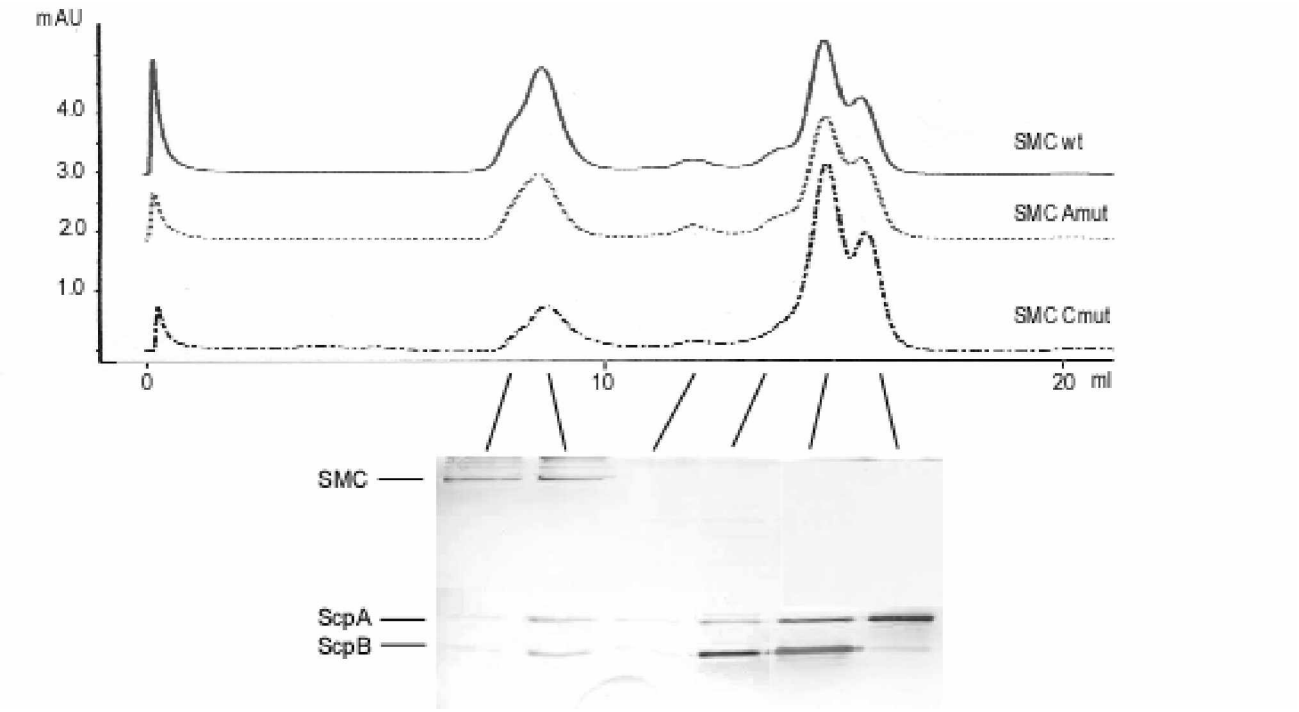

Fig. 34 Analytical gel filtration assays with SMC, SMC WalkerA (A mut), SMC C motif (Cmut), ScpA and ScpB. Purified SMC (0.3 nmole) and its mutants in same concentrations were mixed with ScpA (0.4 nmole) and ScpB (1 nmole). Comparison of gel filtration profiles of wild type SMC and SMC mutants (as noted on the profiles) loaded together with ScpA and ScpB is shown on the graph. Below the gel filtration graph is silver stained SDS-PAGE with fractions loaded corresponding to peaks from gel filtration of SMC Walker A mutant mixed with ScpA and ScpB.

3.10 ATP binding but not hydrolysis is needed for interaction of SMC with DNA

Although it was shown that SMC needs all its domains for proper binding to DNA (see chapter 3.3) and that SMC most likely binds nonspecifically to DNA via ring-like structures, the role of ATPase activity of SMC and importance of this activity for DNA binding remained unclear. To answer this question, DNA binding activity of Walker A and C motif mutants of SMC was tested in native gel shift assay with linear (PCR amplified fragment) and circular (plasmid) DNA as a substrate. Wild type SMC and C motif mutant showed similar shift of bound linear as well as of bound plasmid DNA (Fig. 35 A and B respectively). DNA binding activity of the

Walker A mutant protein, on the contrary, was completely abolished**,** independently on the type of DNA (Fig. 35).

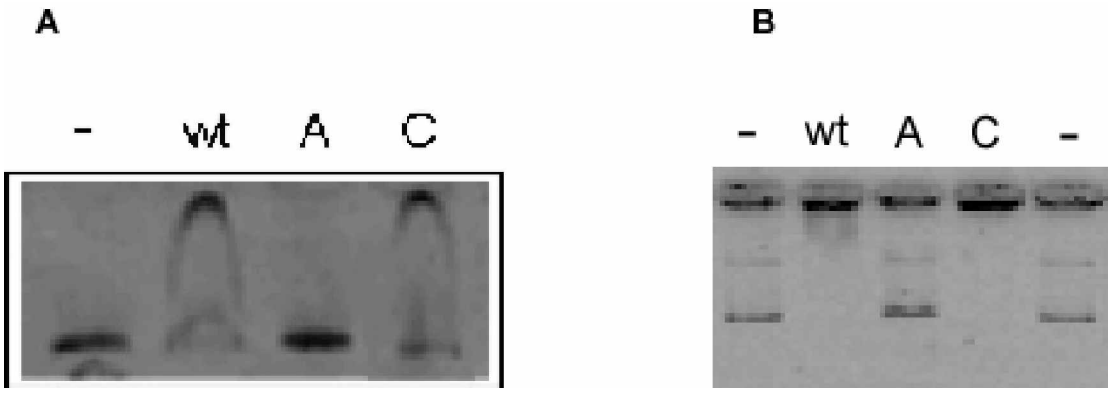

Fig. 35 7.5% Native PAGE shift analysis. (A**)** Lanes 1-4: 1.5 pmol 500 bp linear DNA, lane 2 DNA plus 20 pmol wild type SMC, lane 3 DNA plus 20 pmol Walker A mutant SMC, lane 4 DNA plus 20 pmol C motif mutant SMC. (B) same as in Fig.A but with plasmid DNA instead (~4000 bp), 0.2 pmole in each lane.

Surface plasmon resonance analyses were used to confirm the data obtained with native-PAGE shift assays and for more thorough investigation of DNA binding activity of SMC mutants. PCR amplified 500 bp DNA with two biotinylated ends was immobilized on a streptavidine-coated biacore chip and interaction with proteins was measured. Results were similar to those obtained with gel shift assay, wild type SMC and C motif mutant bound to DNA in a similar fashion and WalkerA mutant showed no detectable activity (Fig. 36).

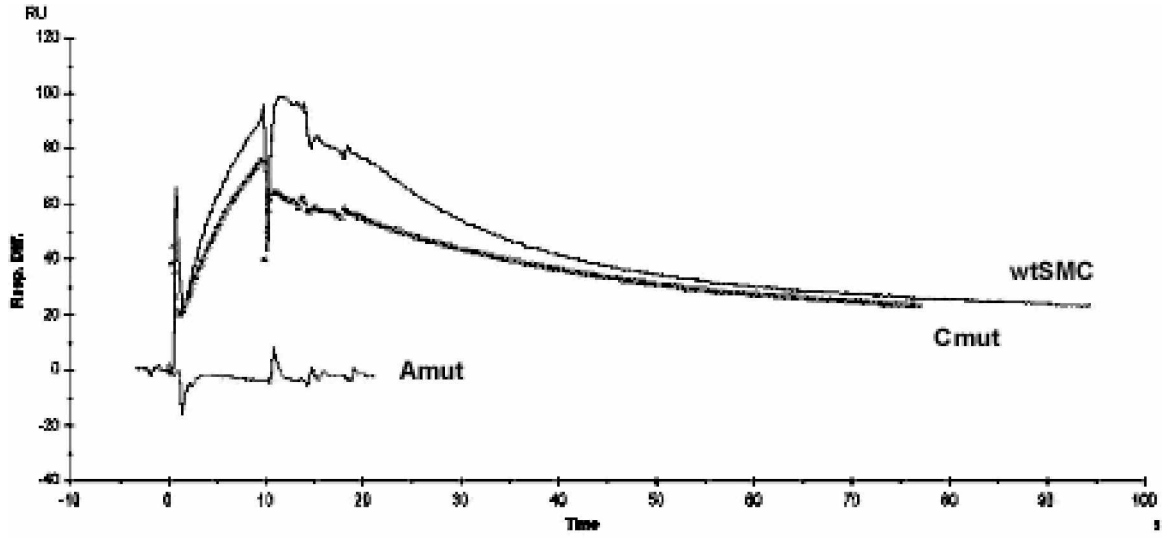

Fig. 36. Fig. 4 Surface plasmon resonance experiments using 500 bp linear DNA immobilized on the chip with both ends (300 RU loaded onto chip). 10 µl of wild

type SMC, Walker A and "C motif" mutants (2 µM) were injected at 0 s at 10 µl/min, and washed with 1500 µl/min of buffer at 10 s.

Although C mutant bound to DNA with a slightly lower affinity its release from DNA rate was also somewhat lower than that of wild type SMC. Conclusion can be made from these facts that ATP binding is crucial for DNA binding while ATP hydrolysis is not required for it, although possibly can affect release from DNA.

3.11 SMC possibly forms aggregates on AFM in solution

In order to visualize SMC molecules *in vitro*, electron microscopy was the first method of choice. Purified SMC was fixed on the mica slide and visualized with help of negative staining technique. As predicted, both "open", with two head domains separated from each other and "closed" state with head domains bound together could be observed (Fig. 37).

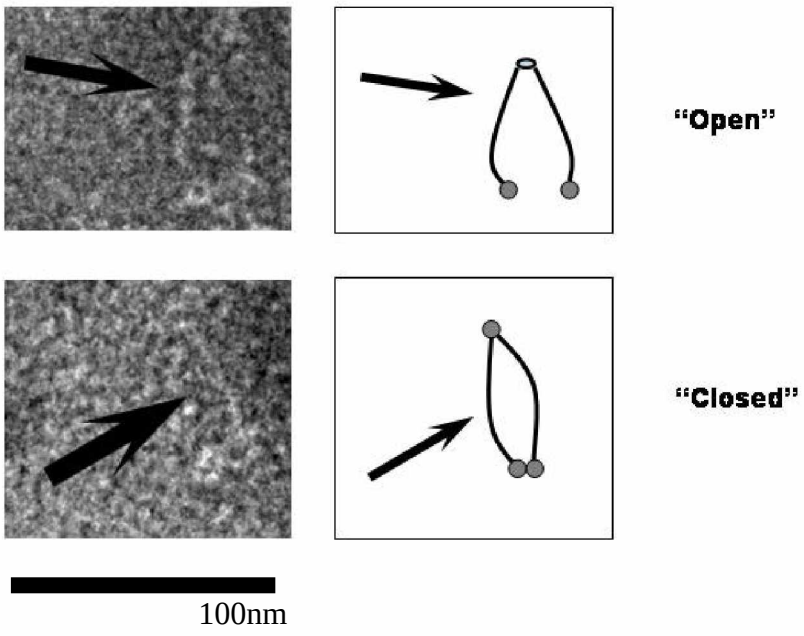

Fig. 37. Electron microscopy for SMC, performed by Jens Schiener, Max-Plank Institute, Biochemie, Munich. Proteins were fixed on mica and negatively stained

prior to analyses on a microscope. Upper picture represents “open state of molecule and lower picture represents “closed” state

Unfortunately, due to thin long arms obtained results were not of a very high quality since thickness of coiled-coil domains is close to the limits of resolution of electron microscope even when rotary shadowing is used. Moreover, protein was immobilized on mica under conditions that were quite far from native, so for this reason additional experiments were made using AFM (atomic force microscopy) technique. AFM appears to be a more accurate method in work with thin objects like DNA or long coiled-coil domains of SMC due to a direct contact of atomic needle to a subject of investigations. Moreover liquid AFM allows to measure proteins in medium unlike electron microscopy. First attempt to measure SMC on AFM was made with made with SMC dialyzed against low salt buffer (10 mM ammonium acetate, pH 8.0) and after application of a sample to the chip it was dried on air so conditions were similar to electron microscopy. As can be seen on the fig. 38A, in this case most of SMC looked like “rings” with a diameter of approximately 50 nm which is in agreement with the length of one SMC arm being about 50nm. Such high amount of ring-like SMCs can be explained by a very low salt condition which might cause binding heads to each other to form the most energetically favorable at this conditions conformation. Alternatively, the rings might be head domains making a ring with coiled-coiles and hinge sticking out, which would agree with AFM data obtained by Munich group showing that picture totally changed when SMC was measured on AFM in liquid medium in original buffer. In this case, mostly large star-like aggregates with a very minor amount of single molecules were observed (Fig. 38B). These star-like structures had a diameter of about 100nm and can give a clue to mechanisms of SMC foci formation *in vivo*.

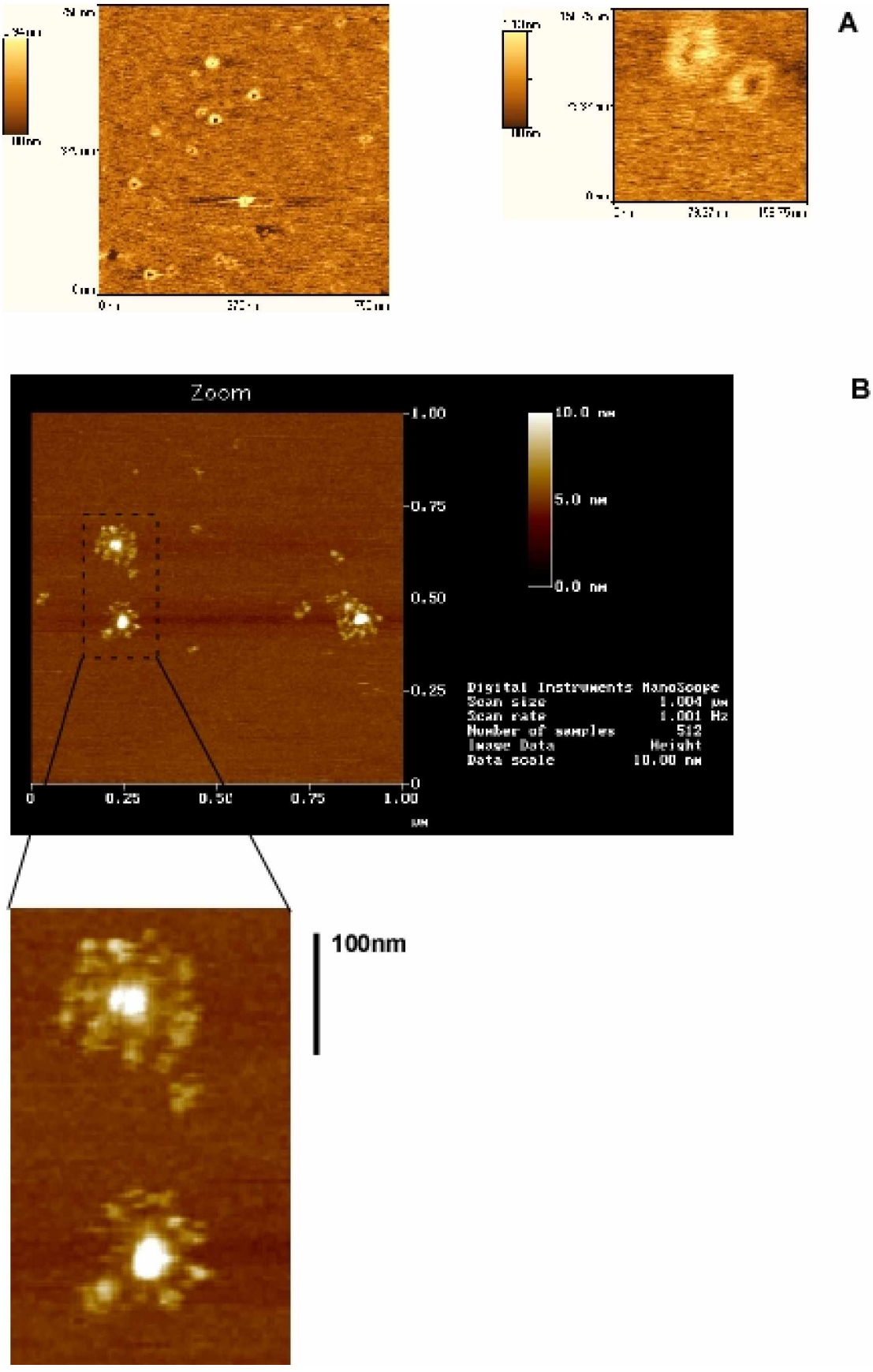

Fig. 38. Atomic force microscopy of SMC in dry state (A) performed by Frank Noll, physikalische Chemie, Philipps-Universität, Marburg and in solution(B) performed by Jens Schiener, Max-Plank Institute, Biochemie, Munich.

3.12 Purification and properties of Thermatoga maritima SMC

SMC proteins can be found almost in all bacteria species with some exceptions. A further aspect of this work was to verify results on a native form of SMC, containing no additional tags or fusions. Ideal candidate for such test experiments was SMC from *Thermatoga maritima.* Since this microorganism is a hyperthermophilic bacterium and its optimal growing temperature is 80°C, most of its proteins are highly stable at temperatures as high as 80°C. This property of its proteins makes them very convenient for purification without any modifications in protein sequence when they are expressed in a mesophilic organism such as *E. coli.* Thus, *T. maritima* SMC was expressed and purified for control experiments. Unfortunately all attempts to purify it resulted in high amounts of chromosomal DNA in all SMC fractions. Attempts to get rid of DNA via precipitation or treatment with DNase, resulted in a lose of SMC making control experiments impossible. Also, ScpA and ScpB were cloned from *T. maritima* for purification. In contrast to SMC, their expression was very low, so another thermophilic system should be used for future work.

3.13 Localization of cold shock proteins to cytosolic spaces surrounding nucleoids in Bacillus subtilis depends on active transcription

During this work I was also involved in a project that was not connected to the main topic of the work. My part of the work in this project consisted of investigation of the pattern of localization of *B. subtilis* cold shock proteins using immunofluorescence microscopy technique, and of the effects of deletion of cold shock genes on sporulation. Complete information on the work can be found in the attached paper in the appendix part.

4. Discussion

At the onset of this work very little was known about possible mechanisms of DNA condensation and cohesion by SMC proteins and of SMC complexes in any cell. *In vivo* studies of *B. subtilis* SMC performed by J. Mascarenhas and P. Graumann in our lab, showed that in the cell, SMC interacts with two novel proteins, ScpA and ScpB. All three proteins are present in certain discrete positions (foci) on the nucleoids, associated with DNA, and the localization pattern is dependent on the cell cycle, and even remains after overproduction of SMC. Although interaction and importance of SMC, ScpA and ScpB was shown *in vivo*, the question remained, how these condensation/segregation centers work and what the function of ScpA and ScpB is in the complex. This work provided biochemical investigation of SMC and the SMC complex with ScpA and ScpB *in vitro*, giving some clues on mechanisms of chromosome condensation and segregation.

All eukaryotic SMC proteins and the *E. coli* analogue of SMC, MukB perform their function in cells in complex with a number of different proteins. Although the function of these subunits of the SMC complex differs dependent on the type of SMC they interact with, the overall structure of all SMC complexes appears to be similar and these proteins interact with SMC in a close proximity to the head domains. Being a very "sticky" protein with a large molecular weight of 135 kDa for a monomer and 270 kDa for a dimer, SMC sets a lot of limitations on purification and work with it. SMC as well as ScpA are very easy to precipitate in attempts to concentrate them or in experiments that require change of salt conditions and pH. In this work I found conditions to purify an active SMC and reconstitute its complex with ScpA and ScpB. It was shown that the *B. subtilis* SMC complex is not an exception in means of complex architecture from eukaryotic SMC complexes and SMC complex proteins: ScpA and ScpB are able to interact with just a head domain and bind either to a part of coiled-coil domain which is very close to head domain (not further than 50 a. a. from head domain) or to the head domain of SMC itself. Experimental data obtained from native PAGE-shift assay and SPR experiments suggest that both ScpA and ScpB are needed to form a stable complex and that most likely ScpB, which is a dimer in solution, interacts with SMC via ScpA (see model on Fig. 39). Unlike ScpB, ScpA can exist in a monomer as well as in a dimer form in solution with possible formation of even higher order multimers. Dimerization (or even a multimerization) of ScpA

bound to ScpB and head domains of SMC might be one of mechanisms by which SMC brings and bridges its head domains together. This mechanism can be found in eukaryotic **c**ohesin complex where head domains of SMC1 and SMC3 are locked by Scc1 protein. This model for *B. subtilis* SMC can be supported by two facts: first one is that terminal parts of ScpA have a sequence similarity to Scc1 and the second fact is that ScpA sequence computer analyses has predicted a high probability of coiled-coils formation**,** indicating that ScpA is very likely to form dimers or multimers**.** Although in case of prokaryotic SMC it is possible that this is not the main mechanism of bridging heads together, dimerization of ScpA still can be a stabilizing factor in interaction of the head domains.

In vitro, ScpA and ScpB were found able to interact with each other and form two different types of complexes in absence of SMC. Analyses of native weights of this complexes showed that the smaller one most likely consists of one ScpA molecule bound to a ScpB dimer while the bigger one is probably composed of two ScpA molecules and two ScpB dimers. Taking in account the possibility of dimer formation by ScpA, the bigger ScpA/ScpB complex can be described as two smaller complexes (one ScpA and one ScpB dimer) dimerized via ScpAs.

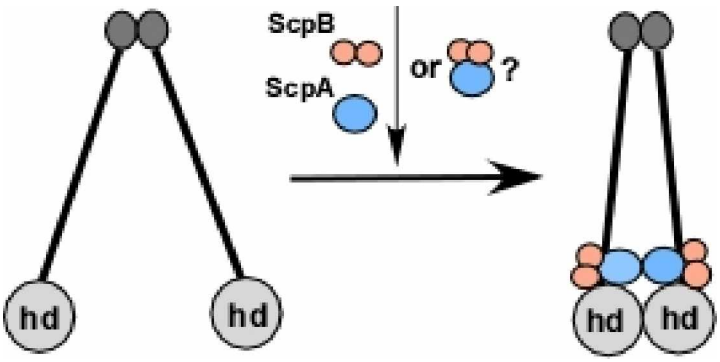

Fig. 39 Model for the SMC/ScpA/ScpB complex formation.

Reconstitution of the SMC complex *in vitro* resulted in formation of a complex with a native weight of approximately 460 kDa. Taking into account gel filtration data for SMC, ScpA and ScpB, analysis of the possible composition of the complex with such native weight resulted in a complex that consists of one SMC dimer and combination of ScpAs and ScpBs with total weight similar to that of a 2ScpA/4ScpB complex. The fact that ScpA and ScpB are able to form stable complexes in the absence of SMC allows us to conclude that most likely SMC complex formation

occurs in two steps. The first step is formation of the ScpA/ ScpB complex and the second step is binding of a big ScpA/ScpB complex (or two small ScpA/ScpB complexes) to SMC. Although, and we cannot exclude the possibility of consequent interaction of SMC with ScpA and ScpB avoiding the step of ScpA/ScpB complex formation (Fig. 39), my data strongly favor the view that SMC interacts with a 2ScpA/4ScpB complex.

Although SMC was shown to have an ATP-dependent single stranded DNA binding activity (Hirano and Hirano 1998) and *in vivo* studies showed association of SMC with DNA in the cell, no interaction of SMC with double stranded DNA could be detected until recently. This work provided the proof of the ability of SMC to bind double stranded DNA *in vitro*. Previous models suggested binding of SMC to DNA via head domains, assuming that DNA binding activity is dependent on ATPase function of head domain. These models were not confirmed by experimental data since SMC demonstrated ability to associate with DNA in absence of ATP and independently of ScpA and ScpB. Moreover, hinge and head domains of SMC, individually showed no DNA binding activity. Although the SMC head domain showed some affinity to DNA**,** it was at least 10 times smaller than that of the complete SMC. ScpA and ScpB were also unable to bind DNA *in vitro*. Thus, DNA binding activity of SMC does not belong to a certain SMC domain and a complete SMC protein with all its domains is needed for a proper function and DNA binding.

In the beginning of investigation of DNA binding activity of SMC in this work, the assumption was made that binding of SMC to DNA could be sequence specific and that SMC binds to certain regions of the chromosome, but experimental data proved this assumption wrong since no experiments showed any specificity in DNA binding for SMC. Rather, the structure of DNA appeared to be much more important than its sequence. While kinetics of SMC binding to DNA seems to be independent both on sequence and structure of DNA, the manner in which SMC releases its substrate differs depending on DNA structure. Native gel shift experiments showed that interaction of the SMC with linear DNA with unfixed ends was not stable and always resulted in a smeared pattern of DNA migration in the gel. In the SPR experiments, SMC could bind nonspecifically to dsDNA and after washing was released from the linear DNA fixed on the surface of the chip only with one end but not from the DNA fixed on the chip with both ends. Therefore, a closed bridge-like structure of the DNA is more important for SMC binding than its sequence. These findings disprove the old model of binding of SMC to DNA via head domains, and

can be explained by the model of formation of a ring-like structure by SMC around DNA (Fig. 40). In this model SMC interacts with DNA by embracing its long arms around substrate and leaving DNA trapped in between its arms by closing of the ring through the interaction of its head domains. In this case, SMC association with DNA will be more stable in case of a "closed" structure of the DNA (for example bridge-like structure on the surface of the Biacore chip) and will easily slip off the linear "open" DNA. This model can also explain smearing of the DNA in the native gel shift experiments with SMC since due to the electric field and gel conditions SMC can easily slip off the DNA during migration in the gel therefore making clean sharp DNA shift impossible. Another reason for smearing can be the fact that because of the sequence independent DNA binding, there is not any defined number of the bound SMC molecules per one DNA molecule and thus shift of each DNA molecule would be different depending on the number of associated SMC molecules. In spite of the fact that "ring" formation by SMC is most likely the main mechanism for DNA binding, it should be mentioned that there is a possibility that small domains with low affinity to DNA exist within coiled-coil domains of SMC which could help in association of SMC with DNA during the "ring" formation.

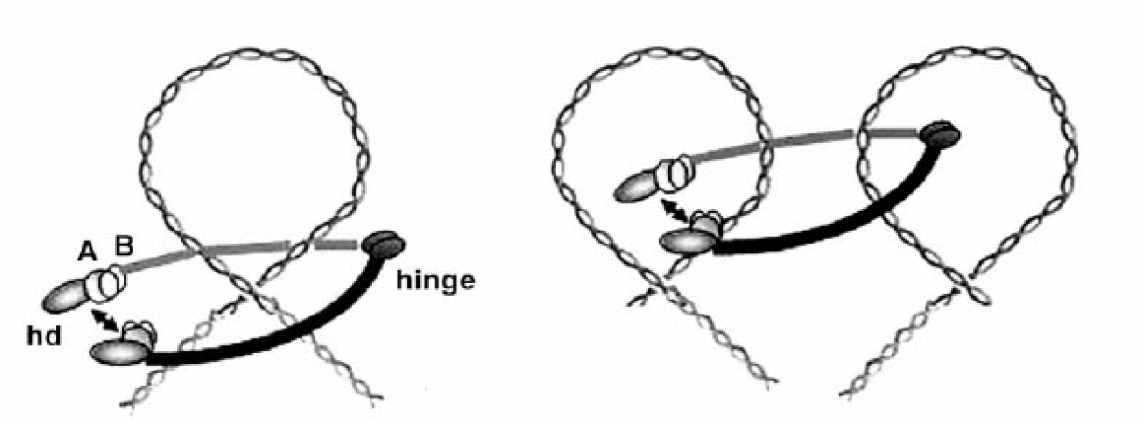

Fig. 40 Model for architecture and DNA binding of the bacterial SMC complex. hd, SMC head domain; A, ScpA; B, ScpB. The SMC complex could condense DNA by introducing loops or by interlocking different DNA loops.

For eukaryotic condensin, using electron spectroscopy imaging (ESI) it was shown that it is able to introduce two or more supercoils into the closed circular DNA in ATP dependent manner *in vitro* (Bazett-Jones, Kimura et al. 2002). In the suggested model each of the globular head domains of condensin wrapped DNA around itself providing two supercoiling turns. Similarly to condensin, prokaryotic

SMC could also provide supercoils into the DNA by means of binding of DNA to low affinity regions while dimerization of the heads would prevent DNA from releasing.

It was mentioned above that the eukaryotic cohesin complex performs its function in sister-chromatid cohesion by a similar mechanism of embracing its arms around chromatids and through Scc1 which serves as a locking mechanism between the head domains and computer analysis of protein sequences showed that Scc1 has a sequence similarity to ScpA. All these facts together allow us to suggest that the prokaryotic SMC complex is an ancestor of cohesin. However, the fact that localization centers of SMC in the *B. subtilis* cells are more close to the cell poles rather to the middle of the cell where chromosome cohesion occurs, suggests that it is a condensation factor and is not involved into cohesion of chromosomes. Taking all the facts mentioned above into consideration we can conclude that SMC most likely condenses DNA via cohesin-like binding, introducing loops into the DNA and locking different supercoils of DNA (see Fig. 40) making thereby the structure of the nucleoid more compact and dense.

Another question addressed in this work was the importance and function of ATPase activity of the head domains of SMC. Previously it was shown (Hirano and Hirano 1998) that SMC is able to precipitate single stranded DNA in the presence of ATP and ATPase activity of SMCs is DNA-dependent. Moreover, ATPase mutants of eukaryotic SMCs are not associated with DNA anymore and in the case of Rad50 mutants with abolished ATPase activity, proteins show reduced ability to dimerize their head domains. However, the role of ATPase activity in the function of SMC remains unclear and not much is known about the regulation of this activity, if it exists at all. Head domains of SMC share the same fold with ATP-binding cassette (ABC) family of ATPases and contain three conserved motifs that are typical for this family: Walker A, Walker B and C motif**,** also known as “signature motif”. While Walker A and Walker B motifs form the ATP binding pocket and therefore are responsible for association of ATPase with ATP, signature motif is responsible for ATP hydrolysis. Crystal structure studies of the *Thermatoga maritima* SMC head domain have shown that in the head domain Walker A and Walker B motifs are topologically separated from the signature motif (which is also typical for all ABC-transporters family) and therefore ATP cannot be hydrolyzed by a single head domain. Crystal structure studies of ATPase domains of ABC-type transporters showed that in presence of ATP they form a dimer with two bound ATP molecules so that each ATPase domain provides one ATP-binding pocket formed by Walker A and

Walker B motifs which will interact with signature motif from the other domain and two functional ATPases will form through dimerization. It was shown that ATP hydrolyses results in a conformational change in the ABC-transporter providing transport of the corresponding molecule through the membrane. Thus, in the same manner, ATPase activity of SMCs can only be established by bringing two head domains together. In other words, binding of ATP to head domains might induce dimerization of head domains so that two ATP molecules would become sandwiched in between the domains, keeping heads together and therefore providing "ring" formation by SMC and association with DNA as described above**.** On the other hand, ATP hydrolysis would cause dissociation of head domains and release of the DNA. One support for this idea was given by protein-protein cross-linking assay, performed by M. Hirano et al. that has shown that ATPase activity is important for interactions between SMCs (Hirano, Anderson et al. 2001). At the same time, the possibility of the ring closing via dimerization of head domains was also confirmed by crystal structure studies of the head domain of Rad50 in presence of ATP. Data obtained in my work from experiments with SMC ATPase mutants gave additional support for this model. The Walker A mutant of SMC, which is unable for ATP binding and therefore according to the model is unable to form a "ring" and bind DNA, showed no DNA binding activity as was predicted. At the same time, the signature motif mutant, with ATP binding activity but with abolished ability to hydrolyze ATP, could bind DNA as wild type SMC with only slightly reduced affinity to DNA. Additional support for this model was given by the DNA binding studies of cohesin complex, performed by Nasmyth and Uhlmann groups (Arumugam, Gruber et al. 2003; Weitzer, Lehane et al. 2003). Similarly to bacterial SMC, it was found that SMC subunits of cohesin are able to form a ring by themselves via ATP dependent interaction of the heads and it was shown that ATP hydrolysis is needed for loading of cohesin onto DNA. These findings fit perfectly with the model of ABC-transporters dimerization. It remains an important point to be investigated how ATPase function of SMC and therefore DNA binding/release are controlled and regulated.

In contrast to its DNA binding activity, complex formation of SMC with ScpA and ScpB was not severely affected by introduction of mutations into Walker A and Walker B motifs. Mutants were still able to form a complex although the affinity to DNA was slightly reduced. That means that ATP binding and hydrolysis are not required for complex formation, but that these activities of SMC have some influence

on the function of the protein. In the case of cohesin, abolishment of ATPase activity has a much more severe effect on the complex formation (Arumugam, Gruber et al. 2003), and ATP binding on SMC1 but not on SMC 3 was needed for association with Scc1, while, similarly to bacterial SMC mutations that blocked ATP hydrolysis had no effect on complex formation.

Analysis of purified SMC has shown that even after all steps of purification it remained associated with a small amount of DNA that could only be removed by treatment with DNase. This strong interaction with DNA made also *Thermatoga maritima* SMC difficult for studying since it was impossible to pull it down separately from chromosomal DNA. Gel filtration analyses of the SMC interaction with ScpA suggested that it is possible that ScpA causes DNA release from SMC while interaction of SMC with ScpA in presence of ScpB has no effect on the bound DNA. This idea is also supported by the fact that cleavage fragment of Scc1 one from cohesin complex blocks interaction of the head domains thereby causing opening of the ring and DNA release (Weitzer, Lehane et al. 2003). ATPase activity studies performed by the Hirano group (Hirano and Hirano 1998; Hirano, Anderson et al. 2001) have shown that ATPase activity is very weak relatively to that of ATPases from ABC family though the structure of the SMC head domain is very similar to the structure of the ABC ATPase cassette. This reduced ATPase activity can be explained if we assume that SMC needs an additional factor for a proper hydrolysis of ATP and that the activity that was detected by Hirano group was just a background activity in the absence of this cofactor. Therefore, combining facts that “ring” formation by SMC and DNA binding require ATP loading onto SMC and DNA release would probably require opening of the SMC ring and thus ATP hydrolysis, with the notion that ScpA probably causes DNA release from DNA, the suggestion can be made that ScpA could be the factor that induces ATP hydrolysis in the SMC complex. Since no DNA release was detected in interaction of SMC with ScpA together with ScpB we can assume that ScpB serves as an inhibitor of ScpA mediated ATPase activity of SMC.

If the described model is correct then in the cell there are possible two ways for SMC after DNA is bound. If both ScpA and ScpB are present in the neighborhood of SMC, then the SMC/ScpA/ScpB complexes will be formed providing DNA condensation, and ScpA/ScpB would prevent SMC rings from opening by ATPase activity inhibition and by possible locking of the rings by ScpA dimerization. If ScpB is not present in the cell, then ScpA would induce hydrolyses of ATP by SMC and no

DNA condensation would occur (Fig. 41). This second scenario is possible when cells are in stationary phase and chromosomal DNA is decondensed. Therefore cells would be able to control condensation state of DNA via control of the ScpB level. This control can be done on the transcriptional or the translational level as well as via proteolysis. However, additional experiments should be done to finally prove the model for ScpA/ScpB control of the DNA binding/release by SMC right (represented by the right half of the figure 41).

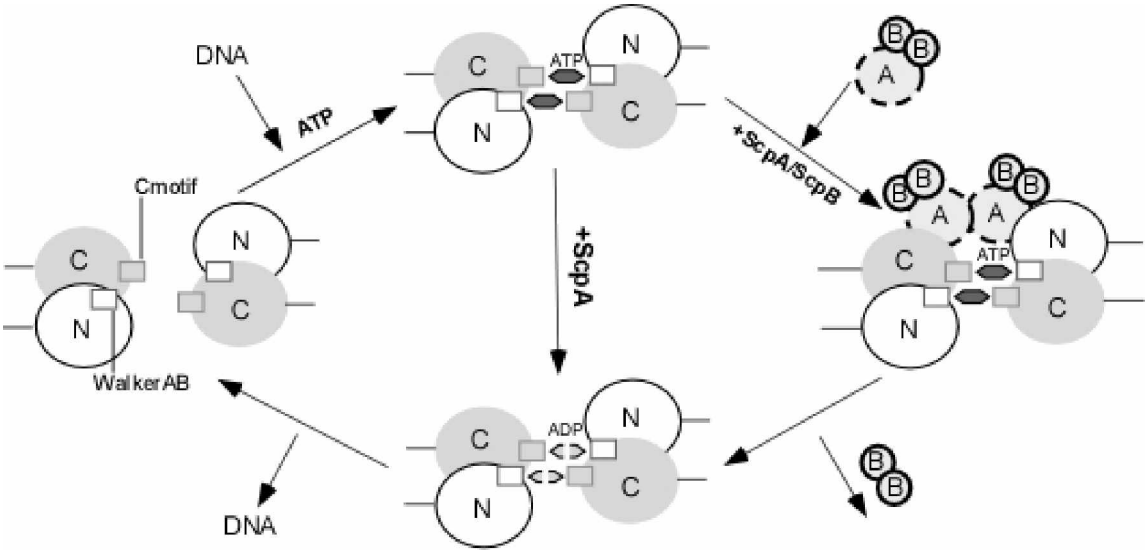

Fig. 41 Model for SMC binding to and release from DNA. ATP binding dimerizes SMC head domains, because the C motif of one head interacts with the Walker A/B binding pocket of the other head, so that two ATP molecules are sandwiched between the domains, similar to ATP cassettes of ABC transporters. DNA is encircled by the long coiled coil arms of SMC, so that dimerization of head domains leads to closure of the SMC ring. ATP hydrolysis induced by ScpA leads to opening of the SMC ring, and thus to DNA release. Alternatively binding of ScpA/ScpB stabilizes head domain dimerization preventing ATP hydrolysis until ScpB release. The ScpAB complex most likely interacts with the open form of SMC, and might trap SMC in the closed form by tightly bridging head domains. However, other binding modes of ScpA and ScpB to SMC are possible.

In vivo, the SMC complex as well as its *E. coli* homologue MukB/E/F are not distributed throughout the cell but are located in certain regions of the cell forming foci**,** and it was shown in our group that in case of *B. subtilis* SMC even its overproduction does not change this localization pattern. AFM experiments helped to visualize SMC *in vitro* and gave some clues about the possible mechanisms of foci

formation. Ring-like structures that were detected with AFM of dried SMC under low salt conditions can be explained either by the “ring” structure model of SMC or by multimers formation by SMCs via multimerization of head domains and formation of circle structures. Ring formation is supported by the fact that estimation of the possible diameter of SMC rings results in a value that is similar to the diameter of rings detected on AFM. However, the equal height of or sectors of the AFM “rings” and the impossibility to distinguish head and hinge domains from coiled-coil domains can be explained by the second model of SMCs multimerization via head domains (Fig. 42). The difficulty to distinguish certain domains of SMC on AFM can be explained by a high mobility and flexibility of the long coiled-coil domains which can be easily shifted by the atomic needle**,** making the signal not very precise.

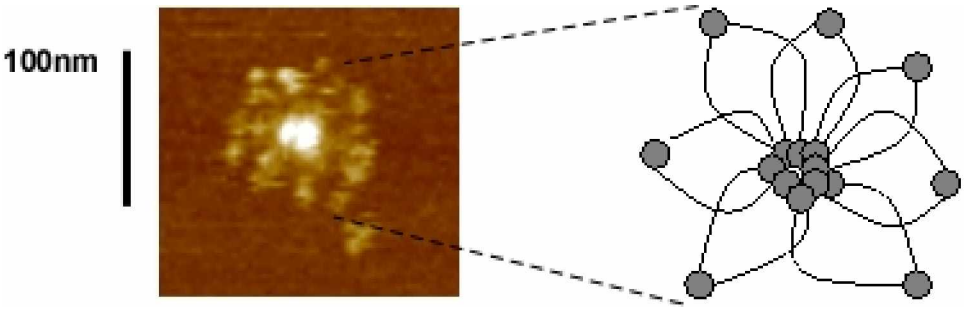

Fig. 42 Model for foci formation by SMC. Head domains of SMCs interact with each other and are accumulated in the middle of the structure while hinges look outside.

“Sun”-like structures obtained on AFM in the liquid medium also supported the model of multimer formation by SMCs. These structures could also be formed by multimerization of SMC via their head domains or by interlocking of multiple SMC via ring formation around each other. In this case because of the close proximity of head domains from different SMCs, it is possible that dimerization could occur between head domains that belong to different SMC molecules. It should be mentioned that we cannot exclude the possibility of the presence of DNA in this “sun”-like structures which cannot be distinguished from coiled-coil domains of SMC on AFM.

In vivo investigation of *B. subtilis* SMC, performed in our group, showed that in the cells SMC are concentrated in the discrete foci. It was found that when replication is blocked or just in the beginning of the replication, SMC complexes are

concentrated in one focus which is located very close to the center of the cell, but as replication goes on this focus divides into two which rapidly move towards cell poles and remain there until next round of replication. Combining these data with AFM data for large structures formation by SMC, we can suggest that SMC is loaded on the newly replicated DNA close to replication forks (possibly in eukaryotic cohesin manner), which are located in the center of the cell, but as replication goes on, SMCs would be pushed with DNA towards the cell poles and there, interacting with other SMC complexes could form similar large structures to what was observed on AFM. Thus, SMC foci that can be seen in the cell can be this “sun” like structures but in a larger scale. Therefore, the compact structure of nucleoid is possibly achieved by introduction of supercoils into DNA through topoisomerases and by interlocking supercoils through the SMC complex, rather than by some mechanical action of SMC.

Obviously all the data presented in this work are just a tip of the iceberg and lots of experiments remain to be done to fully understand the mechanisms of SMC complex formation, action and regulation. In particular, calorimetric studies for interactions in complex and crystal structure studies should be performed for proper understanding of complex structure and additional experiments are needed to prove and enhance models for DNA binding and foci formation, described above.

5. Appendix

5.1 Localization of cold shock proteins to cytosolic spaces surrounding nucleoids in Bacillus subtilis depends on active transcription

JOURNAL OF BACTERIOLOGY, Nov. 2001, p. 6435–6443 Vol. 183, No. 21
0021-9193/01/$04.00+0 DOI: 10.1128/JB.183.21.6435–6443.2001

Localization of Cold Shock Proteins to Cytosolic Spaces Surrounding Nucleoids in *Bacillus subtilis* Depends on Active Transcription

MICHAEL H. W. WEBER, ARSEN V. VOLKOV, INGO FRICKE, MOHAMED A. MARAHIEL, AND PETER L. GRAUMANN*

Biochemie, Fachbereich Chemie, Philipps-Universität Marburg, 35032 Marburg, Germany

Received 18 June 2001/Accepted 21 June 2001

Using immunofluorescence microscopy and a fusion of a cold shock protein (CSP), CspB, to green fluorescent protein (GFP), we showed that in growing cells *Bacillus subtilis* CSPs specifically localize to cytosolic regions surrounding the nucleoid. The subcellular localization of CSPs is influenced by the structure of the nucleoid. Decondensed chromosomes in *smc* mutant cells reduced the sizes of the regions in which CSPs localized, while cold shock-induced chromosome compaction was accompanied by an expansion of the space in which CSPs were present. As a control, histone-like protein HBsu localized to the nucleoids, while β-galactosidase and GFP were detectable throughout the cell. After inhibition of translation, CspB-GFP was still present around the nucleoids in a manner similar to that in cold-shocked cells. However, in stationary-phase cells and after inhibition of transcription, CspB was distributed throughout the cell, indicating that specific localization of CspB depends on active transcription and is not due to simple exclusion from the nucleoid. Furthermore, we observed that nucleoids are more condensed and frequently abnormal in *cspB cspC* and *cspB cspD* double-mutant cells. This suggests that the function of CSPs affects chromosome structure, probably through coupling of transcription to translation, which is thought to decondense nucleoids. In addition, we found that *cspB cspD* and *cspB cspC* double mutants are defective in sporulation, with a block at or before stage 0. Interestingly, CspB and CspC are depleted from the forespore compartment but not from the mother cell. In toto, our findings suggest that CSPs localize to zones of newly synthesized RNA, coupling transcription with initiation of translation.

Cold shock proteins (CSPs) constitute a widespread and highly conserved protein family in bacteria, and multiple copies of CSPs are often present (10, 25). *Haemophilus influenzae* contains a single *csp* gene, while *Bacillus subtilis* contains three *csp* genes and *Escherichia coli* contains nine. The sequence identity for CSPs and the cold shock domain that has been identified in a variety of eukaryotic RNA-binding proteins is remarkably high, suggesting that there is a conserved function for CSPs and the cold shock domain (11).

Synthesis of all CSPs (CspB, CspC, CspD) in *B. subtilis* is strongly induced following cold shock and entry into the stationary phase (for CspB and CspC), while CSPs are also present at 37°C (6, 9). Cold shock induction occurs mainly at the posttranscriptional level, while transcriptional activation of *csp* genes is only modest (6, 19, 31). Deletion of one or two *csp* genes leads to an increase in synthesis of the other CSP(s) and influences the synthesis of many other cytosolic proteins (6). *cspB cspD* and *cspB cspC* double mutants show growth impairment at 15°C as well as at 37°C. These findings suggest that CSPs can complement each other and cross-regulate their synthesis. The presence of at least one CSP is necessary for viability of *B. subtilis* at low and optimal growth temperatures, and depletion of CSPs leads to compromised and deregulated protein synthesis (6). CSPs consist of a five-stranded β-barrel with highly conserved RNA-binding epitopes (RNP motifs) on adjacent β-strands. Mutational analysis has shown that RNP motifs are essential for binding to single-stranded DNA (ssDNA) and to RNA (28). CSPs bind cooperatively to single-stranded nucleic acids, and their affinity for ssDNA is somewhat greater than their affinity for RNA (6, 17). Longer RNA molecules are bound only after heat denaturation, suggesting that CSPs bind to linear single-stranded nucleic acids instead of highly structured nucleic acids. Interestingly, *B. subtilis* CSPs are highly susceptible to proteolysis in vitro, while they are rather stable in vivo. Based on the finding that binding to substrate nucleic acids strongly protects CSPs in vitro, CSPs appear to be heavily associated with ssDNA and/or RNA in vivo (27). It has been suggested that CSPs may act as transcription activators of other cold-induced genes or as RNA chaperones during initiation of translation.

According to recent reports (1, 23), transcription in bacteria seems to occur mostly on the centrally located nucleoid that contains the bulk of the DNA, while translation appears to take place mainly at cytosolic sites surrounding the nucleoid. It has been proposed that the coupling of transcription and translation to insertion of proteins into membranes and transport across the cytosolic membrane pulls DNA towards the membrane, thereby decondensing chromosomes, which otherwise form a more compacted structure (e.g., in the stationary phase) (32). We have proposed a model in which CSPs cooperatively bind to nascent transcripts and prevent formation of secondary structures in RNA that would impair initiation of translation (6). As the affinity of CSPs for ssDNA and RNA is moderate, ribosomes could displace CSPs from RNA and initiate translation on a linear template. Thus, CSPs would strongly affect the coupling of transcription to translation in bacteria. This model was recently supported by biochemical data obtained by Hanna and Liu (13), who reported a strong association of

* Corresponding author. Mailing address: Biochemie, Fachbereich Chemie, Hans-Meerwein-Straße, Philipps-Universität Marburg, 35032 Marburg, Germany. Phone: 49 (0) 6421 2825539. Fax: 49 (0) 6421 2822191. E-mail: graumann@chemie.uni-marburg.de.

TABLE 1. *B. subtilis* strains

Strain	Genotype	Reference
64BCDbt	*cspB*::*spc cspC*::*kan cspD*::*cat* pDGcspB	6
JH642	*pheA1 trpC2*	31
PK9C8	*hbs-gfp* P_{spac}-*hbs*	21
MW1	*amyE*::*xylR*-P_{xyl}-*gfp-cat*	This study
MW2	*cspB-gfp*	This study
MW3	*cspB-gfp cspC*::*kan*	This study
MW4	*cspB*::*cat cspC*::*kan cspD*::*cat* pDGcspB	This study
MW5	*cspC*::*kan cspD*::*cat cspB-gfp* pDGcspB	This study

E. coli CspE with several short transcripts after in vivo cross-linking.

In this study, we investigated the subcellular localization of *B. subtilis* CSPs. We found that all three CSPs are present in cytosolic spaces surrounding the central nucleoid. So far, a similar localization has been reported only for a ribosomal protein in *B. subtilis* (23), suggesting that CSPs function in the same cellular location as ribosomes rather than on the nucleoid. However, inhibition of transcription eliminated specific localization of CspB, indicating that CspB binds to RNA during transcription. We also found that CSPs influence the structure of the nucleoid, which supports the hypothesis that these molecules function in coupling transcription and translation.

MATERIALS AND METHODS

Media and growth conditions. *E. coli* XL1-Blue {*recA endA1 gyrA96 thi-1 hsdR17 supE44 relA1 lac* [F′ *proAB lacI*^{q}ZΔ*M15* Tn*10*(Tet^r)]; Stratagene} was grown in Luria-Bertani (LB) rich medium supplemented with 50 μg of ampicillin per ml when it was appropriate. *Bacillus* strains were grown in 2xYT rich medium or DSM sporulation medium. For expression of green fluorescent protein (GFP) in *B. subtilis* MW1 (see below), Spizizen's minimal medium (14) supplemented with 0.2% (wt/vol) fructose instead of glucose, 50 μg of tryptophan per ml, and 50 μg of phenylalanine per ml was used. Xylose was added to a final concentration of 0.5% to activate the P_{xyl} promoter controlling transcription of *gfp*. Isopropyl-β-D-thiogalactopyranoside (IPTG) (final concentration, 1 mM) was added to the growth medium of *B. subtilis* MW4 (see below) and 64BCDbt (6). For inhibition studies, rifampin, chloramphenicol, kanamycin, or spectinomycin was added to a final concentration of 200 μg/ml. Cells were incubated for 30 min before image acquisition. S750 minimal medium (16) was used for growth for microscopy.

Plasmid construction. By using primers 5′cspB-OrfUp (5′-AGAGAGCTCA GAAAATTTGAAGAAACCAC-3′) and 3′cspB-gfp (5′-AAACCCGGGACGC TTCTTTAGTAACGT-3′) and primers 3′cspB-gfp-Trm3′Orf (5′-GAAAAGCT TAAGCATAAATTGATATGAAAAACT-3′) and 3′cspB-OrfDown (5′-GGAC TCGAGAAATCAGAGATCATTTAAA-3′), a *cspB*-containing upstream fragment that did not include the *cspB* stop codon (5′ fragment, 1,958 bp) and a fragment downstream of the *cspB* gene (3′ fragment) were amplified from *B. subtilis* JH642 chromosomal DNA by PCR. The 5′ fragment was cloned into pCW8 (30) by using *Sac*I and *Sma*I, resulting in plasmid pMW_BGFP-1. Next, the 3′ fragment was cloned into pMW_BGFP-1 by using *Hin*dIII and *Xho*I. The resulting plasmid, pMW_BGFP-2, was linearized by *Hin*dIII digestion and ligated with a 1,660-bp *Hin*dIII fragment obtained from pDG647 (*Bacillus* Genetic Stock Center, Columbus, Ohio) containing an erythromycin resistance cassette, which yielded pMW_BGFP. The integrity of this plasmid was verified by sequencing the entire *cspB* gene, including its 5′ untranslated leader region and promoter region, as well as the junction between *cspB* and *gfp*, using an ABI Prism 310 genetic analyzer. The linker sequence between CspB and GFP is SRAAGIRLEK, and the entire fusion protein comprises 317 amino acids (molecular weight, 35,600; pI 5.50). By introducing *Spe*I and *Bam*HI restriction sites, a DNA fragment carrying the entire *gfp* gene was amplified from pCW8 (30) with primers 5′gfp-Express-pX (5′-ATAAACTAGTAGGAGGTAGAAAAA ATGAGTAAAGGAGAAG-3′) and 3′gfp-Express-pX (5′-CCTAGGATCCAT GCTATTTGTATAGTTCATCCAT-3′), and it was subsequently cloned into the *Spe*I and *Bam*HI sites of the *B. subtilis amyE* integration vector pX (20). Plasmid pMW_gfp was tested for the presence of *gfp* by digestion analysis and by PCR.

Bacterial strains. For construction of *B. subtilis* MW1 (*amyE*::*xylR*-P_{xyl}-*gfp-cat*), plasmid pMW_gfp was linearized with *Sca*I and transformed into *B. subtilis* JH642 (*pheA1 trpC2*), with selection for resistance to 10 μg of chloramphenicol per ml. Double-crossover integration was verified by performing a starch assay with Lugol's solution (Merck, Darmstadt, Germany) on LB medium plates containing 1% starch. Transformation of *B. subtilis* JH642 and 64C (6) with *Sca*I- and *Xho*I-linearized plasmid pMW_BGFP and selection for resistance to 1 μg of erythromycin per ml and 25 μg of lincomycin per ml resulted in *B. subtilis* MW2 (*cspB-gfp*) and MW3 (*cspB-gfp cspC*::*kan*), respectively. To construct MW4 (*cspB*::*cat cspC*::*kan cspD*::*cat* pDGcspB), *B. subtilis* 64BCDbt (6) was transformed with *Sca*I-linearized pX (20). Transformants were selected on LB medium plates containing 30 μg of chloramphenicol per ml. In contrast to parental strain 64BCDbt, strain MW4 did not contain the spectinomycin resistance cassette in the *cat*-disrupted *cspB* gene locus, as determined by PCR analysis of the *cspB* gene locus (Table 1), but instead contained two *cat* genes. For construction of MW5 (*cspC*::*kan cspD*::*cat cspB-gfp* pDGcspB), chromosomal DNA prepared from MW3 was used for transformation of MW4 to obtain MW5 after selection on LB medium plates containing 1 μg of erythromycin per ml and 25 μg of lincomycin per ml. In contrast to 64BCDbt, growth of MW5 was not affected by depletion of IPTG. As determined by PCR, continued growth of MW5 without selection for phleomycin resistance resulted in loss of pDGcspB after approximately 2 weeks, in contrast to growth of 64BCDbt, which did not lose this plasmid.

Immunofluorescence microscopy. Immunofluorescence microscopy was performed as described by Pogliano et al. (26). Anti-CspB, anti-CspC, and anti-CspD sera were used at concentrations of 1:2,500 to 1:10,000. 4′,6′-Diamidino-2-phenylindole (DAPI) was used at concentrations of 200 to 500 ng/ml; FM4-64 was used at a concentration of 1 nM.

Image acquisition. Fluorescence microscopy was performed with an Olympus AX70 microscope by using Xenon epifluorescence. Cells were grown in S750 medium (16) and were mounted on agarose pads containing growth medium on object slides. Images of live cells or images of fixed cells were taken with the same exposure time. For stationary-phase cells, culture supernatant was used for the agarose pads. Images were acquired with a digital charge-coupled device camera, and three-dimensional image reconstitution was generated with the Metamorph program.

RESULTS

Intracellular localization of CSPs in growing cells. To study the subcellular localization of the major CSP, CspB, in *B. subtilis*, we constructed a fusion of CspB to GFP. The fusion was integrated by double crossover into the *cspB* locus of strain JH642 so that the *cspB-gfp* fusion was under the same control as wild-type *cspB*. Western blot analysis verified that the fusion was produced, replacing wild-type CspB. To investigate whether the fusion was active, it was necessary to combine the *cspB-gfp* fusion with *cspD* and *cspC* deletion mutants, since *csp* single

FIG. 1. Fluorescence microscopy of exponentially growing *B. subtilis* cells. Green, GFP; red, DAPI DNA stain; blue, membrane stain; monochrome, Nomarski differential interference contrast. (A) Live cells (MW1) expressing GFP at 25°C. (B) Live cells (MW2) expressing CspB-GFP at 25°C. (C) Immunofluorescence with anti-CspB serum and fixed wild-type cells (JH642) growing at 37°C. (D) Immunofluorescence with anti-CspB serum and wild-type cells 2 h after cold shock from 37 to 15°C. (E) Immunofluorescence with anti-β-galactosidase serum and wild-type cells growing at 37°C. (F) Immunofluorescence with anti-CspB serum and *cspB* deletion strain 64B growing at 37°C. (G) Immunofluorescence with anti-CspB serum and *smc* mutant cells growing at 23°C. (H) Live cells (PK9C8) expressing HBsu-GFP at 25°C. (I) Live cells (MW2) expressing CspB-GFP 4 h after induction of sporulation at 25°C. (J) Immunofluoresence with anti-CspB antiserum and fixed wild-type cells 3 h after induction of sporulation at 37°C.

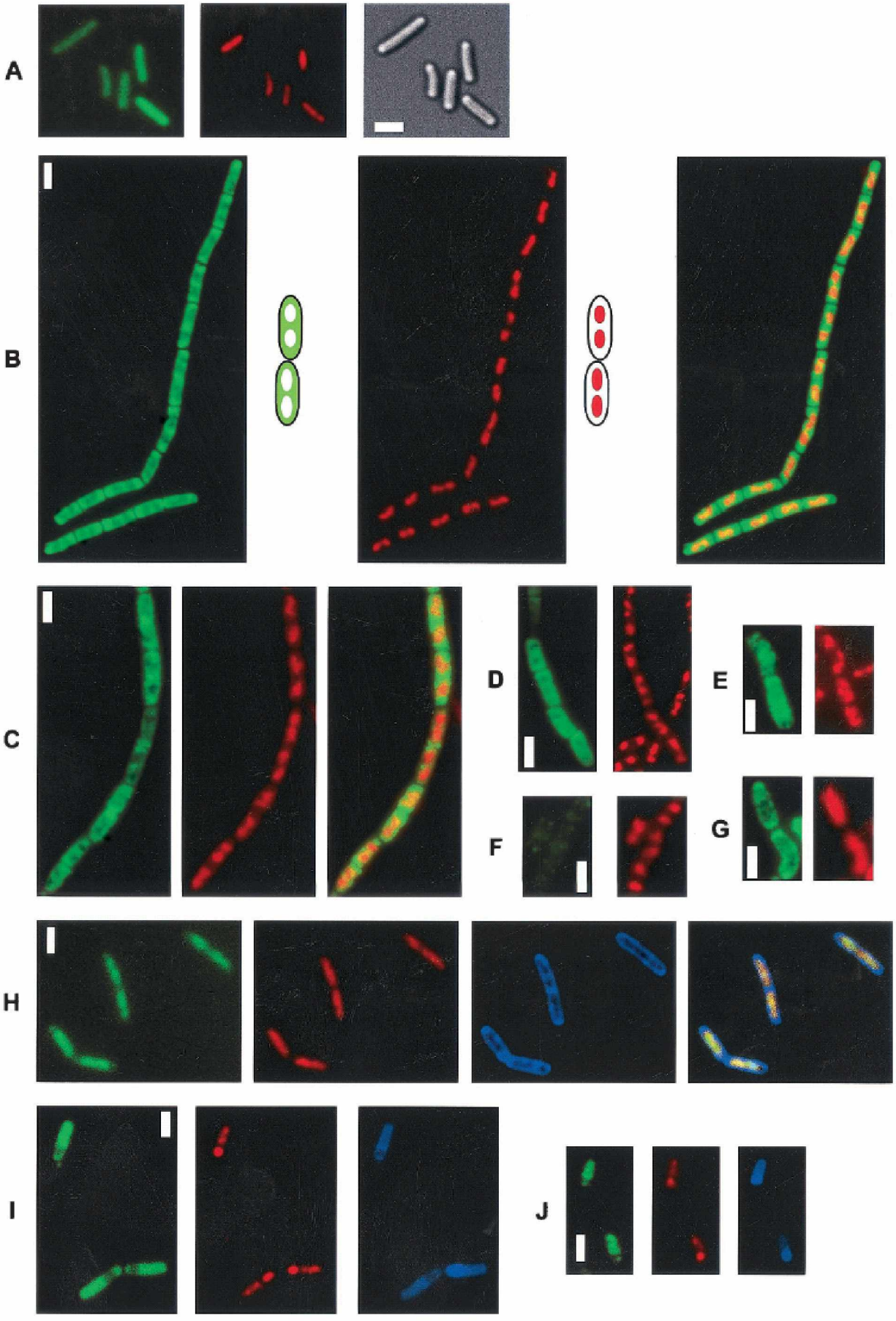
A
B
C
D
E
F
G
H
I
J

mutants had no detectable phenotype (6). A strain carrying *cspB-gfp* and having deletions of *cspC* and *cspD* is viable, whereas cells having deletions of all *csp* genes can survive only when they carry a plasmid encoding *cspB* in *trans* (6). Therefore, the CspB-GFP fusion was able to complement CspB function, at least in part (see below). Fluorescence microscopy of the resulting strain, strain MW2 (*cspB-gfp*), showed that CspB-GFP localized to the cytosol, as expected. However, the pattern of localization was different from that of GFP, which was present throughout the cell (Fig. 1A). CspB-GFP was observed only in cytosolic regions surrounding the nucleoids; most occurred at the cell poles, while nucleoids were devoid of CspB or had a drastically lower concentration of CspB (Fig. 1B). An overlay of GFP fluorescence with DNA stain (Fig. 1B, green-blue panel) revealed little overlay (yellow) of CspB and the DNA stain. To obtain better resolution of the location of the GFP fusion, three-dimensional images were reconstructed from Z sections taken through MW2 cells (data not shown). These analyses showed that central spaces in the cells were mostly devoid of CspB-GFP and that CspB was present not only at the cell poles but also between nucleoids and the membranes along the long axis of the cells. To determine if this pattern of localization is also valid for wild-type CSPs, we performed immunofluorescence microscopy with antisera raised against all *B. subtilis* CSPs (CspB, CspC, and CspD) (6). As shown in Fig. 1C, CspB localized around nucleoids indistinguishable from the CspB-GFP fusion protein; this was also observed for CspC and CspD (data not shown), while background staining was observed in a *cspB* deletion strain (Fig. 1F) (the same results were obtained with *cspC* or *cspD* mutant cells when the corresponding sera were used [data not shown]). In contrast, β-galactosidase was observed throughout the cells (Fig. 1E), without pronounced exclusion from spaces occupied by nucleoids. As a further control, we used HBsu-GFP, which localized entirely to nucleoids (Fig. 1H) (note that the overlay of GFP and blue DNA staining resulted in a yellowish color), as previously reported (21). Thus, HBsu and CSPs localize to two distinct subcellular regions in *B. subtilis*.

The fluorescence intensity was greater in a *cspC* deletion mutant carrying *cspB-gfp* than in wild-type cells and greatest in cells with a deletion of *cspC* and *cspD* (data not shown). This observation is in accordance with the previous finding that deletion of *csp* genes leads to higher levels of the remaining CSPs (6).

Nucleoid structure influences the localization of CSPs. After a shift from 37 to 15°C during the mid-exponential phase in rich medium, *B. subtilis* cells continue to grow, albeit at a very reduced rate, while the level of CSPs increases about twofold (10). Following cold shock, nucleoids in *B. subtilis* cells condensed significantly, as shown in Fig. 1D (Fig. 1C and D, compare the red stains), although the cell size and cell shape remained similar to the cell size and cell shape of cells growing at 37°C. Thus, as in cells in the stationary phase and after a block in translation (see below), cold shock leads to chromosome compaction, probably due to a decrease in the transcriptional and translational capacity of the cell. Immunofluorescence microscopy revealed that CSPs still localized around nucleoids and that the zones of localization increased concomitant with nucleoid compaction (Fig. 1D). Conversely, in *smc* mutant cells growing exponentially at a permissive temperature (23°C) in rich medium, which have a DNA-to-protein ratio similar to that of wild-type cells but strongly decondensed chromosomes (4, 8, 24), the cellular spaces occupied by CSPs decreased, and CSPs were detectable only in small spaces close to the cell membrane (Fig. 1G). Thus, in growing cells, CSP localization depends on the state of compaction of the DNA.

Entry into the stationary phase and inhibition of transcription but not inhibition of translation affect localization of CSPs. CSPs may localize to zones surrounding the nucleoids simply because of exclusion from the nucleoids, or alternatively, they may localize to zones of active transcription and/or translation. CSPs have been shown to bind to ssDNA, as well as to RNA, via a positively charged RNA-binding epitope (28), so there is no repulsion from DNA per se due to their overall negative charge. We therefore analyzed the localization of CSPs in stationary-phase cells, in which chromosomes were more compact (Fig. 2C) than they were in growing cells (Fig. 2A). Nucleoid compaction during the stationary phase was also observed in cells expressing HBsu-GFP (Fig. 2E) and thus is likely to represent the true situation in vivo instead of a fixation artifact. Soon after entry into the stationary phase, CspB-GFP was observed throughout cells (Fig. 2C), in contrast to the pronounced localization around nucleoids in growing cells (Fig. 2A). Similarly, using immunofluorescence, we found that CspB and CspC localized throughout the cytosol in the stationary phase (data not shown).

In order to analyze whether active transcription or translation or both are required for specific localization of CspB, exponentially growing cells were treated with inhibitors of transcription or translation. In contrast to growing cells (Fig. 2A), CspB-GFP was found throughout the cells after addition of rifampin (Fig. 2D), while CspB remained localized around nucleoids after addition of chloramphenicol (Fig. 2B), spectinomycin, or kanamycin (data not shown) in a manner similar to that in cold-shocked cells (Fig. 1D). To confirm relocalization of CspB upon inhibition of transcription, we performed immunofluorescence microscopy using CspB antiserum with wild-type cells and found that CspB localized throughout the cells after addition of rifampin (data not shown). We have no straightforward explanation for our finding that nucleoids decondensed after rifampin treatment, while treatment with translation inhibitors induced nucleoid compaction. In control experiments, we did not observe a noticeable effect on CspB-GFP localization or on nucleoid structure after addition of ethanol and methanol at concentrations used for the chloramphenicol and rifampin experiments, respectively (data not shown). Additional control experiments in which Western blotting was used showed that the CspB-GFP fusion is stable during the stationary phase and after addition of rifampin, eliminating the possibility that delocalized fluorescence might have been due to a GFP-containing proteolysis product of the fusion. These findings show that inhibition of transcription eliminates specific localization of CspB.

Absence of CSPs leads to a defect in nucleoid structure and in chromosome segregation. Two CSPs have been identified as high-copy-number suppressors of chromosome decondensation defects in *E. coli* cells (15, 34). We therefore analyzed nucleoid morphology in *csp* deletion strains during exponential growth. Figure 3 shows nucleoid staining in typical fields of wild-type cells (Fig. 3A) and *cspB cspD* double-mutant cells

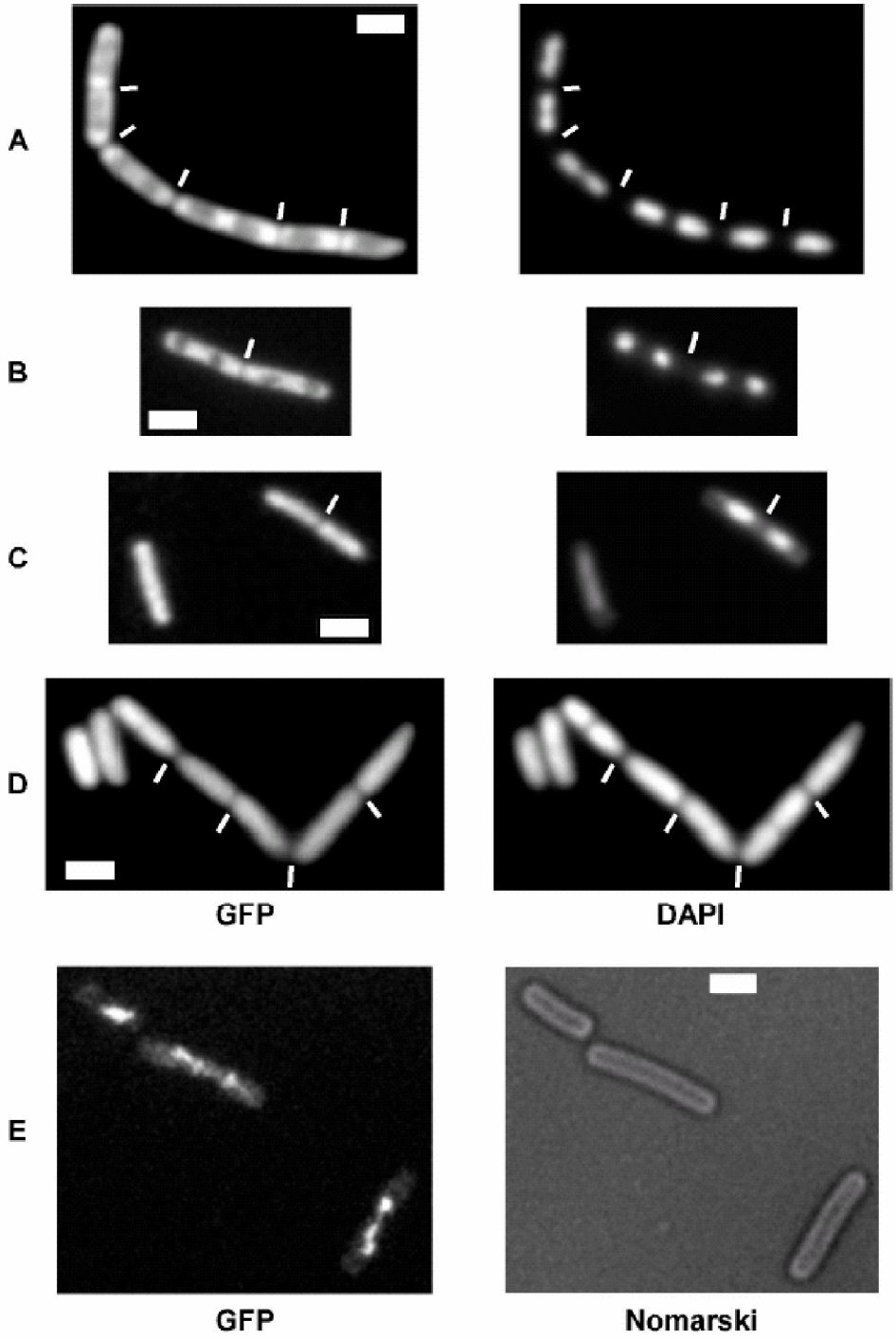

FIG. 2. Fluorescence microscopy of live *B. subtilis* cells grown at 25°C. (A) Exponentially growing cells expressing CspB-GFP (MW2). (B) MW2 cells treated with chloramphenicol for 30 min. (C) MW2 cells 3 h after entry into the stationary phase. (D) MW2 cells treated with rifampin for 30 min. (E) Cells expressing HBsu-GFP 3 h after entry into the stationary phase. The white lines indicate septa between cells. Bars = 2 μm. Note that immunofluorescence using anti-CspB antibodies with fixed wild-type cells confirmed the delocalization of CspB upon inhibition of transcription (D) (data not shown).

(Fig. 3B) grown in rich medium at 37°C. In the mutant strain, nucleoids were generally more condensed (Fig. 3B) and frequently had irregular shapes (this was observed in 5 to 15% of the cells). Similar nucleoid defects were found in *cspB cspC* double-mutant cells (data not shown) and in *cspC* mutant cells containing *cspB*-GFP (indicating that the fusion does not fully complement the wild-type protein). Occasionally, small cells devoid of DNA were detected (0.1 to 0.5% of the cells) adjacent to DNA-free zones in larger mutant cells (Fig. 3C), showing that a defect in CSP function leads to minicell formation. We speculate that in order to function optimally, CSPs need to be small proteins, a requirement which is compromised through

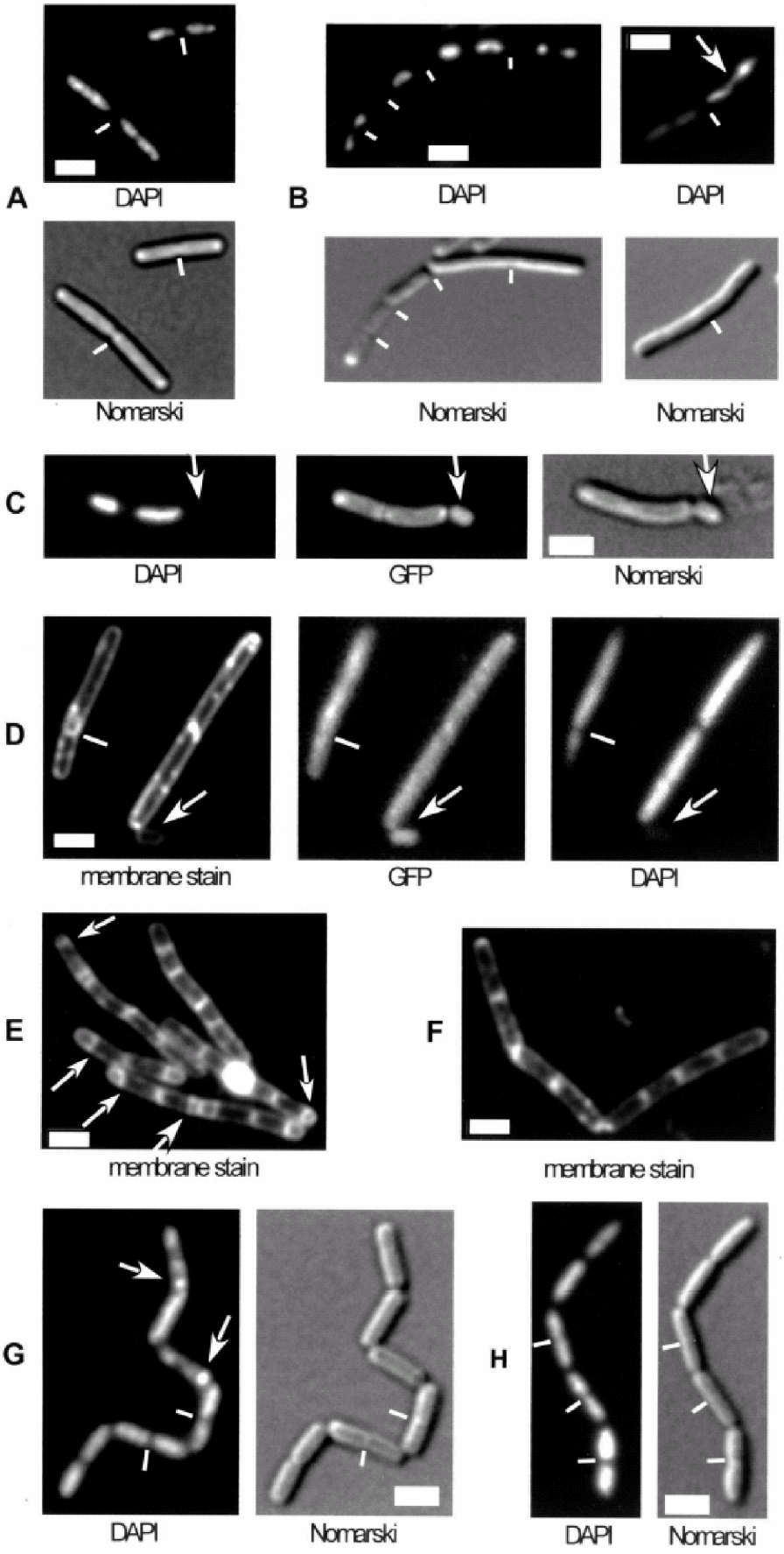
A
DAPI
Nomarski
B
DAPI
DAPI
Nomarski
Nomarski
C
DAPI
GFP
Nomarski
D
membrane stain
GFP
DAPI
E
membrane stain
F
membrane stain
G
DAPI
Nomarski
H
DAPI
Nomarski

the GFP fusion. However, we cannot rule out the possibility that the fusion has an influence on proper folding of CspB. In contrast, depletion of HBsu from cells that constitutively expressed HBsu-GFP and contained wild-type *hbsu* under an inducible promoter led to chromosome decondensation (Fig. 3D), as previously reported (21), as well as to generation of 5 to 10% anucleate cells 2 h after removal of the inducer (when cells were still growing, as judged from the increase in optical density). Note that anucleate cells are generally normal cell size and are generated by guillotining of DNA entrapped by a prematurely closing septum (Fig. 3D, white lines). These findings show that CSPs influence the structure of the nucleoid, although they localize to zones surrounding the chromosomes. Additionally, CSPs influence the position of cell division, probably in an indirect way. In contrast, HBsu has a direct impact on chromosome condensation and segregation, analogous to the impact of the SMC condensation factor.

Sporulation defect in *csp* double mutants. *B. subtilis* has the unique ability to undergo sporulation in response to adverse environmental conditions. This differentiation process involves sequential activation of sporulation genes and synthesis of the corresponding gene products. CSPs have previously been shown to affect protein synthesis in growing cells, so we investigated a possible role of CSPs during sporulation. All *csp* single-mutant strains formed heat-resistant spores comparable to those of wild-type cells (sporulation efficiency, 70 to 80%). In contrast, *cspB cspD* mutant cells were strongly impaired in terms of sporulation, producing only 0.05% spores. Cells with a deletion of *cspB* and *cspC* are defective in adaptation to the stationary phase; such mutant cells lyse after cessation of growth (6). Likewise, only 0.002% viable colonies remained 24 h after the beginning of sporulation in *cspB cspC* mutant cells, compared to wild-type cells. However, the sporulation frequency was 0.03% (compared to viable cells), revealing that the *csp* double mutants did not sporulate. A *cspC* deletion strain expressing *cspB-gfp* formed 0.5 to 1% spores, as well as a number of viable cells comparable to the number formed by the parental strain, showing that a CspB-GFP fusion can substantially but not completely complement the function of CspB during sporulation.

In order to analyze at which stage the block in sporulation occurs, *cspB cspC* and *cspB cspD* mutant cells were stained with FM4-64 membrane stain several hours after entry into sporulation. In contrast to the parental strain, in which polar septation started 2 h after initiation of sporulation (Fig. 3E), no polar septa were detectable in the *csp* double mutants for up to 48 h after entry into sporulation (Fig. 3F). Thus, deletion of *cspD* or *cspC* in addition to *cspB* leads to a defect at stage 0 of sporulation. Recent data suggest that formation of the polar septum during sporulation depends not only on Spo0A activity but also on the migration of replication origins to the extreme cell poles, a process termed axial filament formation (7). To test whether *csp* mutant cells that have more compacted nucleoids during growth are defective in formation of axial filaments, we investigated nucleoid structure at the onset of sporulation. DAPI staining of live cells at the transition to the stationary phase in sporulation medium showed that nucleoids extended to the cell poles (and more or less filled the whole cell) in wild-type cells (Fig. 3G). In *cspB cspC* and *cspB cspD* mutant cells, nucleoids also extended to the poles in a majority of the cells (Fig. 3H). Thus, *csp* mutant cells are not obviously affected in axial filament formation.

Localization of CSPs in sporulating cells. Cells expressing CspB-GFP were used to study the localization of CspB during sporulation. Although CspB-GFP was found to generally localize throughout the cell at the onset of sporulation (data not shown), comparable to what happens in cells entering the stationary phase (Fig. 2C), the amount of fusion protein decreased considerably within the forespore compartment soon after polar septation (Fig. 1I). Likewise, using immunofluorescence as a control, we observed depletion of CspB and CspC from the forespores in wild-type sporangia (Fig. 1J). CspD appeared to be present in the forespore compartment at least until engulfment (data not shown); however, in the absence of an available GFP fusion construct, this finding remains preliminary.

DISCUSSION

The results of this study establish that there is a connection among specific subcellular localization of *B. subtilis* CSPs, active transcription, and nucleoid structure. In growing cells, CSPs localize in cytosolic spaces surrounding the nucleoids, in contrast to histone-like protein HBsu, which localizes exclusively in the nucleoid, as shown previously (21). *B. subtilis* CSPs remained at locations surrounding nucleoids in cells with more condensed nucleoids, such as cells after cold shock, and also in cells with decondensed chromosomes, such as *smc* mutant cells. According to recent reports, ribosomal proteins localize in a manner similar to CSPs, while RNA polymerase subunits and the main sigma factor localize mainly in nucleoids (1, 23). In control experiments, we found that GFP and β-galactosidase localize throughout the cell, providing evidence that nonnucleoid-associated proteins are not generally excluded from nucleoids.

CSPs have been shown to affect the synthesis of other cytosolic proteins at 37°C and after cold shock (5, 6, 18, 22, 33). Two main modes of activation or repression by CSPs have been proposed. Due to their binding to ssDNA, it has been proposed that CSPs may facilitate open complex formation by RNA polymerase through stabilization of ssDNA during transcription initiation (3). In an alternative model, it was sug-

FIG. 3. Fluorescence microscopy of live *B. subtilis* cells growing in rich medium. DAPI, DNA stain; Nomarski, outline of cells; membrane stain, vital stain FM4-64. (A) Wild-type cells. (B) Two fields of 64BD cells (*cspB::spc cspD::cat*) grown at 37°C. The arrow indicates an abnormal nucleoid structure. (C) Strain MW3 (*cspB-gfp cspC::kan*) growing at 25°C. The arrow indicates a minicell devoid of DNA. (D) Cells depleted of HBsu (see text) for 3 h. The arrow indicates an anucleate cell. The white line indicates a septum dissecting a nucleoid. (E) Wild-type cells 3 h after the onset of sporulation at 37°C. The arrows indicate polar septa. (F) 64BD cells (*cspB::spc cspD::cat*) 3 h after the onset of sporulation. (G) Wild-type cells 2 h after the onset of sporulation. The arrows indicate condensed nucleoids in forespore compartments that have proceeded to stage III (engulfment) of sporulation. The white lines indicate septa. (H) Cells of strain 64BD (*cspB::spc cspD::cat*) 2 h after the onset of sporulation. The white lines indicate septa. Note that nucleoids are more decondensed and extended in cells entering sporulation (G and H) than in growing cells (A and B).

gested that CSPs function as RNA chaperones (17) by binding to newly synthesized RNA and by keeping RNA in a linear form (6). This is a prerequisite for translation initiation, which depends on a linear RNA template in bacteria (12). Although our data do not exclude a possible function of CSPs in transcription or in replication initiation, the pattern of localization suggests that the main function of CSPs takes place at sites of translation.

Recently, *E. coli* CSPs were shown to act as antiterminators in transcription of a cold stress-induced operon (2). This finding indicates that coupling of transcription and translation may take place at the interface between the nucleoid and surrounding spaces containing ribosomes. Consequently, CSPs could act mainly on translation initiation within translation areas and could act as antiterminators at the interface between nucleoid and cytosol. In support of this model, we found that in the absence of transcription and during the stationary phase, CSPs localize throughout the cytoplasm, while inhibition of translation retains the specific localization of CSPs. We interpret these findings as an association of CSPs with mRNA, which is preserved upon a block in translation but is eliminated when there is a decrease in RNA synthesis. Our data show that CSPs change their pattern of localization depending on cellular activity, which has not been reported previously for bacterial proteins with respect to transcription and translation.

Intriguingly, although CSPs do not localize to the nucleoid like condensation and compaction factors such as HBsu and SMC, they affect the structure of the nucleoid. In contrast to depletion of HBsu (21) or deletion of *smc* (4, 8), each of which leads to chromosome decondensation, a *cspB cspD* double mutant had more compact nucleoids with frequently abnormal structure than wild-type cells. This finding suggests that through their function, CSPs are involved in decondensing chromosomes in growing cells. Chromosome condensation occurs during the stationary phase, during a block in translation, and after cold shock, as shown in this study. Woldringh et al. (32) proposed a model in which simultaneous insertion into and transport of proteins across membranes and coupled transcription-translation that takes place in bacteria provide expansion forces for chromosome decondensation in growing cells. Our findings are consistent with this model, since a decrease in cellular CSP levels compromises protein synthesis (6) and thereby probably affects chromosome decondensation. The data which we obtained also support the hypothesis that CSPs are important mediators in the coupling of transcription and translation. Moreover, the effect of CSPs on nucleoid morphology discovered in this study is a first clue to why two CSPs in *E. coli* were found to be high-copy-number suppressors of a mutation in condensation factor MukB (34) and confer resistance to chromosome decondensation through camphor (15).

We also found that CSPs are important for the developmental process of sporulation in *B. subtilis*. CSP double mutants were strongly impaired in terms of initiation of sporulation, at a stage before polar septation. In light of a defect in protein synthesis in *csp* mutants during growth (6), it appears likely that absence of CSPs leads to deregulation of protein levels at the onset of sporulation. Interestingly, we found that CspB and CspC were depleted from the forespore compartment but not from the mother cell. The significance of this observation is not clear; however, degradation of CSPs from the forespore may indicate a generally higher rate of proteolysis within the forespore. This may be relevant in compartmentalized proteolysis during sporulation, which, for example, could also lead to degradation of sigma factor E, which is depleted from the forespore (26).

Changes in localization of CSPs during growth, sporulation, and the stationary phase provide evidence not only that membrane and DNA-binding proteins switch their subcellular locations (29) but also that the position of cytosolic, non-DNA-binding proteins is more dynamic in bacteria than anticipated.

ACKNOWLEDGMENTS

Immunofluorescence microscopy experiments were performed primarily in the laboratory of Richard Losick (Cambridge, Mass.).

This study was supported by the Deutsche Forschungsgemeinschaft (Emmie Noether Program and SFB 395).

ADDENDUM IN PROOF

It was recently shown that CSPs colocalize with ribosomes in *B. subtilis* and that localization of ribosomes to sites surrounding nucleoids also depends on active transcription (J. Mascarenhas, M. H. Weber, and P. L. Graumann, EMBO Rep. **2**:685–689, 2001).

REFERENCES

1. **Azam, T. A., S. Hiraga, and A. Ishihama.** 2000. Two types of localization of the DNA-binding proteins within the *Escherichia coli* nucleoid. Genes Cells **5**:613–626.
2. **Bae, W., B. Xia, M. Inouye, and K. Severinov.** 2000. *Escherichia coli* CspA-family RNA chaperones are transcription antiterminators. Proc. Natl. Acad. Sci. USA **97**:7784–7789.
3. **Brandi, A., C. L. Pon, and C. O. Gualerzi.** 1994. Interaction of the main cold shock protein CS 7.4 (CspA) of *Escherichia coli* with the promoter region of *hns*. Biochimie **76**:1090–1098.
4. **Britton, R. A., D. C.-H. Lin, and A. D. Grossman.** 1998. Characterization of a procaryotic SMC protein involved in chromosome partitioning. Genes Dev. **12**:1254–1259.
5. **Graumann, P., and M. A. Marahiel.** 1997. Effects of heterologous expression of CspB from *Bacillus subtilis* on gene expression in *Escherichia coli*. Mol. Gen. Genet. **253**:745–752.
6. **Graumann, P., T. M. Wendrich, M. H. W. Weber, K. Schröder, and M. A. Marahiel.** 1997. A family of cold shock proteins in *Bacillus subtilis* is essential for cellular growth and for efficient protein synthesis at optimal and low temperatures. Mol. Microbiol. **25**:741–756.
7. **Graumann, P. L., and R. Losick.** 2001. Coupling of asymmetric division to polar placement of replication origin regions in *Bacillus subtilis*. J. Bacteriol. **183**:4052–4060.
8. **Graumann, P. L., R. Losick, and A. V. Strunnikov.** 1998. Subcellular localization of *Bacillus subtilis* SMC, a protein involved in chromosome condensation and segregation. J. Bacteriol. **180**:5749–5755.
9. **Graumann, P. L., and M. A. Marahiel.** 1999. Cold shock proteins CspB and CspC are major stationary-phase-induced proteins in *Bacillus subtilis*. Arch. Microbiol. **171**:135–138.
10. **Graumann, P. L., and M. A. Marahiel.** 1999. Cold shock response in *Bacillus subtilis*. J. Mol. Microbiol. Biotechnol. **1**:203–209.
11. **Graumann, P. L., and M. A. Marahiel.** 1998. A superfamily of proteins that contain the cold-shock domain. Trends Biochem. Sci. **23**:286–290.
12. **Gualerzi, C. O., and C. L. Pon.** 1990. Initiation of mRNA translation in procaryotes. Biochemistry **29**:5881–5889.
13. **Hanna, M. M., and K. Liu.** 1998. Nascent RNA in transcription complexes interacts with CspE, a small protein in *E. coli* implicated in chromatin condensation. J. Mol. Biol. **282**:227–239.
14. **Harwood, C. R., and S. M. Cutting.** 1990. Molecular biological methods for *Bacillus*. Wiley, New York, N.Y.
15. **Hu, K. H., E. Liu, K. Dean, M. Gingras, W. DeGraff, and N. J. Trun.** 1996. Overproduction of three genes leads to camphor resistance and chromosome condensation in *Escherichia coli*. Genetics **143**:1521–1532.
16. **Jaacks, K. J., J. Healy, R. Losick, and A. D. Grossman.** 1989. Identification and characterization of genes controlled by the sporulation regulatory gene *spo0H* in *Bacillus subtilis*. J. Bacteriol. **171**:4121–4129.
17. **Jiang, W., Y. Hou, and M. Inouye.** 1997. CspA, the major cold-shock protein

of *Escherichia coli*, is an RNA chaperone. J. Biol. Chem. 272:196–202.
18. **Jones, P. G., R. Krah, S. Tafuri, and A. P. Wolffe.** 1992. DNA gyrase, CS7.4, and the cold shock response in *Escherichia coli*. J. Bacteriol. 174:5798–5802.
19. **Kaan, T., B. Jurgen, and T. Schweder.** 1999. Regulation of the expression of the cold shock proteins CspB and CspC in *Bacillus subtilis*. Mol. Gen. Genet. 262:351–354.
20. **Kim, L., A. Mogk, and W. Schumann.** 1996. A xylose-inducible *Bacillus subtilis* integration vector and its application. Gene 181:71–76.
21. **Köhler, P., and M. A. Marahiel.** 1997. Association of the histone-like protein HBsu with the nucleoid of *Bacillus subtilis*. J. Bacteriol. 179:2060–2064.
22. **La Taena, A., A. Brandi, M. Falconi, R. Spurio, C. Pon, and C. O. Gualerzi.** 1991. Identification of a cold shock transcriptional enhancer of the *Escherichia coli* gene encoding nucleoid protein H-NS. Proc. Natl. Acad. Sci. USA 88:10907–10911.
23. **Lewis, P. J., S. D. Thaker, and J. Errington.** 2000. Compartmentalization of transcription and translation in *Bacillus subtilis*. EMBO J. 19:710–718.
24. **Moriya, S., E. Tsujikawa, A. K. M. Hassan, K. Asai, T. Kodama, and N. Osagawara.** 1998. A *Bacillus subtilis* gene encoding protein homologous to eukaryotic SMC motor protein is necessary for chromosome partition. Mol. Microbiol. 29:179–187.
25. **Phadtare, S., J. Alsina, and M. Inouye.** 1999. Cold-shock response and cold-shock proteins. Curr. Opin. Microbiol. 2:175–180.
26. **Pogliano, K., A. E. Hofmeister, and R. Losick.** 1997. Disappearance of the sigma E transcription factor from the forespore and the SpoIIE phosphatase from the mother cell contributes to establishment of cell-specific gene expression during sporulation in *Bacillus subtilis*. J. Bacteriol. 179:3331–3341.
27. **Schindler, T., P. L. Graumann, D. Perl, S. Ma, F. X. Schmid, and M. A. Marahiel.** 1999. The family of cold shock proteins of *Bacillus subtilis*. Stability and dynamics *in vitro* and *in vivo*. J. Biol. Chem. 274:3407–3413.
28. **Schröder, K., P. Graumann, A. Schnuchel, T. A. Holak, and M. A. Marahiel.** 1995. Mutational analysis of the putative nucleic acid-binding surface of the cold-shock domain, CspB, revealed an essential role of aromatic and basic residues in binding of single-stranded DNA containing the Y-box motif. Mol. Microbiol. 16:699–708.
29. **Shapiro, L., and R. Losick.** 2000. Dynamic spatial regulation in the bacterial cell. Cell 100:89–98.
30. **Webb, C. D., Decatur, A., A. Teleman, and R. Losick.** 1995. Use of green fluorescent protein for visualization of cell-specific gene expression and subcellular protein localization during sporulation in *Bacillus subtilis*. J. Bacteriol. 177:5906–5911.
31. **Willimsky, G., H. Bang, G. Fischer, and M. A. Marahiel.** 1992. Characterization of *cspB*, a *Bacillus subtilis* inducible cold shock gene affecting viability at low temperatures. J. Bacteriol. 174:6326–6335.
32. **Woldringh, C. L., P. R. Jensen, and H. V. Westerhoff.** 1995. Structure and partitioning of bacterial DNA: determined by a balance of compaction and expansion forces? FEMS Microbiol. Lett. 131:235–242.
33. **Wouters, J. A., M. Mailhes, F. M. Rombouts, W. M. de Vos, O. P. Kuipers, and T. Abee.** 2000. Physiological and regulatory effects of controlled overproduction of five cold shock proteins of *Lactococcus lactis* MG1363. Appl. Environ. Microbiol. 66:3756–3763.
34. **Yamanaka, K., T. Mitani, T. Ogura, H. Niki, and S. Hiraga.** 1994. Cloning, sequencing and characterization of multicopy suppressors of a *mukB* mutation in *Escherichia coli*. Mol. Microbiol. 13:301–312.

5.2.1 List of plasmids and strains constructed in this work

E. coli strain	Modified plasmid	Cloned gene	Host/Expression strain	Cloning details	Primers used
AV11	pQE60 (Qiagen)	*scpA* from *B. subtilis*	XL1-Blue/M15	Cloned at *Nco*I/*Bgl*II sites	62, 63
AV12	pQE60 (Qiagen)	*scpB* from *B. subtilis*	XL1-Blue/M15	Cloned at *Nco*I/*Bgl*II sites	60, 61
AV13	pQE60 (Qiagen)	*smc* from *B. subtilis*	XL1-Blue/M15	Cloned at *Nco*I/*Bgl*II sites	77, 116
AV14	pQE60 (Qiagen)	N-terminal part of *smc* from *B. subtilis*	XL1-Blue	Cloned at *Nco*I/*Bgl*II sites	77, 111
AV15	pQE60 (Qiagen)	C-terminal part of *smc* from *B. subtilis*	XL1-Blue	Cloned at *Nco*I/*Bgl*II sites	112, 116
AV16	pQE60 (Qiagen)	*smc* head domain from *B. subtilis*	XL1-Blue/M15	N-terminal domain amplified from pAV14 was cloned at *Xba*I into pAV15	138, 139
AV17	pQE60 (Qiagen)	*smc* hinge domain from *B. subtilis*	XL1-Blue/M15	Cloned at *Nco*I/*Bgl*II sites	70, 71
AV18	pET101D (Invitrogen)	*smc* from *T. maritima*	Top10/BL21 Star™	Blunt-end cloning	274, 275
AV19	pET101D (Invitrogen)	*scpA* from *T. maritima*	Top10/BL21 Star™	Blunt-end cloning	276, 277

AV20	pET101D (Invitrogen)	*scpB from T. maritima*	Top10/BL21 Star™	Blunt-end cloning	278, 279
AV21	pQE60 (Qiagen)	*smc* with K37I mutation, *B. subtilis*	XL1-Blue/M15	Cloned at *Nco*I/*Bgl*II sites, mutation introduced by PCR-based site-directed mutagenesis	230, 231
AV22	pQE60 (Qiagen)	*smc* with D1117A mutation, *B. subtilis*	XL1-Blue/M15	Cloned at *Nco*I/*Bgl*II sites, mutation introduced by PCR-based site-directed mutagenesis	232, 233
AV23	pQE60 (Qiagen)	*smc* with S1090R mutation, *B. subtilis*	XL1-Blue	Cloned at *Nco*I/*Bgl*II sites, mutation introduced by PCR-based site-directed mutagenesis	234, 235

5.2.2List of primers used

Primer	***´Sequence (5´-3)***
60 ypuHhisup	cat gcc atg ggg ctt gat atc gtg
61 ypuHhisdw	tga aga tct ttt tat atc ttc gaa ggt ttg g
62 ypuGhisup	cat gcc atg gaa gaa tat caa gtg aaa att g
63 ypuGhisdw	tga aga tct agc ccc atg aat gga ttc ac
70 smchingeup	cat gcc atg gaa tat gag cag aaa aag cgc
71 smchingedw	tga aga tct gct tct tcc aag gag gg
77 smchisnco	cct gcc atg ggt acc gtg aac ctc g
111 smcN50Bgldw	tga aga tct cga cca ttt acc atg cag c
112 smcC50Nco	cat gcc atg gtg aag ctg att aaa ctc gc
116 smchisbgl3	cga aga tct ctg aac gaa ttc ttt tgt ttc
138 pQEXbaUp	tgc tct aga ccc gaa aag tgc cac ctg
139 pQEXbaDw	tgc tct aga gtt ctg agg tca tta ctg g
158 rrnA100dw	ccg tcc gcc gct aac atc
159 rrnA500dw	gtt agc cgt ggc ttt ctg g
172 rrnAup (5` Biotinylated)	cgg aga gtt tga tcc tgg c
173 rrnA100dw (5` Biotinylated)	ccg tcc gcc gct aac atc
174 rrnA500dw (5` Biotinylated)	gtt agc cgt ggc ttt ctg g
230 K37Iup	gtc ggg ccg aac gga agc gga ata agc aac atc acg gat gcc
231 K37Idw	ggc atc cgt gat gtt gct tat tcc gct tcc gtt cgg ccc gac
232 D1117Aup	gtg ccg ttt tgc gtc ctt gcc gaa gta gag gct gcg c
233 D1117Aup-r	gcg acg cct cta ctt cgg caa gga cgc aaa acg gca c
234 S1090Rup	caa aac tta aac ctc ctg cga ggc gga gag cgt gcg
235 S1090Rup-r	cgc acg atc tcc gcc tcg cag gag gtt taa gtt ttg
274 ThermarSMCup	cac cat gag act gaa aaa act cta ctt aaa ag

```
275 ThermarSMCdw      cta cta cac ctc cag tat ttt ctc cac
276 ThermarScpAup     cac cat gga tct tgt ctt caa act tcc
277 ThermarScpAdw     tca tca ata gcg gcc ttg agc tgc
278 ThermarScpBup     cac cat gca gct caa ggc cgc tat tg
279 ThermarScpBdw     tca tca aga ctc gcc acc atc gc
```

6 References

Anderson, D. E., A. Losada, et al. (2002). "Condensin and cohesin display different arm conformations with characteristic hinge angles." J. Cell Biol. **156**(3): 419-424.

Arumugam, P., S. Gruber, et al. (2003). "ATP hydrolysis is required for cohesin's association with chromosomes." Curr Biol **13**(22): 1941-53.

Bazett-Jones, D. P., K. Kimura, et al. (2002). "Efficient supercoiling of DNA by a single condensin complex as revealed by electron spectroscopic imaging." Mol. Cell **9**(6): 1183-1190.

Buonomo, S. B., R. K. Clyne, et al. (2000). "Disjunction of homologous chromosomes in meiosis I depends on proteolytic cleavage of the meiotic cohesin Rec8 by separin." Cell **103**(3): 387-98.

Chuang, P. T., D. G. Albertson, et al. (1994). "DPY-27:a chromosome condensation protein homolog that regulates C. elegans dosage compensation through association with the X chromosome." Cell **79**(3): 459-74.

Cobbe, N. and M. M. Heck (2004). "The evolution of SMC proteins: phylogenetic analysis and structural implications." Mol Biol Evol **21**(2): 332-47.

Cohen-Fix, O. and D. Koshland (1997). "The anaphase inhibitor of Saccharomyces cerevisiae Pds1p is a target of the DNA damage checkpoint pathway." Proc Natl Acad Sci U S A **94**(26): 14361-6.

Combet C., B. C., Geourjon C. and Deleage G. (2000). "NPS@: Network Protein Sequence Analysis." TIBS **25**(No 3 [291]): 147-150.

Connelly, J. C. and D. R. Leach (2002). "Tethering on the brink: the evolutionarily conserved Mre11-Rad50 complex." Trends Biochem Sci **27**(8): 410-8.

Dubnau, D. (1991). "Genetic competence in Bacillus subtilis." Microbiol Rev **55**(3): 395-424.

Emptage, N. J. (2001). "Fluorescent imaging in living systems." Curr Opin Pharmacol **1**(5): 521-5.

Erickson, H. P. (1991). Protein Structure. Useful calculations for thinking about protein structure at the nanometer level.

Fousteri, M. I. and A. R. Lehmann (2000). "A novel SMC protein complex in Schizosaccharomyces pombe contains the Rad18 DNA repair protein." Embo J **19**(7): 1691-702.

Freeman, L., L. Aragon-Alcaide, et al. (2000). "The condensin complex governs chromosome condensation and mitotic transmission of rDNA." J Cell Biol **149**(4): 811-824.

Fujioka, Y., Y. Kimata, et al. (2002). "Identification of a novel non-structural maintenance of chromosomes (SMC) component of the SMC5-SMC6 complex involved in DNA repair." J Biol Chem **277**(24): 21585-91.

Funabiki, H., H. Yamano, et al. (1996). "Cut2 proteolysis required for sister-chromatid seperation in fission yeast." Nature **381**(6581): 438-41.

Gruber, S., C. H. Haering, et al. (2003). "Chromosomal cohesin forms a ring." Cell **112**(6): 765-77.

Guacci, V., D. Koshland, et al. (1997). "A direct link between sister chromatid cohesion and chromosome condensation revealed through the analysis of MCD1 in *S. cerevisiae*." Cell **91**(1): 47-57.

Haering, C. H., J. Lowe, et al. (2002). "Molecular architecture of SMC proteins and the yeast cohesin complex." Mol. Cell **9**(4): 773-788.

Haering, C. H. and K. Nasmyth (2003). "Building and breaking bridges between sister chromatids." Bioessays **25**(12): 1178-91.

Hagstrom, K. A., V. F. Holmes, et al. (2002). "C. elegans condensin promotes mitotic chromosome architecture, centromere organization, and sister chromatid segregation during mitosis and meiosis." Genes Dev **16**(6): 729-42.

Hagstrom, K. A. and B. J. Meyer (2003). "Condensin and cohesin: more than chromosome compactor and glue." Nat Rev Genet **4**(7): 520-34.

Higgins, C. F. (1992). "ABC transporters: from microorganisms to man." Annu Rev Cell Biol **8**: 67-113.

Hirano, M., D. E. Anderson, et al. (2001). "Bimodal activation of SMC ATPase by intra- and inter-molecular interactions." EMBO J. **20**(12): 3238-3250.

Hirano, M. and T. Hirano (1998). "ATP-dependent aggregation of single-stranded DNA by a bacterial SMC homodimer." EMBO J. **17**(23): 7139-7148.

Hirano, T., R. Kobayashi, et al. (1997). "Condensins, chromosome condensation protein complexes containing XCAP- C, XCAP-E and a *Xenopus* homolog of the Drosophila Barren protein." Cell **89**(4): 511-521.

Hirano, T. and T. J. Mitchison (1994). "A heterodimeric coiled-coil protein required for mitotic chromosome condensation in vitro." Cell **79**(3): 449-58.

Hopfner, K. P., L. Craig, et al. (2002). "The Rad50 zinc-hook is a structure joining Mre11 complexes in DNA recombination and repair." Nature **418**(6897): 562-566.

Hopfner, K. P., A. Karcher, et al. (2000). "Mre11 and Rad50 from Pyrococcus furiosus: cloning and biochemical characterization reveal an evolutionarily conserved multiprotein machine." J Bacteriol **182**(21): 6036-41.

Hopfner, K. P. and J. A. Tainer (2003). "Rad50/SMC proteins and ABC transporters: unifying concepts from high-resolution structures." Curr Opin Struct Biol **13**(2): 249-55.

Hung, L. W., I. X. Wang, et al. (1998). "Crystal structure of the ATP-binding subunit of an ABC transporter." Nature **396**(6712): 703-7.

Jessberger, R. (2002). "The many functions of SMC proteins in chromosome dynamics." Nat Rev Mol Cell Biol **3**(10): 767-78.

Jones, P. M. and A. M. George (2004). "The ABC transporter structure and mechanism: perspectives on recent research." Cell Mol Life Sci **61**(6): 682-99.

Junop, M. S., G. Obmolova, et al. (2001). "Composite active site of an ABC ATPase: MutS uses ATP to verify mismatch recognition and authorize DNA repair." Mol Cell **7**(1): 1-12.

Kimura, K., O. Cuvier, et al. (2001). "Chromosome condensation by a human condensin complex in Xenopus egg extracts." J Biol Chem **276**(8): 5417-20.

Kimura, K. and T. Hirano (1997). "ATP-dependent positive supercoiling of DNA by 13S condensin: a biochemical implication for chromosome condensation." Cell **90**(4): 625-634.

Kimura, K. and T. Hirano (2000). "Dual roles of the 11S regulatory subcomplex in condensin functions." Proc. Natl. Acad. Sci. U S A **97**(22): 11972-11977.

Klein, F., P. Mahr, et al. (1999). "A central role for cohesins in sister chromatid cohesion, formation of axial elements, and recombination during yeast meiosis." Cell **98**(1): 91-103.

Klein W, M. M. (2002). "Structure-function relationship and regulation of two Bacillus subtilis DNA-binding proteins, HBsu and AbrB." J Mol Microbiol Biotechnol **4**(3): 323-9.

Lehmann, A. R., M. Walicka, et al. (1995). "The rad18 gene of Schizosaccharomyces pombe defines a new subgroup of the SMC superfamily involved in DNA repair." Mol Cell Biol **15**(12): 7067-80.

Lieb, J. D., E. E. Capowski, et al. (1996). "DPY-26, a link between dosage compensation and meiotic chromosome segregation in the nematode." Science **274**(5293): 1732-6.

Losada, A., M. Hirano, et al. (1998). "Identification of Xenopus SMC protein complexes required for sister chromatid cohesion." Genes Dev **12**(13): 1986-97.

Losada, A., M. Hirano, et al. (2002). "Cohesin release is required for sister chromatid resolution, but not for condensin-mediated compaction, at the onset of mitosis." Genes Dev **16**(23): 3004-16.

Luo, G., M. S. Yao, et al. (1999). "Disruption of mRad50 causes embryonic stem cell lethality, abnormal embryonic development, and sensitivity to ionizing radiation." Proc Natl Acad Sci U S A **96**(13): 7376-81.

Martinez-Balbas, M. A., A. Dey, et al. (1995). "Displacement of sequence-specific transcription factors from mitotic chromatin." Cell **83**(1): 29-38.

Meyer, B. J. (2000). "Sex in the wormcounting and compensating X-chromosome dose." Trends Genet **16**(6): 247-53.

Muskhelishvili G, T. A. (2003). "Transcription factor as a topological homeostat." Front Biosci. **1**(8): d279-85.

Nasmyth, K. (2001). "Disseminating the genome: joining, resolving, and separating sister chromatids during mitosis and meiosis." Annu Rev Genet **35**: 673-745.

Neuwald, A. F. and T. Hirano (2000). "HEAT repeats associated with condensins, cohesins, and other complexes involved in chromosome-related functions." Genome Res **10**(10): 1445-52.

Ono, T., A. Losada, et al. (2003). "Differential contributions of condensin I and condensin II to mitotic chromosome architecture in vertebrate cells." Cell **115**(1): 109-121.

Ono, T., A. Losada, et al. (2003). "Differential contributions of condensin I and condensin II to mitotic chromosome architecture in vertebrate cells." Cell **115**(1): 109-21.

Pasierbek, P., M. Jantsch, et al. (2001). "A Caenorhabditis elegans cohesion protein with functions in meiotic chromosome pairing and disjunction." Genes Dev **15**(11): 1349-60.

Schleiffer, A., S. Kaitna, et al. (2003). "Kleisins: a superfamily of bacterial and eukaryotic SMC protein partners." Mol Cell **11**(3): 571-5.

Schmitt, L. and R. Tampe (2002). "Structure and mechanism of ABC transporters." Curr Opin Struct Biol **12**(6): 754-60.

Sharples, G. J. and D. R. Leach (1995). "Structural and functional similarities between the SbcCD proteins of Escherichia coli and the RAD50 and MRE11 (RAD32) recombination and repair proteins of yeast." Mol Microbiol **17**(6): 1215-7.

Steffensen, S., P. A. Coelho, et al. (2001). "A role for Drosophila SMC4 in the resolution of sister chromatids in mitosis." Curr Biol **11**(5): 295-307.

Sumara, I., E. Vorlaufer, et al. (2002). "The dissociation of cohesin from chromosomes in prophase is regulated by Polo-like kinase." Mol Cell **9**(3): 515-25.

Sutani, T., T. Yuasa, et al. (1999). "Fission yeast condensin complex: essential roles of non-SMC subunits for condensation and cdc2 phosphorylation of Cut3/SMC4." Genes Dev **13**(17): 2271-83.

Toth, A., R. Ciosk, et al. (1999). "Yeast cohesin complex requires a conserved protein, Eco1p(Ctf7), to establish cohesion between sister chromatids during DNA replication." Genes Dev **13**(3): 320-33.

Uhlmann, F., F. Lottspeich, et al. (1999). "Sister-chromatid separation at anaphase onset is promoted by cleavage of the cohesin subunit Scc1." Nature **400**(6739): 37-42.

Uhlmann, F., D. Wernic, et al. (2000). "Cleavage of cohesin by the CD clan protease separin triggers anaphase in yeast." Cell **103**(3): 375-86.

Verkade, H. M., S. J. Bugg, et al. (1999). "Rad18 is required for DNA repair and checkpoint responses in fission yeast." Mol Biol Cell **10**(9): 2905-18.

Volkov, A. V., J. Mascarenhas, et al. (2003). "A prokaryotic condensin/cohesin-like complex can actively compact chromosomes from a single position on the nucleoid." Mol. Cell Biol. **23**: 5638-5650.

Watanabe, Y., S. Yokobayashi, et al. (2001). "Pre-meiotic S phase is linked to reductional chromosome segregation and recombination." Nature **409**(6818): 359-63.

Webb, C. D., A. Teleman, et al. (1997). "Bipolar localization of the replication origin regions of chromosomes in vegetative and sporulating cells of B. subtilis." Cell **88**(5): 667-74.

Weitzer, S., C. Lehane, et al. (2003). "A model for ATP hydrolysis-dependent binding of cohesin to DNA." Curr Biol **13**(22): 1930-40.

Woldringh, C. L. (2002). "The role of co-transcriptional translation and protein translocation (transertion) in bacterial chromosome segregation." Mol Microbiol **45**(1): 17-29.

Yoshimura, S. H., K. Hizume, et al. (2002). "Condensin architecture and interaction with DNA: regulatory non-SMC subunits bind to the head of SMC heterodimer." Curr. Biol. **12**(6): 508-513.

Zhu, X. D., B. Kuster, et al. (2000). "Cell-cycle-regulated association of RAD50/MRE11/NBS1 with TRF2 and human telomeres." Nat Genet **25**(3): 347-52.

Papers published in the course of this work:

1 Weber MH, Volkov AV, Fricke I, Marahiel MA, Graumann PL
Localization of cold shock proteins to cytosolic spaces surrounding nucleoids in Bacillus subtilis depends on active transcription. J Bacteriol. 2001 Nov;183(21):6435-43.

2. Volkov A, Mascarenhas J, Andrei-Selmer C, Ulrich HD, Graumann PL.
A prokaryotic condensin/cohesin-like complex can actively compact chromosomes from a single position on the nucleoid and binds to DNA as a ring-like structure. Mol Cell Biol. 2003 Aug;23(16):5638-50.

3. . Volkov A, Graumann PL
ATP binding is required for DNA binding activity of *Bacillus subtilis* SMC, but not for complex formation with ScpA and ScpB. Submitted Feb 2004

Conference abstracts

1. A. V. Volkov, J. Mascarenhas, C. Andrei-Selmer, H. D. Ulrich, P. L. Graumann
Compaction of Chromosomes in *Bacillus subtilis* via a Ring Structure of the SMC Complex ASM General Meeting, 2003: May 18-May 22, Washington, DC

2. A. Volkov, C. Andrei-Selmer and P.L. Graumann
Characterization of a condensin-like complex in *Bacillus subtilis* VAAM Meeting, Gottingen, Germany 2002

3. J. Mascarenhas, A. Volkov, C. Andrei-Selmer and P.L. Graumann
Dynamic localization of an SMC-chromosome condensation complex in *Bacillus subtilis* VAAM Meeting, Gottingen, Germany 2002

4. Michael H.W. Weber, Carsten I. Beckering, Wolfgan Klein, Thomas M. Wendrich, Lin Muller, Ingo Fricke, Tilman S. Schlothauer, Arsen V. Volkov, Peter L. Graumann, Mohamed A. Marahiel The cold shock response in *Bacillus subtilis* - Cold shock proteins, Translation Machinery and Membrane Adaptation

Functional Genomics of Gram-positive Bacteria Conference, San Diego, California, USA 2001

Erklärung

Ich versichere, daß ich meine Dissertation ‘Biochemical characterization of the Structural Maintenance of Chromosomes (SMC) complex from *Bacillus subtilis*’ selbständig, ohne unterlaubte Hilfe angefertigt und mich dabei keiner anderen als der von mir ausdrüklich bezeichneten Quellen und Hilfen bedient habe.

Die Dissertation wurde in der jetzeigen oder einer ähnlichen Form noch bei keiner anderen Hochschule eingereicht und hat noch keinen sonstigen Prüfungszwecken gedient.

Marburg, den

Acknowledgements

First of all I would like to thank Dr. Peter Graumann for giving me this opportunity to do my PhD work and for all support and help I always received from him.

I would like to thank Prof. Dr. M. Bölker, Prof. Dr. U. Maier and Prof. Dr. A. Batschauer for their participation in the examination commission.

I am thankful to Prof. Dr. L.-O. Essen, Prof. Dr. M. Marahiel and to all their lab members for discussions and all the help.

Special thanks to Dr. H. D. Ulrich, MPI, Marburg for all the help with Biacore experiments

I am grateful to Dr. Uwe Linne, Gabi Schimpff-Weihland for performance of mass spectroscopy and for the kind gift of AbrB protein

I would like to thank Prof. Dr. G. Muskhelishvili, MPI, Marburg for the gift of Fis protein and Dr. Martin Neeb and Prof. Dr. Norbert Hamp, physicalische Chemie, Philipps-Universität, Marburg for their expert help in sucrose gradient centrifugation.

Many thanks to Dr. F. Noll, physicalische Chemie, Philipps-Universität, Marburg and Dr. J. Schiener, MPI, Biochemie, Munich for performing EM and AFM experiments.

I am very grateful to Judith and all my colleagues for all the help and a wonderful work atmosphere.

Most of all I would like to thank my parents for all the love, support and help I always receive from them.

Curriculum vitae

Arsen V. Volkov

Born on 16 of January, 1978 in Aktubinsk, USSR, to Valeriy N. Volkov and Viktoria V. Volkova

Education:

1985-1994 Primary and high school,
Gimnasium №1, Murmansk, Russia

1994-1997 Bachelors of Science Degree in Physical and Chemical Biology and Biotechnology (major, Applied Mathematics and Physics)
Moscow Institute of Physics and Technology, Moscow, Russia

1997-2000 Master of Science Degree, in Physical and Chemical Biology and Biotechnology, (major, Applied Mathematics and Physics)
Moscow Institute of Physics and Technology, Moscow, Russia

2000-2004 PhD thesis in Biochemical Characterization of the Structural Maintenance of Chromosomes (SMC) complex from *Bacillus subtilis*
Biology, Fachberiech Chemie, Philipps Universitaet Marburg, Germany